SOIL TRANSLOCATION

WITH TILLAGE TOOLS

A Thesis Submitted to the College of

Graduate Studies and Research

in Partial Fulfilment of the Requirements

for the Degree of Doctor of Philosophy

in the Department of Agricultural and Bioresource Engineering

University of Saskatchewan

Saskatoon

By

Karim Sharifat

SPRING, 1999

UNIVERSITY OF SASKATCHEWAN

College of Graduate Studies and Research

SUMMARY OF DISSERTATION

Submitted in partial fulfillment

of the requirements for the

DEGREE OF DOCTOR OF PHILOSOPHY

by

Karim Sharifat

Department of Agricultural and Bioresource Engineering

University of Saskatchewan

Spring 1999

Examining Committee:

Dr. E. de Jong	Dean/Associate Dean, Dean's Designate, Chair College of Graduate Studies and Research
Dr. E. M. Barber	Chair of Advisory Committee, Department of Agricultural and Bioresource Engineering
Dr. R. L. Kushwaha	Supervisor, Department of Agricultural and Bioresource Engineering
Dr. R. J. Ford	Department of Agricultural and Bioresource Engineering
Dr. C. P. Maulé	Department of Agricultural and Bioresource Engineering
Dr. J. N. Wilson	Department of Mechanical Engineering

External Examiner:

Dr. D. Lobb
Department of Soil Science
University of Manitoba
66 Chancellors Circle
Winnipeg, Manitoba R3T 2N2

SOIL TRANSLOCATION WITH TILLAGE TOOLS

A study of soil translocation by tillage tools was conducted in the soil bin facilities of the Department of Agricultural and Bioresourse Engineering, University of Saskatchewan. Initially a 300-mm wide sweep and a 14-mm Conserva-Pac knife opener (narrow tool) were used at three operating speeds with three soil moisture contents and three compaction levels. Soil translocation was measured by the movement of small plastic blocks positioned in the soil. The plastic blocks had a density equal to the soil. New positions of the plastic blocks (x-y-z coordinates) after each test were measured with a special instrument developed for this study and the volume of translocated soil was determined. Effects of compaction level, moisture content, tool shape, and travel speed on soil translocation were studied.

Results showed an exponential relationship between soil movement and depth of operation. Soil movement per unit width was higher for the narrow tool. Therefore, more experiments with different narrow tool shapes at higher speeds of operation were conducted to determine the trend. Four narrow tools with shapes of 45° triangular, 90° triangular, flat and elliptical were used at four levels of speed of 10, 15, 20, and 25 km/h and three compaction and three soil moisture levels. A special device using a simple pendulum principle was used to provide the required speed levels. An instrumentation system was designed to measure the tool speed and the energy used during cutting. Soil lateral movement was determined by recording the soil furrow profile by a laser soil profile meter fabricated for this study. Among the four tool shapes used in high speed

experiments, the 45° and elliptical shaped tools resulted in less soil movement and used less energy.

Based on these data, a mathematical model for soil movement with speed of operation of the tillage tool was developed. Soil physical parameters were included to predict soil movement at different moisture contents, compaction levels, and tool shape factors. The predicted soil movement correlated well with experimental data. Therefore, for minimum soil movement, the tool shape should either be elliptical or 45° triangular. Since it is difficult to model soil parameters, the model needs further refinements.

BIOGRAPHICAL

1958	Born in Bandar Emam, Iran
1984	B. Sc. Farm Machinery, Shiraz University, Iran
1990	M. Sc. Mechanics of farm Machinery, Tehran University, Iran

SCHOLARSHIP

Iranian Ministry of Higher Education

College of Graduate Studies and Research, University of Saskatchewan

PERMISSION TO USE

In presenting this thesis in partial fulfilment of the requirements for a postgraduate degree from the University of Saskatchewan, the author agrees that the Libraries of this University may make it freely available for inspection. The author further agrees that permission for copying of this thesis in any manner, in whole or in part, for scholarly purposes may be granted by the professor(s) who supervised my thesis work or, by the Head of the Department or the Dean of the College in which my thesis work was done. It is understood that any copying or publication or use of this thesis or parts thereof for financial gain shall not be allowed without my written permission. It is also understood that due recognition shall be given to me and to the University of Saskatchewan in any scholarly use which may be made of any material in my thesis.

Requests for permission to copy or to make other use of material in this thesis in whole or part should be addressed to:

Head of the Department of
Agricultural and Bioresource Engineering
University of Saskatchewan
57 Campus Drive
Saskatoon SK S7N 5A9
Canada

ABSTRACT

A study of soil translocation by tillage tools was conducted in the soil bin facilities of the Department of Agricultural and Bioresourse Engineering, University of Saskatchewan. Initially a 300-mm wide sweep and a 14-mm Conserva-Pac knife opener (narrow tool) were used at three operating speeds with three soil moisture contents and three compaction levels. Soil translocation was measured by the movement of small plastic blocks positioned in the soil. The plastic blocks had a density equal to the soil. New positions of the plastic blocks (x-y-z coordinates) after each test were measured with a special instrument developed for this study and the volume of translocated soil was determined. Effects of compaction level, moisture content, tool shape, and travel speed on soil translocation were studied.

The results showed an exponential relationship between soil movement and depth, and the soil movement per travel unit area was higher for the narrow tool. Results also indicated that soil movement per unit width or per frontal area of the narrow tool was higher than for the sweep. Therefore, more experiments with different narrow tillage tools at higher speeds were conducted to determine the trend. Four narrow tools with shapes of 45° triangular, 90° triangular, flat and elliptical were used at four levels of speed (10, 15, 20, and 25 km h^{-1}), three levels of compaction and three levels of soil moisture. A special device, using a simple pendulum principle, was used to provide the required speed levels. An instrumentation system was designed to measure the tool speed and the energy used during cutting. Soil profiles for each test were also measured by a laser soil profile meter fabricated for this study. Among the four tool shapes used in high

speed experiments, the 45° and elliptical shaped tools resulted in less soil movement and used less energy.

Based on these data, a mathematical model for soil movement with speed of operation of the tillage tool was developed. Soil physical parameters were included to predict soil movement at different moisture contents, compaction levels, and tool shape factors. The predicted soil movement correlated well with experimental data. Since it is difficult to model soil parameters, the model needs further refinements.

ACKNOWLEDGEMENTS

The author wishes to express his sincere appreciation to his supervisor, Dr. Radhey Lal Kushwaha, for his continuous assistance, guidance, patience and encouragement during all stages of this study.

Thanks are also extended to my advisory committee members (Professor E. M. Barber, Professor C. P. Maulé, Professor J. N. Wilson, Professor R. J. Ford, and Professor Trever Crowe) and Professor E. deJong and my external examiner Dr. D. Lobb for their valuable contributions.

I acknowledge the financial support from Ministry of Culture and Higher Education of Islamic Republic of Iran, College of Graduate Studies and Research, University of Saskatchewan, and the Natural Sciences and Engineering Resource Council of Canada.

I am also thankful to W. Morley and L. Roth, both from the Agricultural and Bioresource Engineering Department who assisted me in preparing the materials and setting up the experiments.

I would like to thank my beloved family, my wife Nassrin, My son Reza, and my daughter Niloofar for their patience and support during my studies.

I would like to thank God for providing me the opportunity for this study, without his grace the successful completion of this work would not have been possible

TABLE OF CONTENTS

LIST OF FIGURES

LIST OF TABLES

LIST OF SYMBOLS

A	regression constant
B	regression constant
C	soil compaction (Cone Index) (kPa)
C_a	adhesion
C_c	cohesion (*k*Pa).
C_i	initial concentration of ^{137}Cs
C_f	final concentration of ^{137}Cs
$\overline{d}$	mean projected displacement distance in the upslope or downslope direction (m)
D	tillage depth (m)
DD	mean downslope displacement distance of the tracers parallel to the soil surface (m)
D_f	Diffusion coefficient
DM	oven dry soil as percentage of the mass of moist soil collected in trench (kg)
F_n	normal contact force (N)
F_S	frictional force (N)
F_t	tangential contact force (N)
G	slope gradient
H	Brinell hardness number

h height at a given point of the hillslope (m)

k a coefficient (kg m^{-1} $time^{-1}$)

K regression coefficient

H regression coefficient

L length of the step slope measured down the angle β (m)

L_s rate of soil loss (kg m^{-2})

M soil moisture content (% dry basis)

M_s specific mass of the till-layer (kg m^{-2})

N normal force (N)

Q_s flux of soil in the x-direction per unit of the width (kg m^{-1} $time^{-1}$)

$Q_{s.down}$ downslope flux due to downslope tillage

$Q_{s.up}$ upslope flux due to upslope tillage

R enrichment ratio

S speed (km h^{-1})

S.M soil movement (m)

SF speed factor (soil movement predicted by the "speed soil movement model")

t time

T mass of soil translocated per meter width of tillage pass

t_f-t_i final and initial time, separated by n years

U constant

V constant

x distance in the horizontal direction (m)

x	distance in the path of tillage (m)
X	soil movement (m)
Y	soil depth (m)
α	slope angle of original soil surface
μ	coefficient of friction
λ	depth-averaged translocated distance
ϕ	soil angle of internal friction (degrees)
τ	soil shear strength (kPa)
θ	slope gradient (%)
β	slope angle of step
ρ_b	bulk density of the soil (kg m^{-3})
σ_n	normal stress (kPa)
ξ	concentration factor

CHAPTER 1

INTRODUCTION AND OBJECTIVES

1.1 Introduction

Tillage is necessary to provide an optimum environment for seed and plant root development by shearing, loosening, and moving the soil. It is the most energy consuming operation in crop production. In the Prairie region of Canada, about 37.7 million hectares of land are under cultivation. If this land is cultivated to an average depth of 75 mm, nearly 42.5 billion tons of soil are moved in each operation. It is estimated that tillage accounts for about one-half of the energy used in crop production (Kushwaha and Bigsby, 1989). However, not all the energy transferred to soil results in useful work. There is appreciable movement of soil during tillage, of which much is not only redundant but also contributes to soil erosion. There is a lack of experimental data concerning soil movement with currently used tillage tools and particularly the effect of repeated tillage over decades or centuries.

Soil erosion has been known to be a serious agricultural problem for centuries. In fact, when man started to cultivate the soil, erosion of soil by wind and water was accelerated. Erosion adversely affects crop productivity by reducing the availability of water, nutrient, organic matter and restricting rooting depth by depleting the top soil.

Lindstrom et al. (1990) conducted research to calculate the average erosion rate for cultivated soils in the Corn Belt when different tillage practices were used. The study

showed average erosion of 21.50 tonnes ha^{-1} $year^{-1}$ for conventional tillage (fall moldboard, disc) and 8.70 tonnes ha^{-1} $year^{-1}$ for chisel plow with 3.92 tonnes ha^{-1} of residue on the soil surface. The average erosion for no-tillage was 6.50 tonnes ha^{-1} $year^{-1}$ with same amount of residue on soil surface. Soil erosion is an important threat to agriculture and the natural environment, since more than 97% of the world's food comes from the land rather than the water (Pimentel, 1993). Therefore, the control of soil erosion for sustainable agriculture is of a great importance.

In recent years, there has been a growing belief that the use of tillage implements is a major contributor to accelerating wind and water soil erosion. The soil erosion process consists of two principal sequential events: detachment and transportation. In the first event, soil particles are detached from their moorings in the soil mass and made available for transport. In the second event, detached soil particles are transported (Ellison, 1947).

The primary purpose of tillage is loosening of the soil for preparing a good seed bed. The first event that contributes to the erosion process is not only unavoidable, but is necessary to provide desirable soil structure, weed control, water infiltration and incorporation of fertilizers and chemicals. Accompanying this event, the soil is ready for the second event of erosion, the transportation of soil with the tillage tools. The extent of unnecessary soil transportation by tillage tools during tillage practices will affect the rate of soil erosion. On the other hand, considering the high cost of energy, conservation of energy by efficient tillage operations also is of great importance. Therefore, it is important to study soil translocation by tillage tools.

1.2 Objectives

The overall objective of this research was to study soil translocation by tillage tools. The specific objectives were:

- To study the relationship of soil parameters (soil moisture content and degree of compaction) and tool parameters (speed and tool shape) on soil movement and energy usage in tillage.
- To develop a predictive model for soil translocation by tillage tools.

CHAPTER 2

LITERATURE REVIEW

Tillage research is for the most part an empirical science. When there was a need to invert and break apart soil, plows were developed and when there was a need to remove the weeds, cultivators were made. The art of tillage started when cultivation of plants started and the response of plant to certain soil manipulations was noticed. Tillage began as a science when soil conditions and their relation to plant growth became a knowledge. The search for efficient crop production led to investigation of soil response to tillage tools and soil-machine behavior. Diversity of weather conditions and soil properties that have different effects on crop production have made it difficult to establish a classified and overall pattern for this science.

Unsaturated soil can be considered a four-phase system composed of various proportions of water, air, solids, and air-water interface (Fredlund and Rahardjo, 1993). It may have a cohesive component, a load-dependent component, and a strain-dependent component. Existence of these components introduces some difficulties in the study of soil, especially in dealing with soil flow and failure. Some researchers have tried to compare air and aerodynamics with soil and soil dynamics. An airfoil moves through air and a tillage tool moves through soil, but air is a continuous, homogenous medium while soil is non-continuous and non-homogenous. Air particles are much smaller than the air foil moving through them, but soil may contain large aggregates, clods and foreign material whose sizes are large relative to tillage tool size. Thus, explaining soil behavior

is much more complex than that of air. This is why the study of soil dynamics is not as advanced as aerodynamics (Schafer and Johnson, 1982).

Soil erosion models have been developed for designing erosion control systems but these models have not been linked to soil movement by tillage since a model to quantify soil movement by tillage is not available in the literature.

Lobb et al. (1999) studied the soil loss by tillage erosion. It was found that tillage erosivity, the potential for tillage events to erode soil within a landscape, was a function of several physical and human parameters, including: tillage tool shape and arrangement within a tillage implement, tillage implement length and width, tractor-implement match, tillage depth, ground speed, and tillage operator response to varying landscape conditions.

Lobb et al. (1995, 1999) conducted some experiments to determine soil translocation by tillage. Plots of soil in different fields were labeled by Cesium-137 and chloride as tracers and the concentration of the tracers was measured after tillage operations. Distribution of the tracers was used to describe soil translocation by tillage. It was concluded that tillage erosion was responsible for at least 70 % of the total soil lost on the upper slope landscape position based on estimates of total soil loss using resident Cesium-137.

In the model proposed by Lobb and Kachanoski (1997) tillage erosion was calculated as the net translocation at specified points in the landscape, by determining the difference between the soil translocated into a point and the soil translocated out from that point during a single tillage operation. The translocation into and out from a point was calculated from forward and backward differences in topographic conditions.

Therefore, the model predicted soil redistribution from forward tillage translocation along two-dimensional landscape profiles.

Sibbesen et al. (1984) studied the soil movement in one horizontal direction by repeated tillage. They proposed a simple mathematical model to approximate the movement of soil. The model describes the development with time of a concentration substance by means of the solution of a diffusion equation. The model is suitable for use in situations where the same cultivation practices are repeated many times in alternating directions.

Few researchers have studied soil flow path and movement. Nichols and Reed (1934) reported the results of experiments by Ashby on the inversion of the soil and accompanying forward movement during moldboard plowing. Most of the soil movement studies were concentrated on the soil movement by tillage on slopes. Mech and Free (1942) reported high amounts of movement downslope caused by tillage. Chase (1942) noted that a sweep with a larger rake angle increased overall lateral soil displacement. Söhne (1960) studied soil movement perpendicular to the travel direction with a wide tool in high-speed plowing and observed that the magnitude of lateral soil displacement increased with the lateral directional angle at the end of the moldboard. Goryachkin (1968) developed three theories to describe soil flow over inclined tillage tool surfaces by using a trihedral wedge. According to the crushing theory of Goryachkin, absolute soil motion was normal to the tool surface. In lifting theory, it was assumed that the relative position of soil aggregates within the soil slice remained the same. Shearing theory considered that the soil motion was parallel to planes of shear failure in soil and flow path depended on the angle of soil shear failure.

Lindstrom et al. (1990) studied the possibility of soil movement by tillage as a contributing factor to apparent soil erosion present on many ridge tops. Steel hexagonal nuts were used as soil movement detection units by inserting them in the soil at definite places and measuring their positions after tillage. It was concluded that soil movement by tillage, particularly when using a moldboard plow was considerable and slope was an important factor. Hanna et al. (1993a) compared the soil flow path on a sweep with the Goryachkin theory. The conclusions of this study supported the Goryachkin model in identifying rake angle and excluding speed and depth as factors influencing soil flow path.

2.1 Soil Movement Models

Little information is available in the literature about soil movement models. Most of the soil movement studies have been conducted on slopes, and the models developed are related to slope, rather than the effect of tillage tool design factors, operating conditions, and relation to some physical properties.

2.1.1 Soil movement models in manual tillage

Turkelboom et al. (1996) in their studies on tillage erosion rates, used three complementary methods for measuring soil flux in manual tillage: the tracer method, the trench method, and the step method.

Tracer method In the tracer method, white painted stones were placed randomly in a 200 mm narrow furrow below a reference line, and the furrow was refilled with soil. The tracers were inserted in four strips of 1 m wide on six transects. On each strip, 10 holes of 300 mm deep were drilled at approximately 100 mm intervals. One tracer was inserted in

each hole and its location was recorded. A certain amount of fine, white sand was poured in the hole, filling the hole over 60 mm, and the next tracer was placed. This was repeated until the hole was completely filled. It was assumed that the movement of stones was similar to soil clods and would be a representative indicator of soil movement. Average tillage depth and the displacement distances of the tracers were measured. Since the experiment was carried out on a slope, the tillage depth was measured vertically in the field, and transformed to tillage depth perpendicular to the soil surface by multiplying by the cosine of the slope angle. The mass of soil that passed a unit contour length for one tillage pass was called "soil flux". The flux of soil was calculated using the following equation.

$$\text{Soil flux (kg m}^{-1} \times \text{tillage pass)} = DD \times D \times \rho_b \qquad (2.1)$$

where :

DD = mean downslope displacement distance of the tracers parallel to the soil surface, (m)

D = mean tillage depth measured perpendicular to the soil surface (m)

ρ_b = dry bulk density of the soil (1100 kg m-3)

Trench method In the Trench method, a trench four meters long and half a meter deep was dug at the bottom of each plot and lined with a plastic sheet to measure soil flux directly. The soil flux was measured by Equation 2.2.

$$\text{Soil flux (kg m}^{-1} \times \text{tillage pass)} = \frac{M.DM}{W} \qquad (2.2)$$

where

M = mass of moist soil collected in trench (kg)

DM = oven dry soil as percentage of M (87-90%)

W = observation width (4 m)

Step method Appearance of a small step at the top of the plot is an indicator of soil movement by manual tillage. At this place, soil was moved downwards but not replaced by any soil from the further upslope. It was assumed that the volume of this scar should correspond with the amount of soil moved into the trench at the bottom of the plot. The soil flux was calculated using Equation 2.3.

$$\text{Soil flux (kg m}^{-1} \times \text{tillage pass)} = \frac{\sin(\beta - \alpha) \times \sin\beta \times L^2 \times \rho_b}{\sin\alpha \times 2} \qquad (2.3)$$

where

α = slope angle of original soil surface

β = slope angle of step

L = length of the step slope measured down the angle β (m)

ρ_b = dry bulk density of soil (1100 kg m^{-3})

The soil flux measured for one tillage pass ranged from 39 to 87 kg m^{-1} depending on slope. For slopes less than 60%, the soil flux did not change substantially with slope. For slopes more than 60 to 82%, the soil flux was increased due the rolling of the clods downhill once the angle of repose has been exceeded.

The result of experiments by using the above methods showed that the tracer method and the step method gave very similar results. The step method followed a linear trend, while the tracer method showed a slightly exponential relationship. The trench method was supposed to provide more accurate results since in this method the

transported soil was collected directly. On the contrary, it showed much smaller soil flux values with a slightly increasing soil flux with increasing slope. The reason given for underestimation of soil flux was formation of a physical barrier hampering free tillage on plastic lined trenches. The step method was suggested to be accurate and fast. The tracer method is slightly more accurate but more time consuming.

2.1.2 Soil movement models in tillage with machinery

Continuity equation model Sibbesen et al. (1984) introduced a simple mathematical model for approximating soil movement in horizontal dimension by repeated tillage with one or more tillage tools in alternating directions. The model used the solution of a diffusion equation to describe the development with time of a concentration gradient of a substance. It was assumed that the soil was distributed according to a diffusion equation with a diffusion coefficient D_f. The soil was labeled with ^{32}P along an infinitely long vertical plane. The initial concentration of the labeled soil considered 1 in the plane at x = 0 and 0 at any distance x from the plane. After n tillage operations across the plane, the concentration C_o of the labeled soil at any distance x from the plane was given by the following equation:

$$C_o = C(x,n) = \frac{1}{\sqrt{4\pi D_f n}} \exp\left(-\frac{x^2}{4D_f n}\right) \tag{2.4}$$

A Gaussian normal distribution with mean $\mu = 0$ and the variance $\sigma^2 = 2D_f n$ gives the probability of finding a labeled soil particle. Hence, the average distance the labeled

particles were transported after n tillage operation is $\sqrt{4D_f n/\pi}$. Equation 2.4 implies that the distribution of labeled soil is symmetrical around x = 0.

A term z (positive or negative) was introduced to account for a systematic displacement of the distribution from operation to operation or from year to year.

$$C_o(x,n) = \frac{1}{\sqrt{4\pi D_f n}} \exp\left(-\frac{(x+z)^2}{4D_f n}\right) \tag{2.5}$$

Govers et al. (1994), using the experimental data with a moldboard and a chisel plow and those available in literature, proposed a universal approach to the modeling of soil redistribution by tillage. Soil redistribution was described by a diffusion-type equation and tillage redistribution intensity was characterized by a single number called the diffusion constant. This value is associated with slope gradient coefficient. This coefficient varies between 100 and 400 kg m^{-1} $year^{-1}$. To measure soil movement, numbered plastic spheres with a metal core and diameter of 15 mm and density of ≈1750 kg m^{-3} were used as a tracer in a variable textured soil ranging from silty loam to loamy sand. The tracers were inserted in four strips of 1 m wide on six transects. On each strip, 10 holes of 300 mm deep were drilled at approximately 100 mm intervals. One tracer was inserted in each hole and its location was recorded. A certain amount of fine, white sand was poured in the hole, filling the hole over (≈60 mm) and the next tracer was placed. This was repeated until the holes were completely filled. After a tillage operation, the new locations of the tracers were recorded and the mean projected displacement distances were calculated. It was found that the mean projected displacement distance was

significantly related to slope gradient. Soil redistribution by tillage on a hillslope section of infinitesimal length and unit width was described by the continuity equation:

$$\rho_b \frac{\partial h}{\partial t} = -\frac{\partial Q_s}{\partial x} \tag{2.6}$$

where :

ρ_b = bulk density of the soil (kg m^{-3})

t = time

h = height at a given point of the hillslope (m)

Q_s = flux of soil in the x-direction per unit width (kg m^{-1} $time^{-1}$)

X = distance in the horizontal direction (m)

The displacement distance is a function of slope gradient and can be calculated by:

$$\overline{d} = K + HG \tag{2.7}$$

where:

$\overline{d}$ = mean displacement distance in the up- or downslope direction per tillage operation (m)

G = slope gradient (tan). Positive when tractor movement is upslope, negative when it is downslope.

K, H = coefficients, obtained by regression analysis

Considering the downslope direction as the positive direction for the x-axis, the flux per unit width per tillage operation corresponding to a given mean displacement distance is:

$$Q_{s.down} = \rho_b \overline{d}_{down} D \tag{2.8}$$

for movement in downslope direction, and

$$Q_{s.up} = -\rho_b \bar{d}_{up} D \tag{2.9}$$

for movement in the upslope direction.

where:

D = tillage depth (m)

$Q_{s.down}$ = downslope flux due to downslope tillage (kg m^{-1} $time^{-1}$)

$Q_{s.up}$ = upslope flux due to upslope tillage (kg m^{-1} $time^{-1}$)

Considering one tillage operation per year, the average net downslope flux per unit width per year for a given transect perpendicular to the slope will be

$$Q_s = \frac{Q_{s.down} + Q_{s.up}}{2} \tag{2.10}$$

or

$$Q_s = \frac{D\rho_b(\bar{d}_{down} - \bar{d}_{up})}{2} \tag{2.11}$$

as, on a single transect

$$G_{down} = -G_{up} = \frac{\partial h}{\partial x} \tag{2.12}$$

The net soil flux on a single transect, due to a single tillage operation can be determined by calculating the average of the flux during the up and downslope movement of the tracer. The flux during upslope movement is considered negative.

$$Q_s = \frac{D\rho_b[(K + HG_{down}) - (K + H(-G_{down}))]}{2} \quad (2.13)$$

i.e.

$$Q_s = D\rho_b HG_{down} \quad (2.14)$$

Q_s will be positive as both H and G_{down} are negative. The analysis is valid for across-slope tillage, provided that the soil is thrown upslope and downslope in alternate years. The average downslope flux must be calculated by taking into account the average flux over two consecutive tillage operations.

Based on Equation 2.14, the net flux due to tillage may be written as:

$$Q_s = -k\frac{\partial h}{\partial x} \quad (2.15)$$

where:

k = a coefficient (kg m^{-1} $time^{-1}$)

$$= -D\rho_b H \quad (2.16)$$

If several tillage operations are carried out in one year, then the value of k may be calculated on a per tillage operation basis and then summed to obtain a yearly value. Second order effects due to small changes in slope after each tillage operation are ignored. Using Equation (2.15), Equation (2. 6) may then be rewritten as:

$$\rho_b \frac{\partial h}{\partial t} = k\frac{\partial^2 h}{\partial x^2} \quad (2.17)$$

which is a diffusion-type equation. The intensity of a diffusion-type process may be characterized by a single constant k, the diffusion coefficient. Using finite difference approximation and yearly time units, the equation (2.17) may be solved. The value of k is representative of the yearly soil movement by tillage.

Lobb and Kachanoski (1996) in their study on the impact of tillage translocation and tillage erosion on the estimation of soil loss using Cesium-137, found that significant amounts of soil were redistributed within topographically complex landscapes by tillage erosion. Soil was translocated, or displaced in excess of 3 meters during one sequence of tillage. Tillage was simulated on a hypothetical landscape for 10 sequences of conventional tillage (moldboard plough, two passes of tandem disc, and C-tine cultivator) in one direction. The redistribution of the soil within the till-layer during translocation was approximated by:

$$T = \frac{M_s}{\lambda e^{\frac{x}{\lambda}}} \tag{2.18}$$

where:

T = mass of soil translocated per meter width of tillage pass (kg m^{-1})

M_s = specific mass of the till-layer (kg m^{-2})

λ = depth-averaged translocated distance (m)

x = distance in the path of tillage (m)

The redistribution of soil within the landscape was approximated by:

$$T = 116 + 6.5\,\theta \tag{2.19}$$

where θ is the slope gradient (%).

Data from Lobb et al. (1995) were used to estimate the parameters of Equation (2.18) and (2.19). The initial Cesium-137 concentration was 3000 Bq m^{-2} with no additions due to atmospheric deposition and no losses due to radioactive decay. Tillage depth was spatially and temporally uniform at 0.2 m, and soil bulk density was spatially and temporally uniform at 1500 kg m^{-3}. Actual soil loss was compared to that estimated using Cesium-137 concentration and Equation (2.20) (deJong et al., 1983) and Equation (2.21) (Walling and Quine, 1990; Kachanoski, 1993).

$$L_s = M_s \frac{(C_i - C_f)}{\frac{C_i}{(t_f - t_i)}} \tag{2.20}$$

$$L_s = \frac{M_s}{R(1-\frac{C_f}{C_i})^{\frac{1}{n}}} \tag{2.21}$$

where

L_s = rate of soil loss (kg m^{-2})

C_i and C_f = initial and final concentration of Cesium

t_f-t_i = final and initial time, separated by n years

R = enrichment ratio (assumed to be 1.0)

Some researchers in studies not related directly to soil movement, have developed some methods that can be considered in soil translocation measurements. Plante et al. (1998) developed a tracer method for studying soil aggregate dynamics. Labeled tracer particles were used to study the incorporation and release of soil particles as aggregates form and degrade, to obtain an indication of the dynamics of aggregates. They used the

findings of Staricka et al. (1992) to use a ceramic material as a tracer. The ceramic tracers are manufactured by Kinetico Inc. (MN, USA) under the tradename Macrolite. A powerful detection instrument, INAA (Instrumental neutron activation analysis) was used in the process. A sample was bombarded with neutrons and the γ-ray spectrum produced was measured as the induced radionuclides decay. The University of Alberta SLOWPOKE II reactor was used as the neutron source. Dysprosium (Dy) was selected as the label and therefore the tracer sphere detection was by measurement of Dy content of samples. Although the developers believe that the method is simple and effective and can be used in studies of soil mass transport by tillage, their technique does not seem to be easily applicable because of the complex instrumentation and the expenses involved.

Boyd and Windisch, (1966) used Cine' Flash x-ray technique to determine the deformation characteristics occurring in the soil mass under a given loading condition as a function of position and time. Markers were made from a composition of 94% lead and 6% Antimony in the form of a three dimensional cross with six orthogonal arms each of length 3 mm, giving a maximum dimension of 7 mm. This shape and size made it possible to measure translational and rotational movements of the marker. Markers were buried in the soil at a depth of 38 mm below the soil surface and the translations, rotations, and velocities of them relative to depth and the wheel position at any instant were measured by using X-ray pulses. The major limitations of this method is that it requires extensive radiation screening for the safety of the operator and high operating cost of X-ray Cine' Photography.

2.2 Soil Bin Experiments

Soil bins generally have two major components. A bin that contains the soil required for the experiments and a fixture that holds the tool and transducers used for measuring required parameters. There are two basic types of soil bins. In one design the tool carriage moves while the soil is in a stationary bin. In other type of soil bins, the tool fixture remains in a fixed position, while the bin moves on guide rails. Each has been used for many years by Army Mobility Research Center, US Army Engineers Waterways Experiment Station, Deere and Company Technical Center, Iowa State University, and the National Soil Dynamics Laboratory. There are a lot of advantages in using soil bins. Soils with different physical properties could be used in one location for different experiments. The soil in the bin could be cleaned of stones and foreign materials to provide a more precise research medium compared to field soil. Soil bins provide the opportunity of carrying out experiments under a controlled environment in all seasons. They provide an excellent tool-soil relative position. Compared to field experiments, better data acquisition and control system could be used. Soil bins are widely used in studying soil-machine relations.

In spite of their enormous advantages, there are some problems in using soil bins that should be taken into account. Soil bins are practically limited to remolded soil conditions. Another limitation is the possibility of stress-strain distortion due to the close proximity of the sides and bottom. Depending on the place of a soil bin in a building, air flow through the air conditioning system of the building may cause differential drying across the soil surface. One of the problems in a soil bin is that the soil preparation operations that run the length of the soil bin may leave invisible bands of soil with low

penetration resistance. There are usually differences in the vertical profile. It is impossible to reproduce exact soil conditions on a regular basis. Excessive soil working often destroys the soil structure. Soil should not be worked at high moisture content where structural damage usually occurs. Soil reconditioning operations should be devised and executed to counter the structural degradation that accompanies severe soil handling operations Chancellor (1994).

CHAPTER 3

SOIL PROPERTIES AND SOIL DYNAMICS

3.1 Overview

Soil particles are not strongly bonded together in the way that the crystals of a rock are. Soil particles are relatively free to move with respect to one another, although not as freely as fluid particles. That is why studying soil behavior can not be done completely through the science of solid mechanics and fluid mechanics. If a force is applied to soil, contact forces develop between adjacent particles as shown in Figure 3.1. For convenience, the contact forces are resolved into normal (F_n) and tangential components (F_t). These contact forces deform the particles. Deformation of particles may lead to bending, crushing, enlarging the contact surface, etc. When the shear stress at the contact becomes larger than its shear resistance, relative sliding between particles occurs. The overall strain of the soil mass is the result of deformation of the individual particles and their relative sliding. Since the sliding is a nonlinear and irreversible deformation, the strain-stress behavior of soil will be strongly nonlinear and irreversible. To understand soil behavior it is necessary to study the phenomena at the contact points and the related parameters like friction and adhesion. The number of contact points in a soil mass are extremely high. For example, there are about 5 million contacts within 1 cm^3 of fine sand (Lambe and Whitman, 1969).

Even if the particles behavior at contact points is understood, it is impossible to construct the stress-strain law for soil from the contact points behavior. However, since the soil resistance to deformation is strongly dependent on the shear resistance at contact between particles, the knowledge of the possible magnitude of this shear resistance and of the factors affecting it is important. Another parameter that has some influence on soil shear resistance is cohesion of soil, which strongly depends on interlocking of the particles or the packing density.

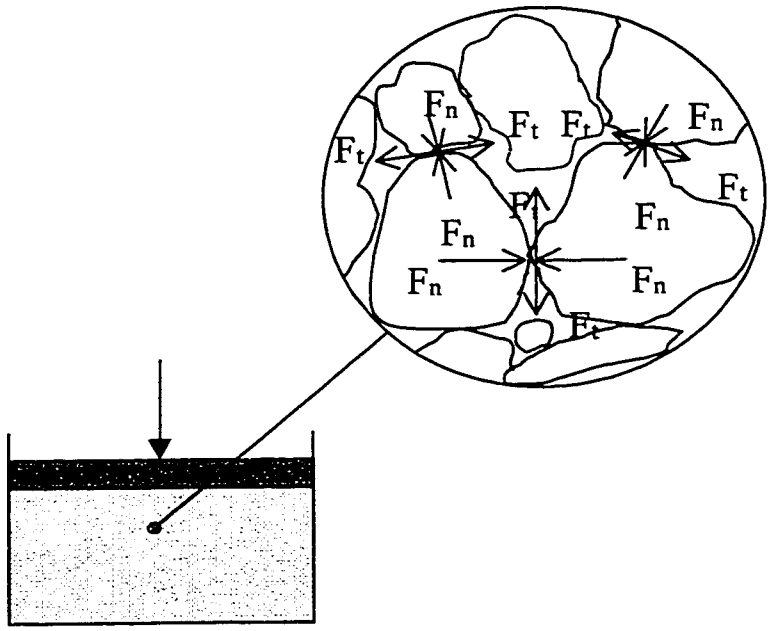

Fig. 3.1 Schematic representation of force transmitted through soil.

3.2 Shear Strength Mechanism

Attractive forces between soil particles and chemical bonds at points of contact of the surfaces are the sources of shear resistance in soil particles. The number of bonds at the interface between particles is influenced by the physical and chemical nature of the

surfaces of the soil particles. Total shear resistance is proportional to the normal force that is pushing the two particles together. Part of the total shear resistance is independent of the normal force pushing the particles together. It comes from cohesion between soil particles. Soils, containing a mixture of fine and coarse particles that are partially saturated with water, have cohesive and frictional shear strength properties. The maximum shear strength for this soil is given by Equation 3.1, which is often referred to as the Mohr-Coulomb equation in classical soil mechanics (Fredlund and Rahardjo, 1993).

$$\tau_{max} = C_c + \sigma_n \tan \phi \qquad (3.1)$$

where:

τ = soil shear strength (kPa),

σ_n = normal stress (kPa),

ϕ = soil angle of internal friction (degrees),

C_c = soil cohesion (kPa).

Saturated, fine grained soils are examples of cohesive soils that exhibit negligible friction and have almost constant shear strength regardless of normal total stress on the failure plane. The shear strength of these soils comes from the soil cohesion, the part of shear strength which is independent of normal stress and is calculated by the following equation.

$$\tau = C_c \qquad (3.2)$$

Dry sand exhibits negligible cohesion and is regarded as a purely frictional material. Depending on the density and the properties of its particles, the angle of internal friction, ϕ for dry sand ranges from 18 to 55 degrees (McKyes, 1989). The shear strength of the cohesionless soil is governed by:

$$\tau = \sigma_n \tan \phi \tag{3.3}$$

It should be noted that the Equation 3.1 does not represent shear yield in all soil conditions and does not contain any information about soil behavior prior to shear failure. Soil cohesion (C_c) and soil angle of internal friction (ϕ) are usually referred to as real physical properties of soil. In reality, soil cohesion (C_c) and soil angle of internal friction (ϕ) are only parameters of the assumed yield equation. Their logical existence can be explained only by an interpretation of the equation and not from the physical nature of the soil itself (Gill and VandenBerg, 1968).

3.2.1 Angle of internal friction of soil (ϕ)

The sum of the total energy required to overcome interlocking of particles, their sliding and rolling in the soil mass constitutes total frictional energy and is expressed by ϕ, the angle of internal friction. Angle of internal friction (ϕ) is affected by soil porosity, moisture content, normal stress, and grain size distribution. In general, a decrease of soil porosity and normal stresses increase the angle of internal friction. Time rate of shear strain has no effect on angle of internal friction. Angle of internal friction (ϕ) also depends on the nature of the surfaces of the contact points. In sands, all the shear resistance is due to friction, rolling and interlocking of particles. The angle of internal

friction of sands depends on a large number of variables. For example, the smaller the void ratio or the larger the relative density, the larger the value of the angle of internal friction is. Sands with sharp edge particles have a greater angle of internal friction than those with round edge particles. Well-graded sands have a larger angle of internal friction compared to uniform sands. In an unsaturated agricultural soil, angle of internal friction varies from 25° for moist, loose, fine textured soils to about 45° for dry, dense, coarse textured soils (Koolen and Kuipers, 1983).

3.2.2 Cohesion (C_c)

The nature of soil cohesion is not fully understood. It may be considered as the strength of the soil that does not depend on the applied force. Based on cohesional properties, clay soils are termed "cohesive" soils and soils like sand and gravel are considered "frictional" or "non-cohesive" soils. Soil cohesion, generally increases logarithmically with soil density.

3.2.3 Soil moisture

Soil moisture influences soil behavior and the soil condition produced by a tillage tool. For many soils, the coefficient of friction increases with an increase in soil moisture up to an intermediate value and then decreases. Although Kuiper and Kroesbergen, (1966) reported decrease of soil cohesion with increasing soil moisture content, Chancellor (1994) noted that the soil cohesion (C_c) increases with moisture but it is maximum at some intermediate level. It is more noticeable in fine-grained soils than coarse-grained. When soil moisture content increases from low to medium values, the soil to metal bonding that depends on soil moisture tension increases and as a result

adhesion C_a increases. At higher soil moisture contents, positive pore pressure develops in soil under load and tension decreases which, in turn, results in decrease of adhesion and an increase in the lubrication effect of moisture. An increase in moisture content of cohesive soils reduces the coefficients of friction and adhesion (Neal, 1966).

3.2.4 Soil compaction

When a tillage tool starts to move in the soil, crushing of soil aggregates occurs. Soil particles then try to rearrange themselves. This rearrangement decreases the porosity and pushes out some of the air in the soil. Some of the soil water may also be squeezed out. Some of the air in the soil is sealed by water and can not escape. Further movement of the tool compresses the entrapped air in the soil pores. This results in the reduction of the soil volume in front of the tool. As soil becomes more dense and the porosity decreases, adhesion increases, but the coefficient of friction is not much affected by change in soil porosity (Chancellor, 1994).

Cone Penetrometer Cone penetrometers have been used for evaluating soil properties for many years. It is a pointed device that is pushed into the soil and the force required to overcome the penetration resistance is measured and divided by the base area of the cone which forms the point of the device. The specification of the most common design used in agricultural applications is specified by ASAE standard: ASAE S313.1 (ASAE, 1984). The penetrometer has a polished steel cone with a 30-degree included angle at the tip and a 3.23 cm^2 base area. Based on the above mentioned standard, the rate of insertion is 1.83 mm/min. The penetration resistance force depends on the cone base area, tip angle, soil-cone friction angle, soil properties and penetration velocity. The dependency of

penetration resistance on soil properties is determined by soil type, soil compaction, soil moisture content, and soil structure. Its ease of use and rapidity to make several measurements in a short time has made it one of the most frequently used devises in comparative soil property measurements.

If one type of soil is considered, cone resistance varies with cohesion and angle of internal friction. (Koolen and Kuipers, 1983). For a given cone it can be expressed as:

$$CI = f(\text{cohesion } (C_c) \text{ and angle of internal friction}(\phi))$$

The function can be determined through experiments and can be used to determine C_c (or ϕ) by a cone penetrometer if ϕ (or C_c) is known from another source. Cone resistance can also be expressed as a function of soil physical properties. For a given cone:

$$CI = f(\text{moisture content, compaction, soil type, and soil structure})$$

In this function it is difficult to quantitatively express soil structure. In experiments with artificially prepared soil, it is often acceptable to neglect soil structure as a factor. For one type of soil, the CI will become dependent on soil moisture and soil compaction.

$$CI = f(\text{moisture content, compaction})$$

This function can also be determined by experiments. By using the result of the experiment, the cone penetrometer can be used to determine the moisture content of the

soil under the same compaction level. It can also be used to measure compaction level of the soil under the same moisture content.

3.2.5 Soil-tool friction

When a soil mass moves relative to or in contact with another material such as tillage tool or another soil mass, frictional forces are developed. Coulomb friction is defined as:

$$\mu = F_s / N \tag{3.4}$$

Or in per-unit area terms:

$$F_s / A_r = \tau = \mu N / A_r = \mu \sigma_n \tag{3.5}$$

where:

μ = coefficient of friction

F_s = frictional force tangent to the surfaces required to produce sliding

N = normal force perpendicular to the surfaces of the materials

σ_n = normal stress

τ = shear stress

A_r = area of mutual contact

The coefficient of friction between soil and the tool surface depends largely on tool surface roughness. A tillage tool with a rusted steel surface may have a coefficient of friction as high as soil internal friction (Koolen and Kuipers, 1983). Soil moisture also affects soil-tool friction. At high moisture content, soil water may act as a lubricant and

lower the friction. The moisture range where this occurs is known as the lubricative phase of soil friction.

Sometimes the shear stress in the soil and tillage tool interface is so high that sliding of soil on the tool surface will not occur, and shear planes are formed in the soil body. This happens when the sliding resistance is greater than the soil internal strength. Shear stresses between the soil and tool just before the movement is static friction and differs from the shear stresses after the start of the movement, which is dynamic friction. Nichols (1931) found the static coefficient of friction before movement for steel and dry sand to be 0.26. The coefficient of dynamic friction after the start of the movement was found to be 0.23. This change in coefficient of frictions could be attributed to the change in soil particle arrangement, position, and water tension.

The value of μ varies with soil condition, soil type, and type of tillage tool surface material. The value of μ for soil on steel ranges from 0.2 to 0.7 (Schafer and Johnson, 1982). Value of μ must be measured for each situation since a predictive model relating it to factors like soil condition, soil type, and tillage tool surface material has not been fully developed. Koolen and Kuipers (1983) proposed an equation for determination of coefficient of friction of soil with steel of various levels of hardness.

$$\mu = 0.37 - 0.00015\ H \tag{3.6}$$

where:

H = Brinell hardness number

The Brinell hardness number for very hard tempered steel is 650 and for low carbon steel is 125. Nichols (1931) suggested an equation for calculating the coefficient of friction of soil on steel for small sliding paths based on soil texture.

$$\mu = U + V \times (\text{percent of clay content in soil}) \qquad (3.7)$$

where U and V are arbitrary constants.

When the clay content is less than 32 percent, U and V are considered 0.23 and 0.005 and when it is more than 32 percent, U and V are 0.37 and 0.0 respectively. Zhang et al., (1986) in a study with soils of up to 45% clay content, found that the coefficient of friction increased with increase of clay content above the level suggested by equation (3.6). This shows that the fine textured soil have a higher coefficient of friction compared to coarse textured soils (Koolen and Kuipers, 1983).

There is disagreement between researchers who have studied soil-metal friction. Stafford and Tanner (1983) studied the effect of sliding speed on the soil-metal friction of a clay and a sandy loam soil on mild steel. It was found that the friction angle increases logarithmically with sliding speed over a wide range of soil moisture content and tool speed, but Payne (1956) reported that soil-metal friction is independent of speed at low normal stresses (maximum 20 kPa). Nikiforov and Bredun (1965), in their study on moist soil and very low normal stress (maximum 25 kPa), noted a decrease of friction angle with speed in the range of 1-5 m s^{-1}.

3.2.6 Adhesion (C_a)

Adhesion is the tension force required at the mutual contact surface of two rigid bodies to separate them. It is the result of bonding forces between the soil and other materials. Adhesion decreases with increasing speed and increases with moisture content for clay soil (Stafford and Tanner, 1983). Adhesion of the soil to tillage tools causes a normal force on the contact surface. Since the frictional force is a function of the normal load, adhesion increases the frictional force. Equation (3.5) has been modified to include adhesion.

$$\tau = \mu \sigma_n + C_a \tag{3.8}$$

where C_a is the adhesion.

3.3 Soil-Tool Interaction

To study soil-tool interaction, it is important to have a fundamental understanding of the soil failure and the factors affecting it. Tillage tool geometry and soil properties and conditions must be considered in any soil-tool interaction studies.

State properties have been used to describe a soil without any reference to its intended use. On the other hand, behavioral properties describe the reaction of a soil to an applied force system. Although it is possible sometimes to relate behavior of a material to its state properties, the state properties may not rationally describe the material behavior. A tillage tool applies force to the soil and moves the soil and changes its condition. So, to describe the soil reaction to tillage tools, its behavioral properties should be considered. State properties have been probably used because of their ease of quantification (Gill and

Vanden Berg, 1968). Many experiments have been conducted to study soil-tool interaction. Since soils are composite materials, their behaviors are not easy to explain. They may have elastic, plastic, viscoelastic, viscoplastic, and elastoplastic characteristics.

Passive earth pressure theories for retaining walls and bearing load for footings have been used by most researchers in explaining the soil failure by tillage tools. For these, they have assumed that the yielding of soil in shear obeys the Mohr-Coloumb criterion and distinct rupture surfaces form in front of the tillage tools. During the interaction of tillage tool with soil, complex stresses will develop in soil, which go above the elastic limit. They reach a maximum value in the range of soil plastic deformation. When this stress exceeds the shear strength of the soil, shearing of soil occurs and one part of the soil slides over the other parts. The fracture surface is not satisfactorily defined yet, but it is known that the failure pattern is successively generated ahead of the tillage tool. Initial failure surface is suddenly created with soil moving vertically upward, propagating cracks in soil mass that may extend to the soil surface. The tool body may cause secondary failure in the already failed soil mass.

Some researchers believe that agricultural soil fails by mechanisms that are different from simple shear (Rajaram and Oida, 1992). Depending on tool shape and soil condition any combination of shear, bending, tensile, compression, and soil flow may exist.

3.4 Soil Failure

In tillage operations, boundary surfaces develop between adjacent soil bodies and also between soil and the tillage tool surface. In general, there is stress acting across the surface element between two bodies. The tangential component of that stress is the shear

stress due to friction at surface element (Koolen and Kuipers, 1983). If a small shear stress is applied, a small relative movement will occur. Application of a greater shear stress initiates a relative movement that continues. If a so-called soil wedge sticks to the tool surface or if a thin layer of soil adheres to the tool surface because of surface roughness, or soil properties, smaller relative movement will occur.

Most of the soil failure studies have been conducted on soil failure with narrow tillage tools. Different two and three dimensional soil failure models have been introduced to describe the failure characteristics of soil by narrow tillage tools.

3.4.1 Two-dimensional models

Terzaghi's passive earth pressure theory was used to develop a two-dimensional soil-cutting model by wide blades. It was assumed that a failure zone exists in front of a cutting blade and the soil in the failure zone was in the critical failure state. (Kushwaha et al., 1993).

3.4.2 Three-dimensional models for narrow tools

Some researchers introduced three-dimensional models for soil cutting with narrow tillage tools. Payne (1956) was the first who introduced a three-dimensional model for soil failure in front of a narrow tool. The failure zone in this model consisted of a triangular center wedge, a center crescent, and two side blocks.

The O'Callaghan and Farelly model (O'Callaghan and Farelly, 1964) consisted of a forward failure above the critical depth and a horizontal failure under the critical depth. The critical depth was considered to be equal to tool width for a smooth blade and half its

width for a free surface with a normal restraint. Their model did not consider the effect of adhesion and friction between soil and tillage tool.

Hittiaratchi and Reece (1967) also proposed a three-dimensional model. The failure zone in their model was divided into forward failure, ahead of the soil-tool interface, and transverse failure, horizontal movement away from the centerline. The model considered the soil properties, tool geometry, and soil-tool properties.

Godwin-Spoor model (Godwin and Spoor, 1977) included two separate failure patterns, one three-dimensional crescent failure above the critical depth, and two two-dimensional lateral failure below the critical depth. The three-dimensional crescent failure was like a parallel center wedge flanked with two curved side crescents. The lateral failure zone below the critical depth was similar to the Hettiaratchi-Reece and O'Callaghan-Farelly models.

McKyes and Ali (1977) proposed a model that consisted of a failure wedge with plane bottom surface, ahead of the cutting tool and two side crescents with a straight line at the bottom.

In the Perumperal-Grisso-Desai model (Perumperal et al., 1983), the side crescents flanking the center wedge were replaced by a set of two forces acting on the center wedge.

The above mentioned models are static models and do not consider the effect of tool travel speed. Sweek and Perumperal (1988) introduced a dynamic model by considering the tool travel speed. The failure zone consisted of a center wedge and two side crescents with a straight rupture plane at the bottom. Zeng and Yao (1992) developed another dynamic model. The failure zone was similar to McKeys-Ali model.

The model included the acceleration, dumping effect, and the relation between soil-metal friction and sliding speed. Several other researchers proposed a number of models to use FEM analysis of soil tillage process.

In all analytical models a failure zone was assumed, and some simplification of the failure zone such as circular side crescents, and straight bottom rupture plane have been made to develop the force equations. The accuracy of the results with these models depends on the closeness of the assumed failure zone with the developed failure zone under the influence of soil condition and tool shape.

3.5 Tool Shape

Tool shape influences the stress distribution in soil and is an important factor in the tillage process. It determines the path of soil particle flow with respect to the tillage tool. Depending on the shape of the tillage tool and soil condition, the tool may slide through the soil like a knife without soil sticking to its surface. Here the soil to metal friction becomes the main factor in describing the soil-tool interaction. It may create a compacted soil body sticking to the tool surface which becomes a part of tool and soil to soil friction becomes mainly active in explaining the soil-tool interaction. As the shape of the tool face approaches the soil body, the tendency for soil to slide on the tillage tool increases and as a result the frictional resistance decreases, and the force required to move the tool in soil decreases. According to Zelenin (1950), the compacted core appears when the angle of face exceeds 50° (Figure 3.2).

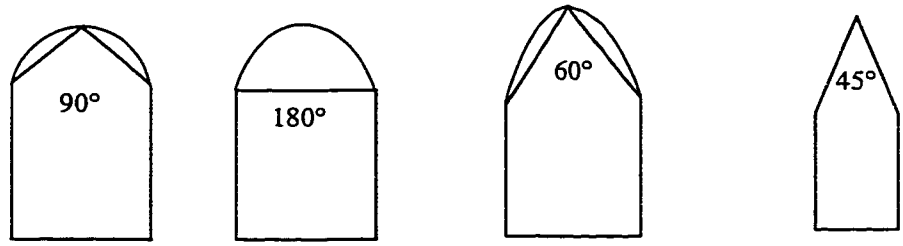

Fig. 3.2 Effect of the form of the tool face on the form of the dense core in a cohesive soil (from Zelenin et al., 1950).

3.6 Tool Operational Speed

The idea of increasing the tool speed to increase the capacity is an acceptable one since increasing the speed, increases the output of the tool without adding much to the size and weight of tractors. The major limiting factor is an increase in draft due to an increase in speed. Several researchers have studied the relationship of draft and speed. They reported that the draft increases linearly with increased tool travel speed for most of tines and soil cutting tools, and with the square of the speed for moldboard plows, disc tools and sub-soilers in the normal range of operation (2-10 km h^{-1}). For higher speeds of operation (10-55 km h^{-1}) the rate of increase in draft decreases with increase in speed. Above the speed of 55 km h^{-1} the rate of draft increases again. It is generally accepted that as the velocity of tillage tool increases the resistance to motion increases. However, this is true up to a certain level. Increasing tool operational speed increases the soil movement. Motion of soil particles during tillage is the result of two motions, a motion with the tillage tool and a motion relative to tillage tool. A particle with a longer flow path over the surface of the tillage tool needs more time to travel along its flow path, and consequently will be dragged over a larger distance.

3.7 Summary

The process of soil movement by tillage tools is a complicated process. Since the number of the factors affecting the soil movement is large, determination of soil movement by tillage tools becomes a difficult task. Some of the soil parameters like soil cohesion and soil angle of internal friction affect soil shear strength that is an important factor in soil movement. In studying soil movement by tillage tools some other factors play important roles. Factors affecting the soil-tool interaction such as soil moisture, soil compaction, tool operational speed, and tool shape are also important. Effects of all these factors and their interactions on the soil movement create a complex process that can not be analyzed with conventional methods. The effects of some of these factors on soil movement can not be calculated separately. There are also disagreements between researchers on the effects of some of soil parameters and their interaction as mentioned in Section 3.2.3.

The process of soil movement by wide tillage tools, like sweeps is different from narrow tools since in wide tools, the soil must pass over a larger surface area of the tool surface and that is why tool surface roughness becomes important. Narrow tools like knife openers will slide through the soil and unlike wide tools they have comparably less interaction with the soil. Tool shape determines the path of flow of soil particles around the tool. While moving through the soil some of the tool shapes create a compacted soil body that attaches to the soil and changes the tool shape. This phenomena changes the nature of the friction to soil-soil friction from tool-soil friction. The compacted soil body will not develop in front of the tool shapes with tip angles of the less than 50° degree. Generally speaking, increasing tools operational speed increases the soil movement.

CHAPTER 4

SOIL MOVEMENT WITH WIDE AND NARROW TOOLS

4.1 Overview

Different methods that were used by the researchers to quantify soil movement were explained in Chapter 2. One of the widely used methods is the "tracer method". In this method a tracer is placed in the soil and after running the tillage tool in the soil, the position or concentration of the tracers are measured. New positions or concentration of the tracers are correlated to the soil movement. White painted stones, steel hexagonal nuts, ^{32}P, Cesium-137 and chloride are some examples of the tracers used in soil movement measurement experiments. The tracer method was selected for this study and plastic blocks with density nearly equal to that of soil (1.2 Mg m^{-3}) were used as the tracer. This study was conducted on a narrow tillage tool (knife opener) and a wide tillage tool (sweep) in the soil bin facilities of the Department of Agricultural and Bioresource Engineering, University of Saskatchewan. Depth of tillage was measured to be 75 mm.

4.2 Materials and Methods

In this part of the study, the forward movement of soil and the furrow profile was measured with the following factors:

1- Tool shapes (Figure 4.1)

- 300-mm wide bent shank Sweep (McKay 50-12K)

- 14-mm Knife opener (Conserva Pac)

2- Speed

- 5.0 km h^{-1}

- 6.5 km h^{-1}

- 8.0 km h^{-1}

3- Soil condition

- Three moisture contents

  - Low (10-11 %)

  - Medium (13-13.5%)

  - High (15-16 %)

- Three compaction levels

  - Low

  - Medium

  - High

To determine soil movement, plastic blocks (15 x 15 x 11mm) with density nearly equal to that of soil (1.2 Mg m^{-3}), were placed in a vertical slot prepared perpendicular to the direction of travel of tillage tool in the soil. The total width of the blocks layer was 315 mm and a total of 126 blocks were placed in 6 layers to a depth of 90 mm. Block positions were specified by different colors for rows and numbers for columns (Figure 4.2).

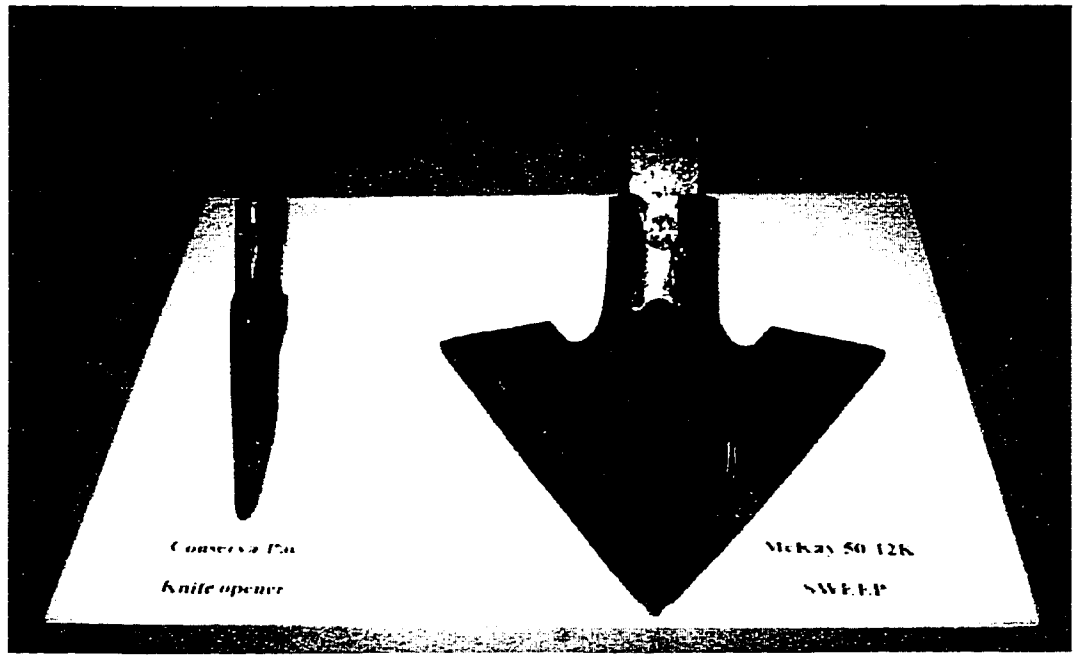

Figure 4.1 14-mm Conserva-Pac knife opener (left); McKay 50-12K sweep (right).

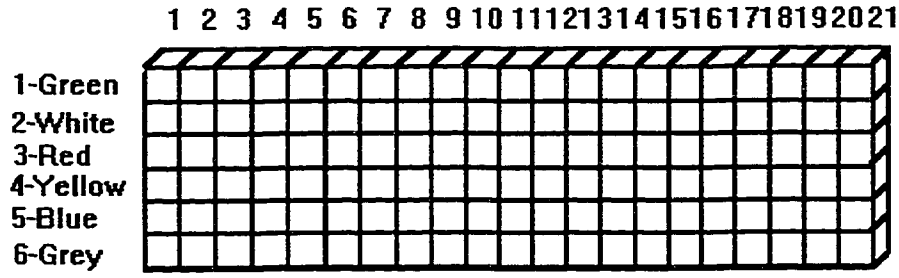

Figure 4.2 Block configuration.

Assuming the soil movement is comparable with the movement of blocks, the new positions of blocks after each test were measured. New positions of the plastic blocks (x-y-z co-ordinates) and the furrow profile were recorded by a special instrument and a soil profile-meter developed for this study.

4.2.1 Experimental Procedure

To find the effects of three variables (speed, moisture content, and compaction) on soil movement with two different tools, a 2x3x3x3 factorial experiment with random design was used. Twenty seven tests with three replicates (a total of 81 tests) were conducted with each tillage tool under different conditions. Measurements of the x-y-z references of every point in the soil bin were provided by the instrumentation system.

4.2.2 Soil preparation

Soil bin facilities of the department of Agricultural and Bioresource Engineering of the University of Saskatchewan includes a soil bin of 1.75 m width and 12.2 m length, (Figure 4.3) containing clay loam soil (sand 47%, silt 24%, and clay 29%)

The soil preparation equipment included a roto-tiller, a flat surface packing roller (Figure 4.4), a sheep-foot roller (Figure 4.5), a soil leveller, and a spray boom to add water for maintaining the soil moisture content. A six-load cell force transducer installed on the carriage of the soil bin enabled the measurement of the three soil reacting forces on the tillage tool. Travel speed of the tool was controlled by using a variable speed drive electric motor connected to soil bin carriage. The required moisture contents were obtained by spraying a certain amount of water into the soil depending on the initial moisture content. Four spray nozzles provided uniform distribution of water. The added

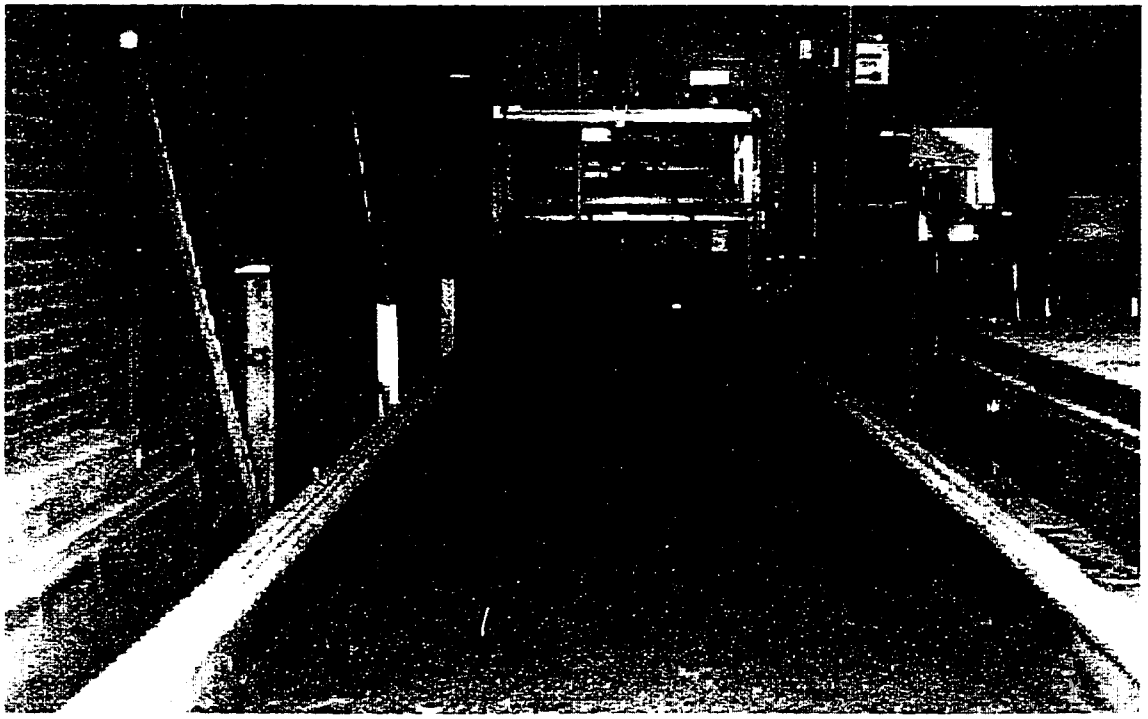

Figure 4.3 Soil bin.

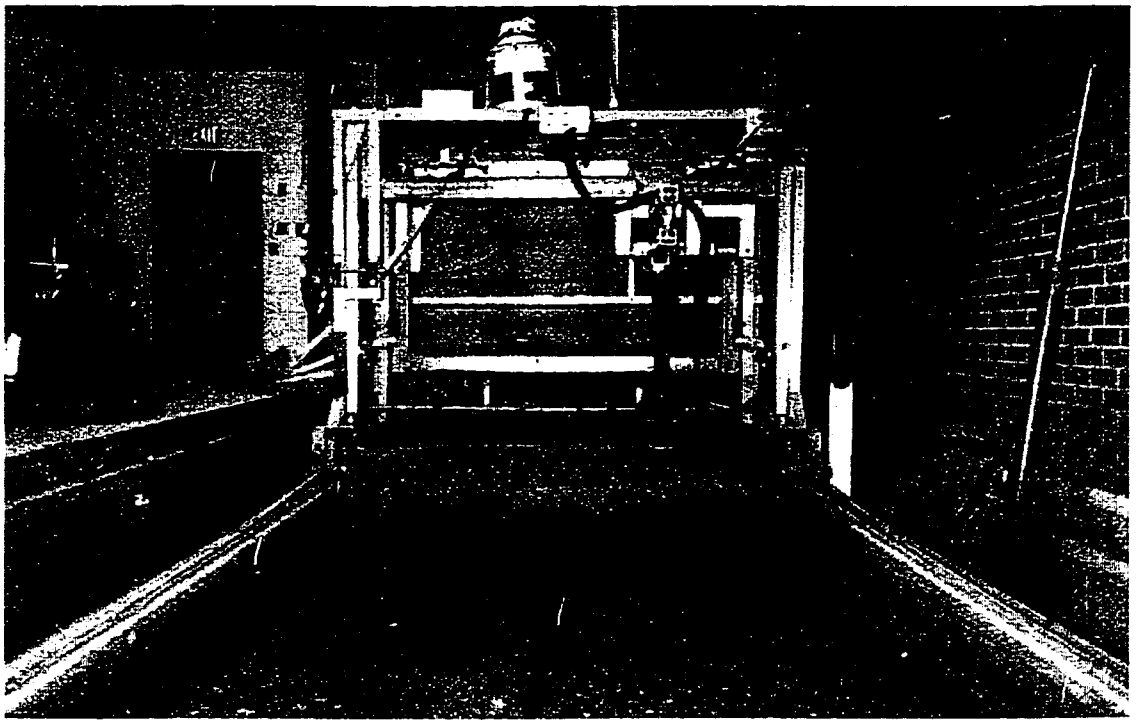

Figure 4.4 Flat surface packing roller.

water was allowed to soak in the soil and then mixed with the roto-tiller. The three oven dry based moisture content levels of 10, 13, and 15% were selected as the low, medium, and high moisture level, respectively.

The compaction levels required for the experiments were obtained by packing the soil at two levels of packing. The sheep-foot roller was used to pack the subsoil followed by levelling the soil surface to fill the depressions left by the packer. Once the subsoil packing was completed, the flat surface packer was used to pack the surface soil to provide a smooth surface. Three compaction levels were considered for the tests. Two passes (back and forth) of the sheep-foot roller plus two passes of the flat surface roller were considered as "low compaction level". For "medium compaction level", four passes of the sheep foot roller plus two passes of the flat surface roller were used. Six passes of the sheep foot roller plus two passes of the flat surface roller were used for "high compaction level". Cone-Index measurements were taken to quantify the compaction level (Table 4.1).

4.2.3 Data acquisition

Soil moisture was measured before the tests by taking five random soil samples along the soil bin. All samples were weighed immediately and dried in an oven at the temperature of 110°C for 24 hours. The moisture content of different tests is given in Table 4.1. Soil compaction levels of the tests were measured by Cone Index measurements with a cone penetrometer. Five sets of readings of penetration resistance were taken randomly along the soil bin before each test to obtain "Average Cone Index" of the soil. Soil penetration resistances were measured at the surface, 25, 50, 75, and 100 mm depths. The average Cone Index for different tests is given in Table 4.1.

Table 4.1: Bulk density, soil moisture and cone index measurements for the experiments with the sweep and the knife opener.

Test conditions		Bulk density	Sweep		Knife opener	
Compaction	Moisture	(Mg m^{-3})	Moisture content (%)	Cone index (kPa)	Moisture content (%)	Cone index (kPa)
	Low	1.26	10.1	205	10.3	220
Low	Medium	1.34	13.1	220	13.8	220
	High	1.43	16.1	210	16.2	215
	Low	1.26	10.1	296	10.2	292
Low	Medium	1.35	13.5	304	13.8	300
	High	1.41	15.2	323	15.4	321
	Low	1.26	10.2	412	10.4	415
Low	Medium	1.35	13.5	423	14.1	425
	High	1.42	15.9	431	16.5	432

An instrumentation system was developed to measure the final position of the blocks after each test (Appendix-C). Some modifications were made in the soil bin, so that the device can be used in any place along the soil bin to measure the x-y-z references of any point in the soil bin. The device had a pointer, which was movable in x-y-z directions. Three potentiometers were used to measure the movements of the pointer in the x-y-z directions. A portable identification device with digital readouts was designed to enter the color code and the number of each block manually. The pointer of the measuring system was positioned on the center of each block. By pushing the digitising button, the x-y-z references of the block along with its specifications were printed out and simultaneously recorded in the computer. Soil translocation at different depths was determined using the recorded x-y-z references (Figure 4.6).

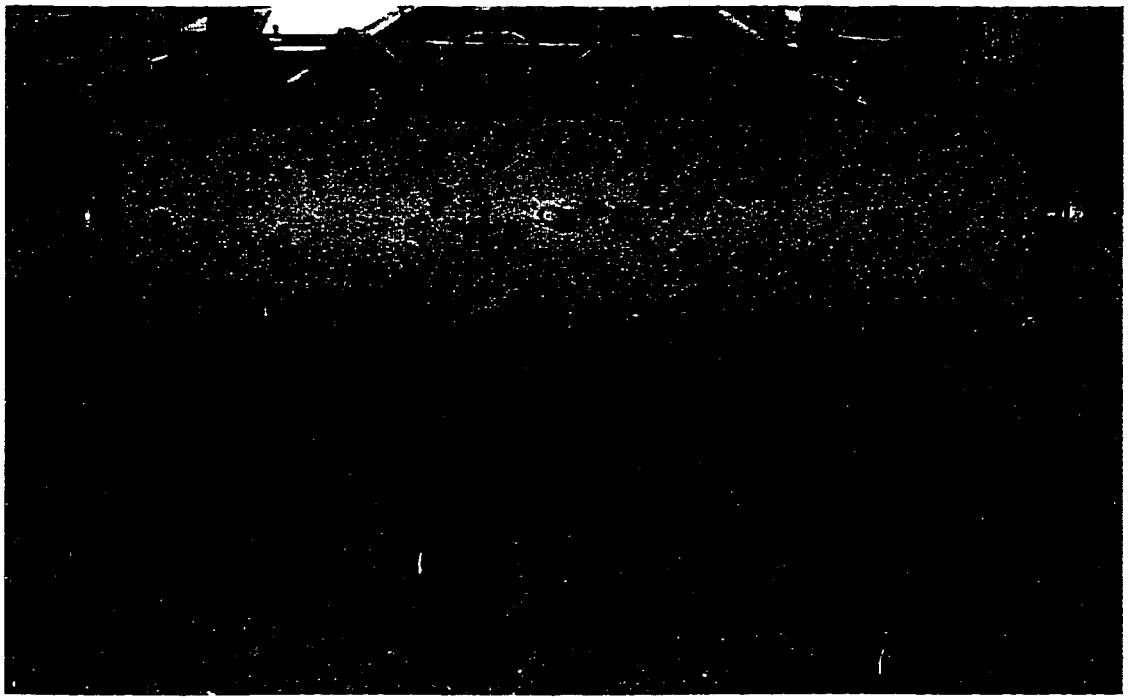

Figure 4.5 Sheep-foot roller.

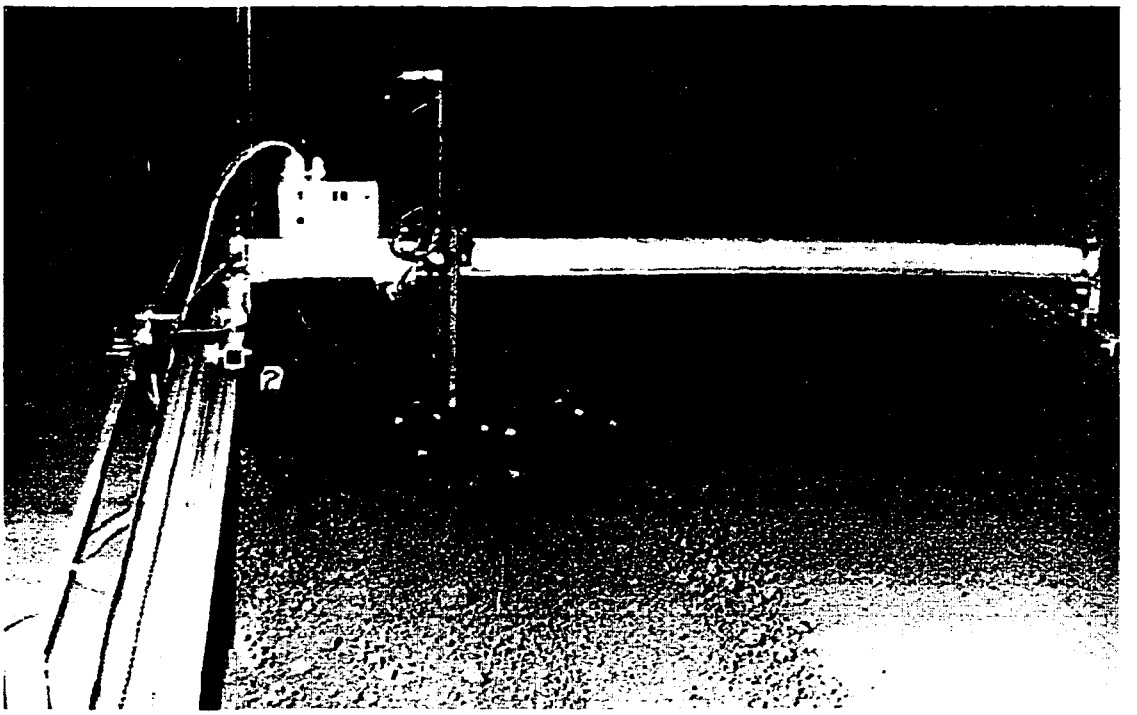

Figure 4.6 The reference (x-y-z) measuring system.

4.3 Results and Discussion

Figures 4.7 and 4.8 show the typical forward movement of plastic blocks at different depths by a sweep and knife opener used in this experiment, respectively. The results obtained from the soil movement measurement tests showed that, in general, for both openers the amount of movement of soil particles was inversely proportional to their distance from the center line of the tool in the direction of travel. An increase in lateral distance from the center line of the tool resulted in less forward movement of the particles. Those particles located on the center line moved considerably greater distance. The difference in the amount of movement of soil particles by the sweep was due to the difference in their flow path over the tool surface. Motion of the particles during tillage is the result of two motions, a motion with the tillage tool and a motion relative to the tillage tool. A particle with a larger flow path over the surface of the tillage tool needs more time to travel along its flow path, and consequently will be transferred over a larger distance.

According to Goryachkin's lifting theory depicted in Figure 4.9, flow path of particles along the trihedral tool surface (LSF) is parallel to flow path LJ. Going from L to S along the line LS, the length of the lines drawn parallel to LJ decreases. Consequently, the flow path of the particles that come in contact with the trihedral wedge along the line LS decreases from L to S. Considerably larger movements of the particles located on the center line of the tool travel, might be due to their impact with the tool shank as seen in the videotapes taken from some tests in the soil bin. This causes the particles to travel further.

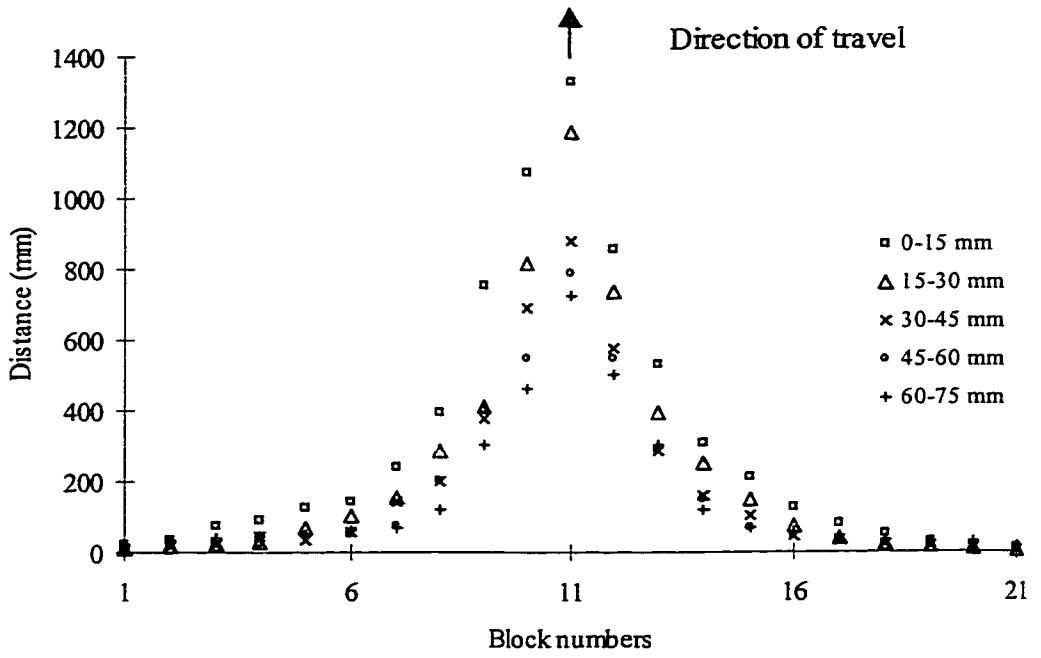

Figure 4.7 Forward movement of plastic blocks at different depths by the sweep at high compaction, high moisture, and 8 km h^{-1} speed.

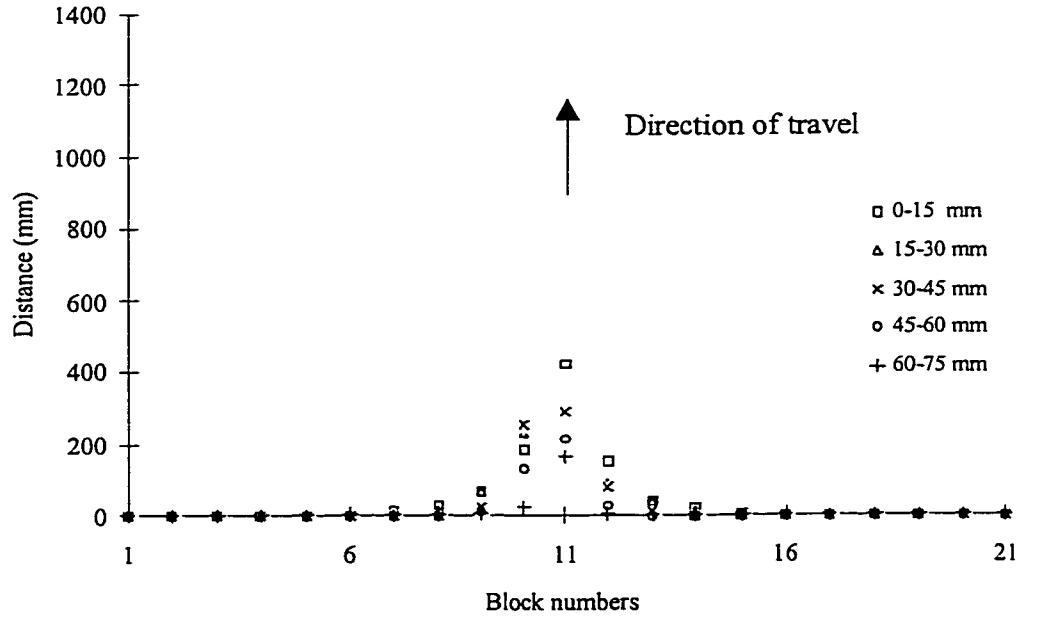

Figure 4.8 Forward movement of plastic blocks at different depths by the knife opener at high compaction, high moisture, and 8 km h^{-1} speed.

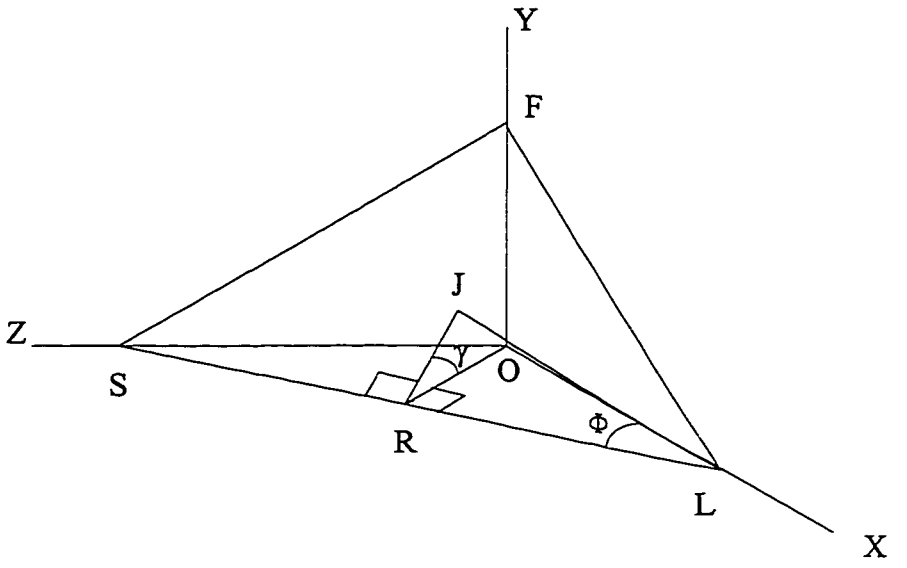

Figure 4.9 Goryachkin's lifting theory showing relative soil aggregate flow path parallel to line LJ. (From Hanna et al., 1993a).

The result of soil movement measurements in different soil conditions with the sweep and the knife opener show that a sweep moves soil particles over a larger distance.

The results of movements of different layers showed that the block's movement was inversely proportional to the depth of the block layer. Blocks located at the soil surface resulted in the largest movement while blocks in the bottom layer had the least movement. Although the lowest block layer was the first one to come in contact by tool, however the undisturbed soil in front of it acted like a cushion preventing movement of blocks. The upper layers faced partially disturbed soil under the influence of disturbance in lower layers, resulting in less cushioning property in front of the blocks. This resulted in a larger movement of blocks located in upper layers.

Figures 4.10 and 4.11 are typical charts representing the effect of increasing speed from 5 km h^{-1} to 8 km h^{-1} on soil movement by sweep and knife opener on the top layer of the blocks. Increasing the speed by a factor of 1.6 (from 5 to 8) increased the average forward movement of the blocks 1.3 – 1.7 times for the sweep and 1.4 - 2.0 times for the knife opener. Closeness of the ratio of increase in soil movement by the sweep with the ratio of speed, can be related to Goryachkin's theory of soil flow (Goryachkin, 1968).

According to this theory, increasing the speed did not change the flow path of soil particles on the tool surface. Hence, by increasing the speed, with no change in flow path, particles were transferred over a larger distance by the tillage tool. A small difference between the corresponding ratios of tool speeds and soil movements, may have been caused by the fact that commercial sweeps are not simple inclined planes, as that assumed by Goryachkin in developing his theories.

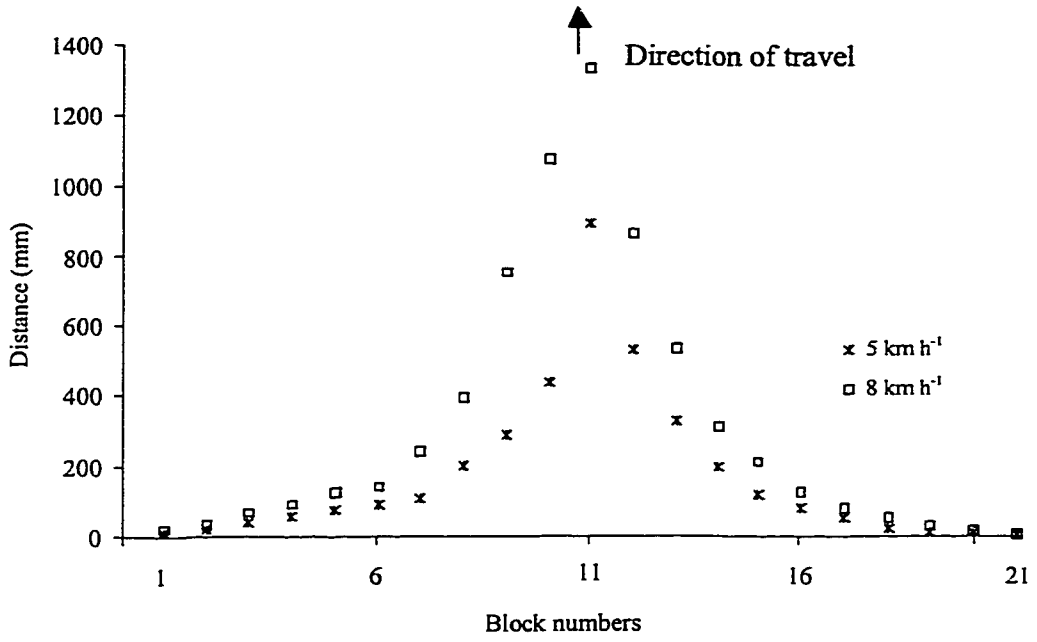

Figure 4.10 Forward movement of plastic blocks by the sweep at 5 and 8 km/h speed (high compaction, high moisture, 0-15 mm depth).

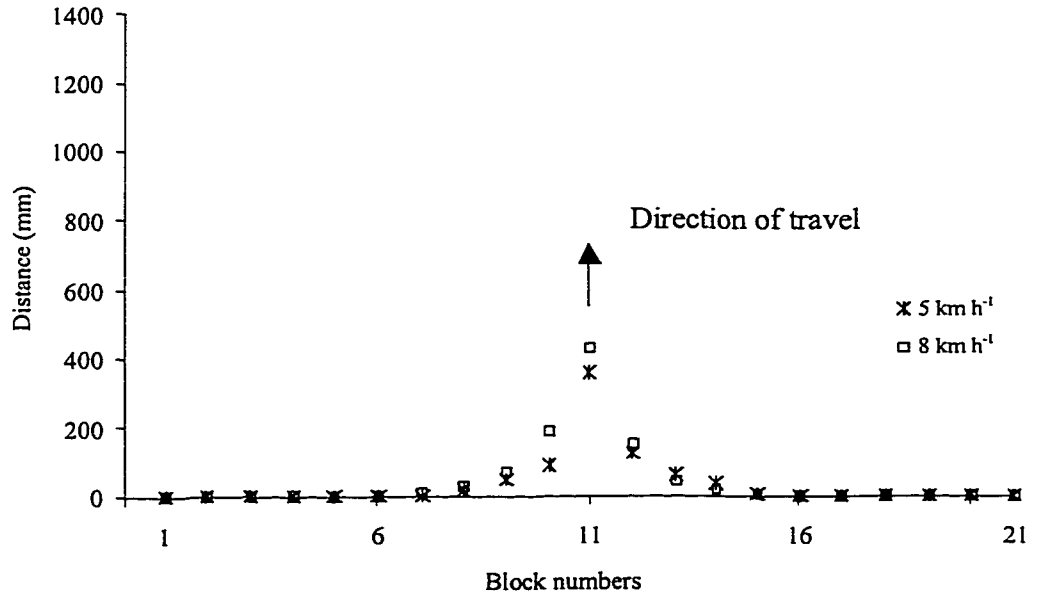

Fig. 4.11 Forward movement of plastic blocks by the knife opener at 5 and 8 km/h speed (low compaction, low moisture, 0-15 mm depth).

Figures 4.12 and 4.13 are typical charts representing the effect of increasing moisture on soil movement by the sweep and knife opener. Increasing the moisture from 11% to 16%, resulted in an 18% increase in soil movements by the sweep. The effect on movement by the knife opener was not significant. Increase in the moisture from 11% to 16% may have resulted in increased adhesion of soil to the surface of tillage tool, which would have decreased the relative velocity of the particles flowing over the tillage tool surface, thus causing the variations in soil movement.

Figures 4.14 and 4.15 represent typical charts showing the effect of increasing compaction level on soil movement by sweep and knife opener respectively. At the test moisture levels, increasing the compaction increased soil shear strength, resulting in less soil movement on a volumetric basis. In most of the tests, soil movement decreased with an increase in soil compaction level. In some tests, there were some discrepancies with what have been expected. One of the possible reasons might be found in the combination of soil moisture and compaction levels of the tests. According to the Proctor density test (Fredlund and Rahardjo, 1993), applying the same compactive effort on a certain soil with two different moisture contents will not result in the same compaction level.

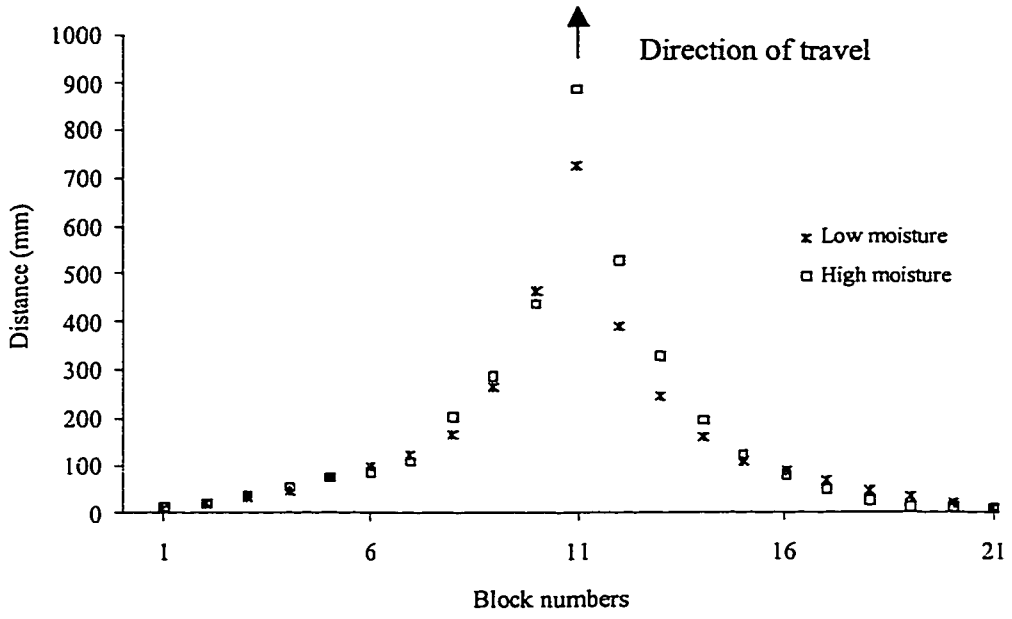

Figure 4.12 Forward movement of plastic blocks by the sweep at two different moistures (high compaction, 5 km h^{-1} speed, 0-15 mm depth).

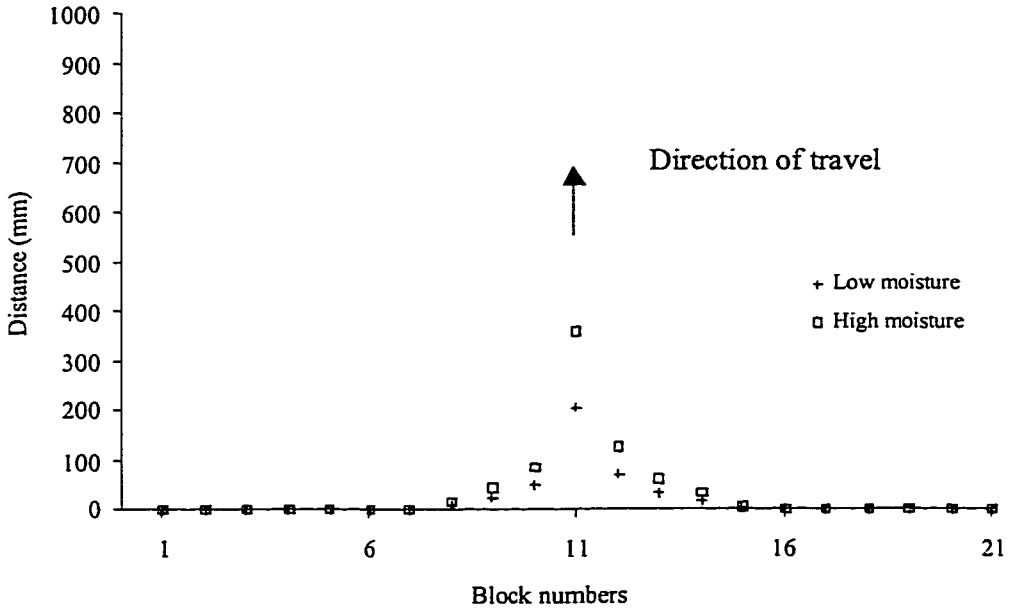

Figure 4.13 Forward movement of plastic blocks by the sweep at two different moistures (high compaction, 5 km h^{-1} speed, 0-15 mm depth).

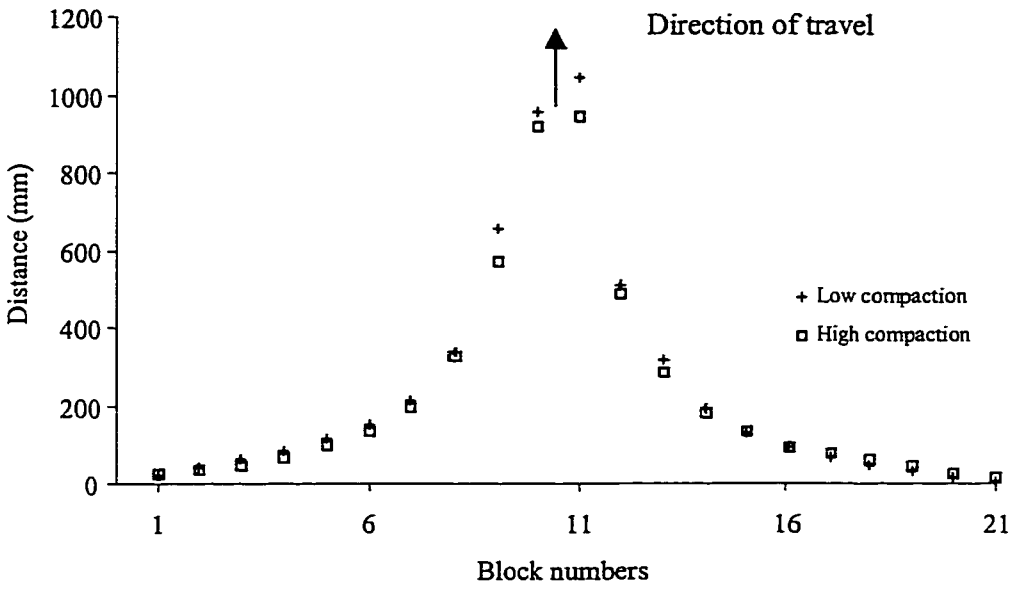

Figure 4.14 Forward movement of plastic blocks by the sweep at two different compaction levels (low moisture, 8 km h^{-1} speed, 0-15 mm depth).

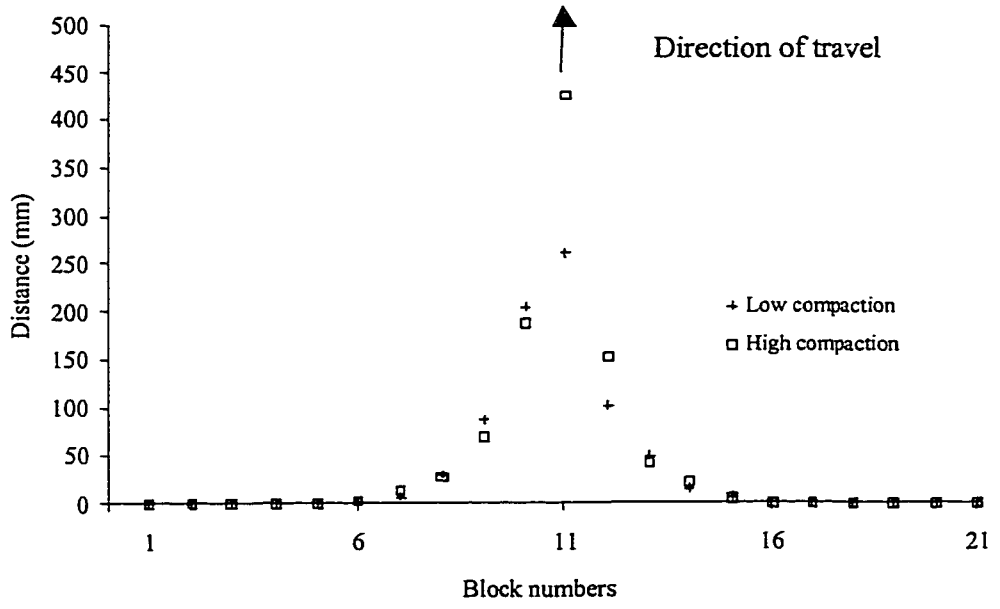

Figure 4.15 Plastic blocks movements by the knife opener at two different compaction levels (high moisture, 8 km h^{-1} speed, 0-15 mm depth).

4.3.1 Data analysis

Results of the soil translocation experiments (Table 4.2) show that the total soil translocation by the sweep was higher than by the knife opener at the same soil moisture content and compaction levels.

This may not be an appropriate basis to compare the function of the sweep with the knife opener. Other ways are comparing the soil movement per unit of frontal area or soil movement per unit width of the sweep and the knife opener. Lobb et al. (1995) used width-averaged and depth-averaged values for a known tool spacing. The frontal areas of the sweep and knife opener were measured to be 12600 mm^2 and 956 mm^2, respectively. This gives a ratio of 13.2 which means that the frontal area of sweep is 13.2 times greater than the frontal area of the knife opener. Tables 4.3 and 4.4 show that the soil movement per unit width or soil movement per unit of frontal area of the sweep is less than the knife opener for different soil moisture contents and compaction levels. However the data indicate that the total soil movement by the sweep was larger than that of knife opener under all test conditions. Thus, it can be concluded that the use of knife opener instead of sweep for the same job reduces the soil movement.

A factorial analysis of variance was conducted for each tool as well as for the whole data from the tests with both tools for translocated soil. Analysis of variance for the sweep and the knife opener (Appendix A - Table I) shows that the effect of moisture, compaction, and speed on soil translocation by the sweep and the knife opener is highly significant. Results of the analysis of the variance for all the data set shown in Appendix-A, Table II indicates that the effects of tool, speed, moisture, and compaction are highly

Table 4.2: Total soil movement for the sweep and the knife opener.

Compaction	Moisture	Speed (km h^{-1})	Total soil movement (m)	
			Sweep	Knife opener
Low*	low†	5.0	12.81	1.23
		6.5	14.78	2.14
		8.0	16.80	2.63
	medium††	5.0	13.28	1.70
		6.5	16.80	2.31
		8.0	20.28	2.97
	high†††	5.0	14.16	1.70
		6.5	17.54	2.57
		8.0	20.90	3.07
Medium**	low	5.0	10.75	1.34
		6.5	14.00	2.00
		8.0	18.52	2.70
	medium	5.0	12.89	1.57
		6.5	16.45	2.14
		8.0	19.93	2.87
	high	5.0	12.69	1.91
		6.5	17.09	2.29
		8.0	21.54	2.82
High***	low	5.0	5.32	1.23
		6.5	10.06	1.63
		8.0	14.17	2.20
	medium	5.0	9.99	1.34
		6.5	13.87	1.76
		8.0	17.54	2.37
	high	5.0	13.65	1.40
		6.5	14.22	1.92
		8.0	21.74	2.26

* 205-220 kPa
** 292-323 kPa
*** 412-432 kPa
† 10.1-10.4%
†† 13.1-14.1%
††† 15.2-16.5%

Table 4.3: Soil movement/unit frontal area.

Compaction	Moisture	Speed (km h^{-1})	Soil movement/unit frontal area	
			Sweep	Knife opener
Low*	Low†	5.0	1.02	1.29
		6.5	1.17	2.24
		8.0	1.33	2.75
	Medium††	5.5	1.05	1.78
		6.5	1.33	2.42
		8.0	1.61	3.11
	High†††	5.0	1.12	1.78
		6.5	1.39	2.69
		8.0	1.66	3.21
Medium**	Low	5.0	0.85	1.40
		6.5	1.11	2.09
		8.0	1.47	2.82
	Medium	5.0	1.02	1.64
		6.5	1.31	2.24
		8.0	1.58	3.00
	High	5.0	1.01	2.00
		6.5	1.36	2.40
		8.0	1.71	2.95
High***	Low	5.0	0.42	1.29
		6.5	0.80	1.71
		8.0	1.12	2.30
	Medium	5.0	0.79	1.40
		6.5	1.10	1.84
		8.0	1.39	2.48
	High	5.0	1.08	1.46
		6.5	1.13	2.01
		8.0	1.73	2.36

* 205-220 kPa
** 292-323 kPa
*** 412-432 kPa
† 10.1-10.4%
†† 13.1-14.1%
††† 15.2-16.5%

Table 4.4: Soil movement/unit width.

Compaction	Moisture	Speed (km h^{-1})	Soil movement/unit width	
			Sweep	Knife opener
Low*	Low†	5.0	42.70	87.86
		6.5	49.27	152.86
		8.0	56.00	187.86
	Medium††	5.0	44.27	121.43
		6.5	56.00	165.00
		8.0	67.60	212.14
	High†††	5.0	47.20	121.43
		6.5	58.47	183.57
		8.0	69.67	219.29
Medium**	Low	5.0	35.83	95.71
		6.5	46.67	142.86
		8.0	61.73	192.86
	Medium	5.0	42.97	112.14
		6.5	54.83	152.86
		8.0	66.43	205.00
	High	5.0	42.30	136.43
		6.5	56.97	163.57
		8.0	71.80	201.43
High***	Low	5.0	17.73	87.86
		6.5	33.53	116.43
		8.0	47.23	157.14
	Medium	5.0	33.30	95.71
		6.5	46.23	125.71
		8.0	58.47	169.29
	High	5.0	45.50	100.00
		6.5	47.40	137.14
		8.0	72.47	161.43

* 205-220 kPa
** 292-323 kPa
*** 412-432 kPa
† 10.1-10.4%
†† 13.1-14.1%
††† 15.2-16.5%

significant. It also shows that tool-speed and tool-moisture interactions are highly significant. The interaction among tool and compaction is also significant.

4.3.2 Soil movement at different depths

Drawing the graphs of soil movement with respect to depth for different layers of soil under different conditions showed that soil movement with depth approximately follows an exponential function for both the knife opener and the sweep.

Knife opener model Figures 4.16 and 4.17 are typical curves showing the soil movement by knife opener at soil conditions of (10.3% moisture content, and 220 kPa Cone Index) at 5 and 8 km h^{-1} tool speed.

Different curves were fitted to the data from experiments with knife opener and it was found that an exponential function model is the best model to describe the soil movement at different depths. The r^2 of the fitted curves varied in the range of 0.98 – 1.00 for different soil conditions and tool's operational speed. The Exponential Model for the knife opener is:

$$X=Ae^{-Y/B}$$

where:

X= soil movement

Y= soil depth

The coefficients A and B were found from the multiple regression of the coefficients of the fitted curves with soil moisture content, compaction level, and tool speed and are as follows.

$A = - 440 + 219\ S + 0.43\ M^2 - 2.12x10^9/C^3$

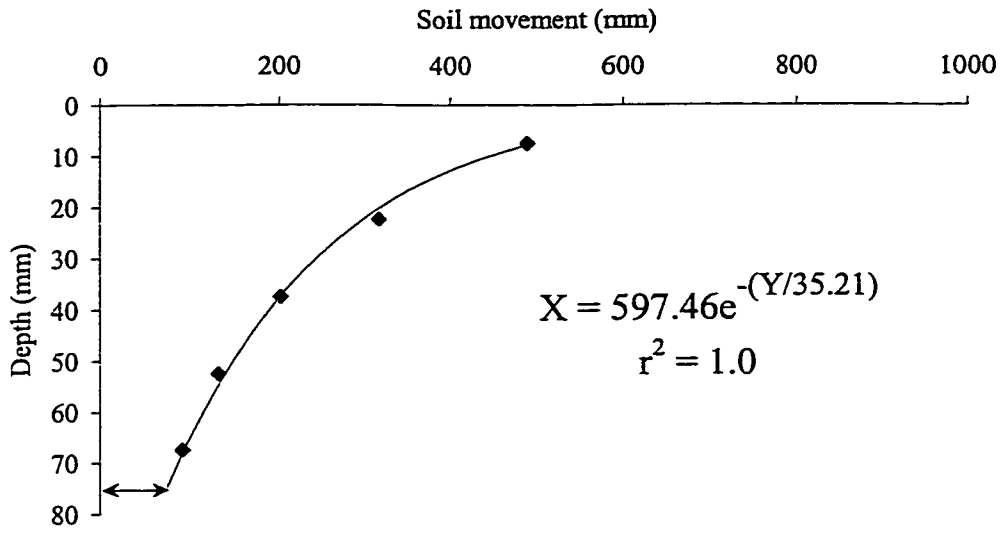

Figure 4.16 Soil movement at different depths by the knife opener at 10.3% soil moisture and 220 kPa Cone Index at 5 km h^{-1} tool speed.

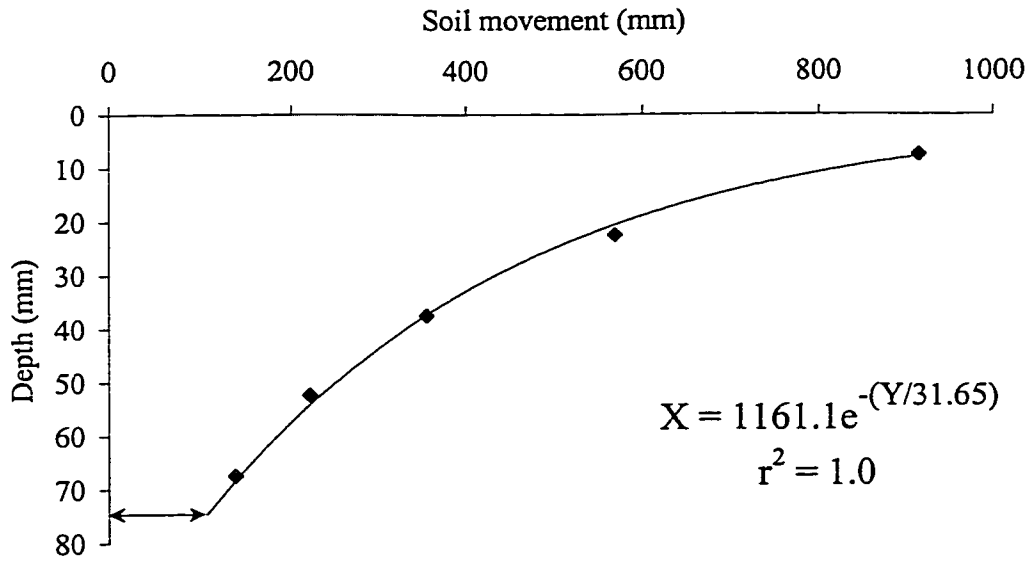

Figure 4.17 Soil movement at different depths by the knife opener at 10.3% soil moisture and 220 kPa Cone Index at 8 km h^{-1} tool speed.

$B = 49.93 - 2.04\ S + 0.03\ M^2 - 4.92x10^7/C^3$

where:

S = speed (km h^{-1})

M = mass soil moisture content (%)

C = soil compaction (Cone Index) (kPa)

The r^2 for the multiple regression of the coefficients A and B are 0.92 and 0.87, respectively. Tables III and IV in Appendix-A show the statistical analysis of the data for estimation of coefficients A and B.

Increasing the coefficient A in the exponential function shifts the curve to the right, which represents an increase of soil movement. Decreasing the coefficient B turns the curve in the clockwise direction that means more soil movement for the soil particle close to soil surface. Increasing tool travel speed increases soil movement for all depths. Although soil movement changes with the 2^{nd} power of soil moisture content, but compared to speed it has a lesser effect. Increasing soil compaction decreases the coefficient A, which results in less soil movement. Compared to soil moisture content and tool travel speed, compaction has less effect in soil movement.

Sweep model Figures 4.18 and 4.19 are typical curves showing the soil movement by sweep at soil conditions of 10.1% moisture content and 205 kPa Cone Index at 5 and 8 km h^{-1} tool speed.

Different curves were fitted to the data from experiments with sweep and it was found that an exponential function model is the best model to describe the soil movement at different depths. The r^2 of the fitted graphs varied in the range of 0.91-0.97

The Exponential Model is:

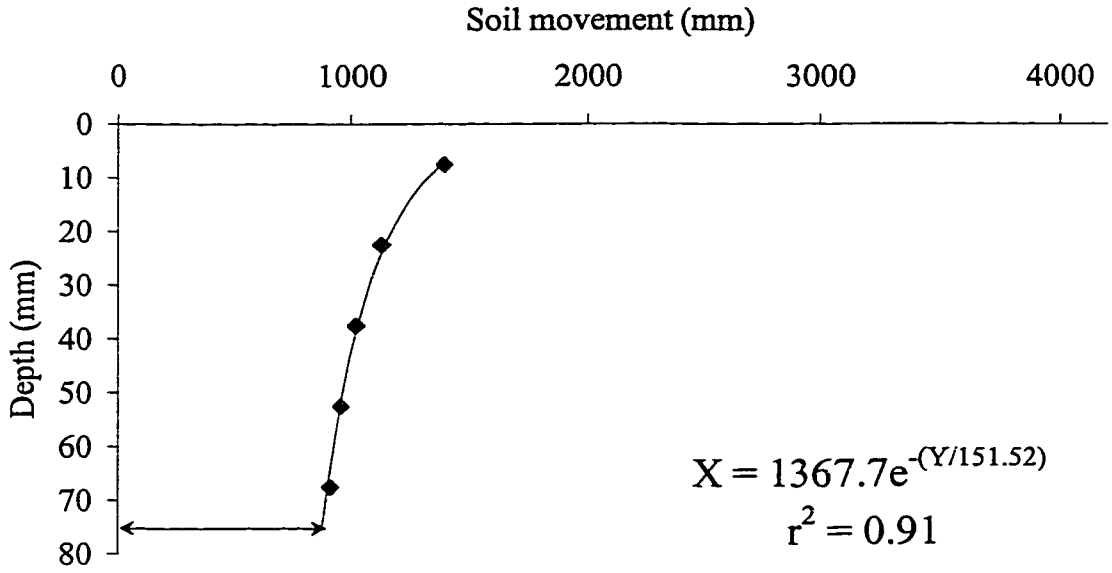

Figure 4.18 Soil movement at different depths by the sweep at 10.1% soil moisture and 205 kPa Cone index at 5 km h^{-1} speed.

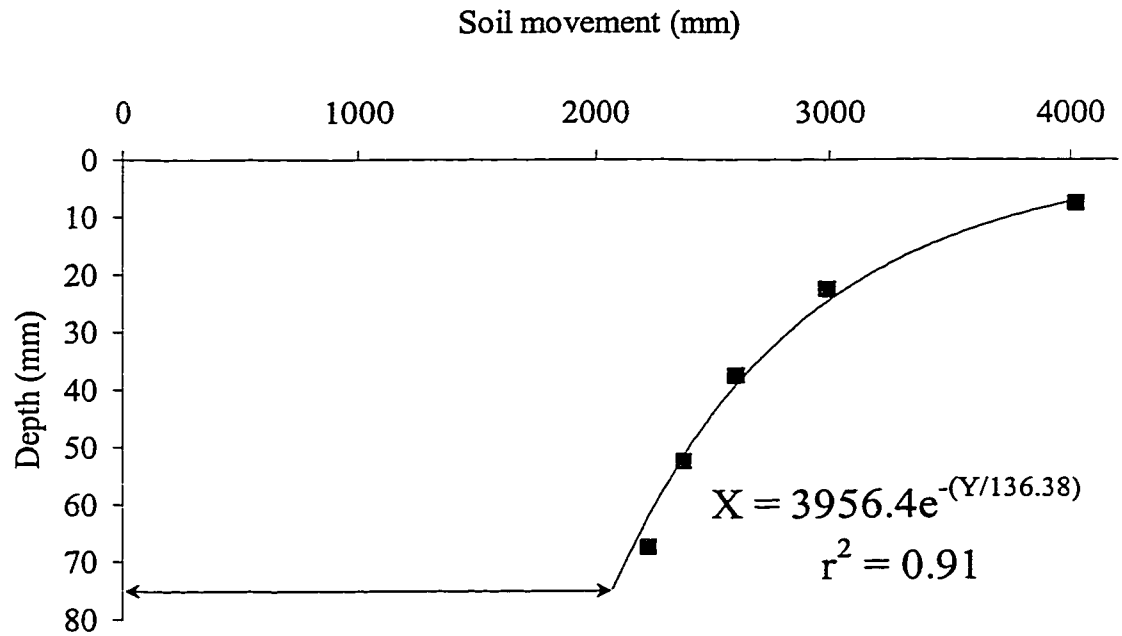

Figure 4.19 Soil movement at different depths by the sweep at 10.1% soil moisture and 205 kPa Cone Index at 8 km h^{-1} speed.

$$X=Ae^{-Y/B}$$

where:

X= soil movement

Y= soil depth

The coefficient A and B were found from the multiple regression of the coefficients of the fitted curves with soil moisture content, compaction level, and tool speed and are as follows.

$$A = - 3802 + 1.68\ C + 204\ M + 781\ S$$

$$B = 260 + 5108/C^{6} - 67.6\ M^{0.5} + 531/S$$

where:

M = mass soil moisture content (%)

S = speed (km h^{-1})

C = soil compaction (Cone Index) (kPa)

The r^2 for the multiple regression of the coefficients A and B are 0.97 and 0.76, respectively. Tables V and VI in Appendix A show the statistical analysis of the data for estimation of coefficients A and B.

The parameters in coefficient A suggest that the tool travel speed has a significant effect on soil movement followed by soil moisture content. From the distribution of soil movement by sweep it can be concluded that since soil particles will travel over the surface of sweep, increasing the soil moisture content will increase soil adhesion to the surface of the sweep. Having more adhesion to the sweep surface, the relative speed of

soil particles to the sweep decreases and it takes more time for soil particles to travel over the sweep surface and, hence, they will be carried over a longer distance by the sweep. This results in more soil movement due to soil moisture increase with the sweep. Compared to tool travel speed and soil moisture content, soil compaction has a lesser effect on soil movement by the sweep volumetrically.

At 75 mm (depth of tool operation), the soil is in a transition phase. The particles coming in contact with tool will move a distance shown in Figures 4.16-4.19 at 75 mm depth marked by the arrows. Different values show the effect of soil and tool operating parameters. At this transition phase, the particles coming in contact with tool will shear and move. However, the particles just beneath this operating depth will tend to move, but will remain partially displaced. In other words, the depth of influence due to tool speeds will be when the soil movement is zero. This will again depend on soil and tool operating parameters. However, this can not be determined by extending the curve or setting the value of x=0 since the nature of linking of inter-molecular soil particles is difficult to estimate.

4.3 Summary

Soil translocation by a wide and a narrow tillage tool were measured in different soil conditions of moisture and compaction. A 300-mm wide sweep and a 14-mm Conserva-Pac knife opener were used at 3 different operating speeds with two soil moistures and compaction levels. Soil translocation was simulated by the movement of small plastic blocks having equal density with soil, positioned in the soil. The new positions of the plastic blocks (x-y-z co-ordinates) after each test were measured with a special instrument developed for this study and the volume of translocated soil was

determined. The effect of compaction level, moisture content, tool shape, and tool operational speed were studied. Results of the soil movement measurements showed that:

- The soil movement by the sweep was greater than knife opener, but a larger soil movement per frontal area by the knife opener was observed.
- Soil movement was inversely proportional to the block layer depth.
- Increasing tool travel speed from 5 to 8 km h^{-1} increased soil movement by the sweep and the knife opener by factors of 1.3 – 1.7 and 1.4 – 2.0, respectively.
- Increasing moisture content of the soil from 10-11% to 15-16% resulted in an 18% increase of soil movement by the sweep. Its effect on soil movement by the knife opener was not significant.
- Effect of soil compaction on soil movement in the range considered for this study was not significant.
- Soil movement at different depths were measured and analysis of the data and regression analysis showed that there is an exponential relation between depth and soil movement.

CHAPTER 5

SOIL TRANSLOCATION IN HIGH SPEED TILLAGE

5.1 Overview

The high cost of energy in crop production encouraged scientists to do research on conserving the energy in farming through efficient tillage operations. Efforts have been concentrated in finding ways to increase the output and decrease the cost. In addition to soil conditions, tool geometry and speed of operation are considered to be important factors in energy consumption in tillage. Most of the energy used to operate tillage tools goes to overcome sliding frictional resistance as soil moves over the tool surface. Any contributing factor to this resistance must be considered in describing soil behavior. Results of the previous experiments by Sharifat and Kushwaha (1997) on soil translocation with tillage tools at low speeds of operation in the soil bin showed that the effect of tool shape and speed of operation were highly significant. Therefore, tool geometry and speed of operation become two important factors in tillage considerations. It was also noticed that soil translocation per unit width or per unit frontal area of the narrow tool used in the study (knife opener) was more than for the wide tool (sweep). These results prompted further research on measurements of soil translocation with different shapes of narrow tillage tools at higher speeds.

Different tool shapes were attached to the pendulum and the pendulum was released from pre-determined heights to provide the desired speed. A special

instrumentation system was designed to measure the tool speed during cutting. The height of release and the final height of the pendulum were also measured by the instrumentation system to calculate the used energy.

5.2 Materials and Methods

Since the equipment of the soil bin of the Department of Agricultural and Bioresource Engineering of the University of Saskatchewan was not suitable for conducting the proposed tests, a special device (Figures 5.1 and 5.2) using simple pendulum principles was fabricated to provide the required speed levels. Four narrow tools with different shapes, 90° triangular, flat, elliptical, and 45° triangular (Figure 5.3) were used at four speed (10, 15, 20, and 25 km h^{-1}) and three compaction and three soil moisture levels. The same procedures as for low speed experiments were used for soil preparation. The length of the soil to be cut by the tillage tools was considered to be 200 mm, with a maximum depth of cut of 50 mm. Two slots on both sides of the test area were prepared for entrance and exit of the tool to test area. Small plastic blocks were used as tracers for soil movement measurements. Blocks were installed in a 10-mm deep vertical slot prepared in soil.

5.2.1 Instrumentation system

Using the simple pendulum principles, a pendulum was fabricated (Figure 5.2). It was installed on the soil bin carriage by means of two bearings. The soil bin carriage was used as the frame of the pendulum and made it possible to use the pendulum in all parts of the soil bin. Pendulum length was considered practically as high as possible to reduce the variation in cutting depth. The length of the soil sample for cutting was considered as

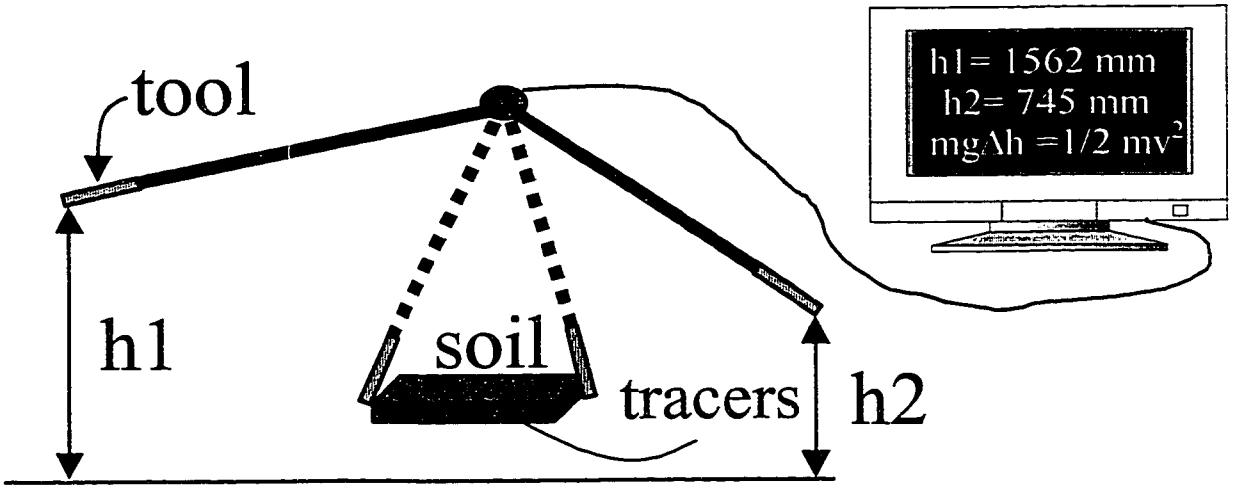

Figure 5.1 Schematic representation of the pendulum system.

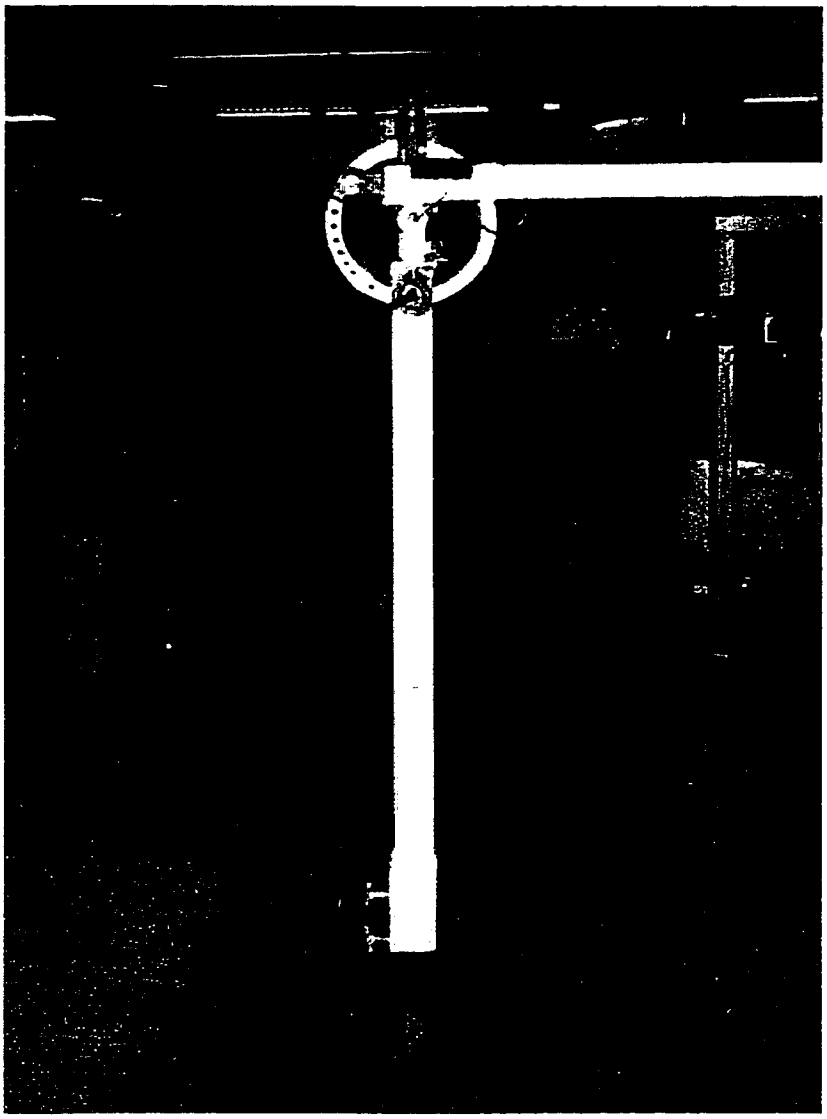

Figure 5.2 The pendulum system used in high speed tillage experiments.

(a) (b) (c) (d)

Figure 5.3 Narrow tool shapes used in high speed experiment. a) 45° triangular (T4), b) Elliptical (T3), c) Flat (T2), and d) 90° triangular (T1).

200 mm. To establish the test speeds, the release height of the pendulum for different speeds was calibrated.

To measure the height of release and the final height of the pendulum after soil cutting, a rotary potentiometer was used. The difference between the height of release and the final height of the center of mass of the pendulum was used to calculate the energy used by pendulum to pass through the soil and overcome friction (Figure 5.1). To measure the tool speed before, during, and after cutting, infrared transmitter and receiver sensors were installed on the carriage. A slotted plate was attached to the pendulum in such a way to cross the path of the infrared light between sender and receiver sensors while tool was cutting the soil. A program to collect and transfer the data from the sensors to computer was developed to sample the data at 34000 samples per second. Based on the number of samples collected between two slots by knowing the sampling rate and the width of the slots, the tool speed was calculated at different positions. The difference between the tool speed before and after cutting the sample was used to determine energy used by the tool to pass through the soil and accelerate the soil particles.

5.2.2 Experimental Procedure

The experiments were conducted under the following conditions:

1- Tool shapes (Figure 5.3)

- 90° triangular (T1)
- Flat (T2)
- Elliptical (T3)

- 45° triangular (T4)

2- Speed

- 10 km h^{-1}
- 15 km h^{-1}
- 20 km h^{-1}
- 25 km h^{-1}

3- Soil conditions

- Three moisture contents
  - Low (11-11.5 %)
  - Medium (14-14.5%)
  - High (17-17.5%)
- Three compaction levels
  - Low (C.I = 60 kPa)
  - Medium (C. I =160 kPa)
  - High (C. I. =320 kPa)

Soil was prepared at one moisture and one compaction level. A tool was attached to the pendulum and tests were conducted at various speeds in a random manner. This procedure was repeated until all tool, speed, and soil condition parameters were tested. To determine soil movement, plastic blocks (10 x 10 x 11mm) with density nearly equal to that of soil (1.2 Mg m^{-3}) were placed in a vertical slot prepared perpendicular to the direction of movement of tillage tool in the soil. Assuming the soil movement is comparable with the movement of blocks, the new position of blocks after each test were

measured. Movement of all plastic blocks in each test were summed and defined as "Soil Movement Index" for that test.

5.3 Results and Discussion

Data obtained from tests were grouped for presenting the results. Figure 5.4 is a typical graph showing the effect of speed on soil movement index and consumed energy at the tool's speed of 10, 15, 20, and 25 km h^{-1} at 11.2% moisture content and 300 kPa Cone Index. The flat tool (T2) had highest and the 45° triangular (T4) had the lowest soil movement and energy consumption. The relationship suggests that the 45° triangular tool had a better performance in low moisture.

Figure 5.5 shows that increasing the speed resulted in an increase in soil movement index in all tools up to 20 km h^{-1} speed. Further increase in speed reduced the slope of the curve for the flat tool (T2) and the 45° triangular tool (T4) and reduced the soil movement index for the elliptical tool (T3). The energy measured in the experiments is the total energy that is used to move the tillage tool through the soil. The used energy accounts for different activities that are taking place while tool is moving in the soil. Some of this energy is used for cutting the soil and overcoming the soil cohesion and soil internal friction. Some is used for accelerating and moving the soil particles. Some is used to overcome the friction forces resulted from of soil-tool adhesion and soil-soil friction. Quantifying most of these energies separately, was not possible.

5.3.1 Statistical Analysis

Analysis of data for the experiments was carried out using the MINITAB statistical package. Results of the analysis of variance for the soil movement index are

shown in Appendix-A, Table VII. Effects of tool, soil moisture content, coil compaction, and speed are highly significant. Effect of Block is not significant.

Mean values for the whole experiment are also shown in Appendix-A, Table VII. The results show that the soil movement index means were increased by increasing the moisture from low to medium. But further increase in soil moisture resulted in a decrease in the mean value of the soil movement index. It seems that the increase of moisture from low to medium has increased soil adhesion to tool and increased the soil movement. Further increase in soil moisture to the high level resulted in a lubrication effect reducing the amount of soil that is moved. Increasing the compaction resulted in decrease in soil movement mean values. Increase of speed, resulted in increase in soil movement means. The 45° triangular tool (T4) had the lowest soil movement index mean and the flat tool (T2) had the highest followed by the 90° triangular tool (T1) and the elliptical tool (T3).

Results of the analysis of variance for the used energy are shown in Appendix-A, Table VIII. The effects of tool, soil moisture content, soil compaction, and speed are highly significant. Effect of Block is not significant. Mean values for the whole experiment are also shown in Appendix-A, Table VIII. The results show that increasing the moisture, compaction, and tool operational speed increased the mean values of energy consumption. The 45° triangular tool (T4) exhibited the lowest energy consumption and the 90° triangular tool (T1) had the highest followed by the flat tool (T2), and the elliptical (T3). While equal width of the tools may suggest equal energy usage for different tool shapes, effects of tool shape in reducing energy required for cutting the soil can not be neglected.

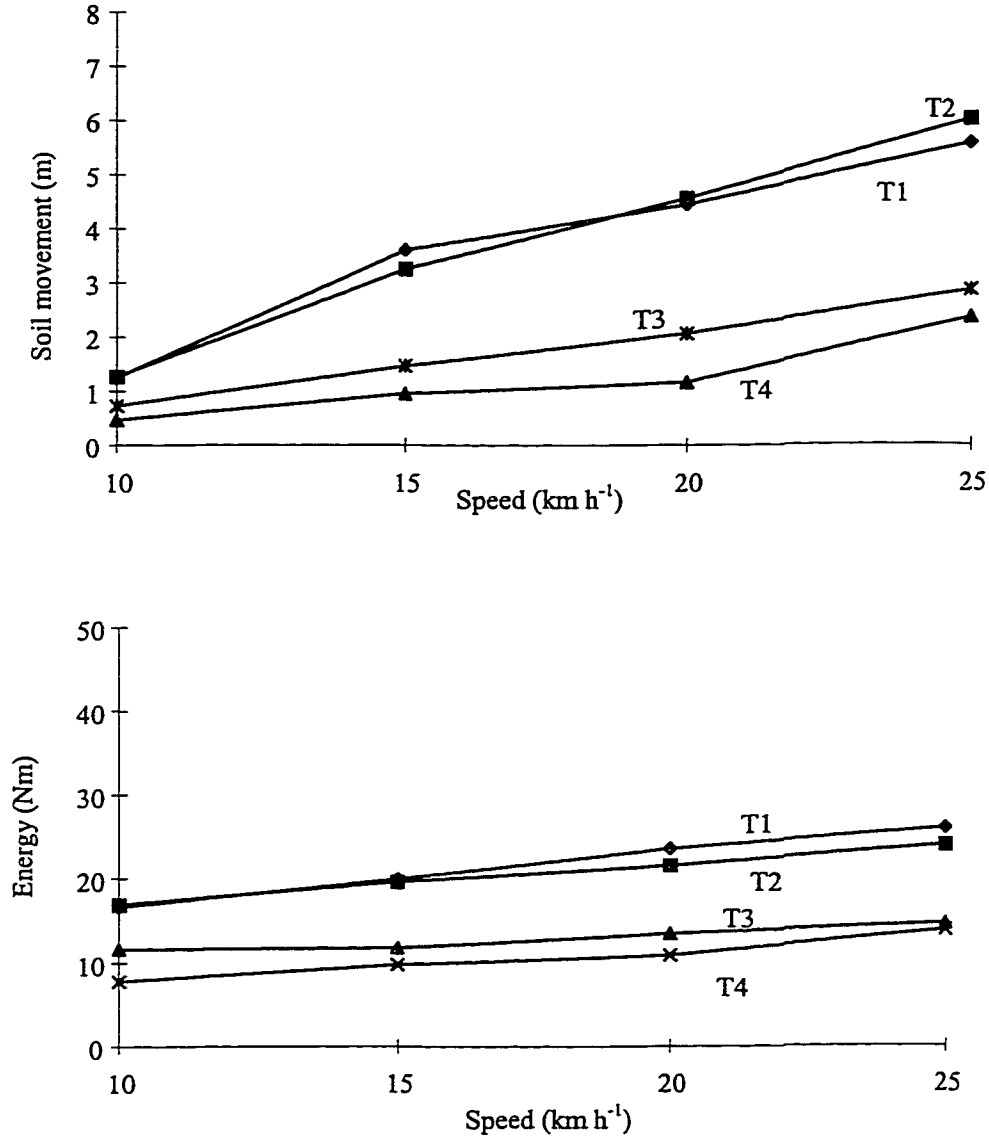

Figure 5.4 Soil movement and used energy with different tools at 11.2% soil moisture, 300 kPa Cone Index, and 10, 15, 20, and 25 km h^{-1} speeds.

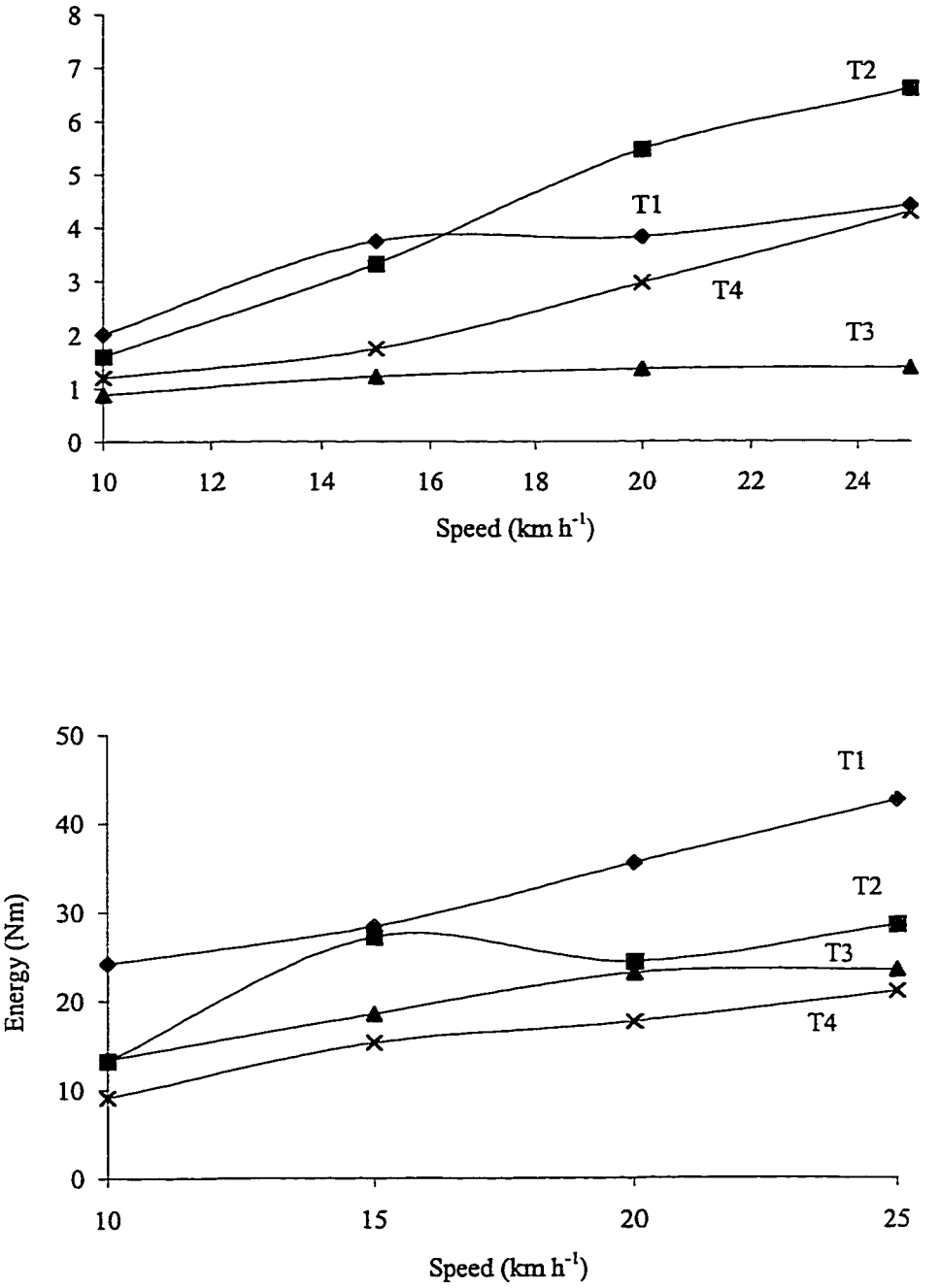

Figure 5.5 Soil movement and used energy with different tools at 15.1% soil moisture, 300 kPa Cone Index, and 10, 15, 20, and 25 km h^{-1} speeds.

Figures 5.6 to 5.9 show the energy used by different tool shapes at 11.2%, 14.6%, and 17.6% soil moisture contents and 60 kPa Cone Index. Assuming a linear relationship between tool travel speed and energy usage, the fitted lines for each tool at different soil moisture contents have close intercepts. The intercepts for the 90° triangular (T1) are 1.65-1.84, for the flat tool (T2) are 2.59-2.86, for the elliptical tool (T3) are 1.14-1.31, and for the 45° triangular tool (T4) are 1.54-1.79. These numbers could be considered as the energy required by different tool shapes to cut the soil at zero speed, which is an indication of soil potential strength. The 45° triangular (T4) showed the lowest soil movement. Soil did not stick to the 45° triangular (T4) and it acted like a sharp wedge facilitating its movement through the soil and as a result required less energy and moved less soil. Some of the differences in the amount of energy used by different tool shapes could be explained by the changes that occur in the frontal area of the tool.

Depending on soil conditions and the tool shape, a compacted soil body was formed on the surface of the tillage tool. This phenomenon changed the attributes of the surface of the tool facing the soil. Compacted soil body became a part of the tillage tool and moved with it. Thus, soil flowing around the tillage tools would have to overcome the soil-soil friction instead of soil-metal friction. Table 5.1 shows the compacted soil body index in the experiments. Compacted soil body index was defined as the ratio of the average length of the compacted soil body to the tool width. Figures 5.10 to 5.13 show compacted soil body index of 1, 2, 3, and 4 respectively. Large soil bodies were observed to form on the 90° triangular tool (T1) and the flat tool (T2), followed by the elliptical tool (T3). The energy used for moving the tillage tool in the soil can not be considered as a measure for comparing soil movement by different tillage tool shapes.

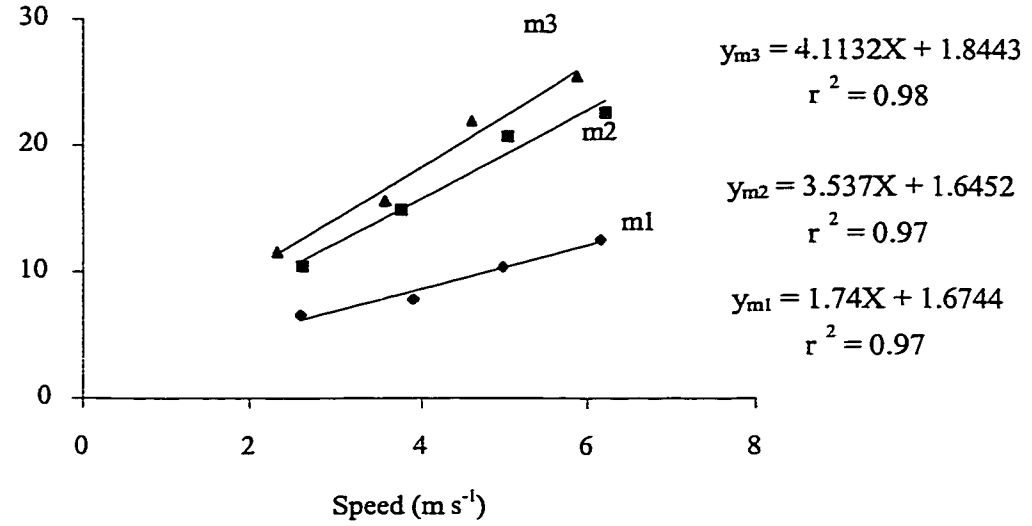

Figure 5.6 Energy used by tool the 90° triangular (T1) at different speeds at 60 kPa Cone Index and 11.2%, 14.6%, and 17.6% soil moisture (m1, m2, and m3).

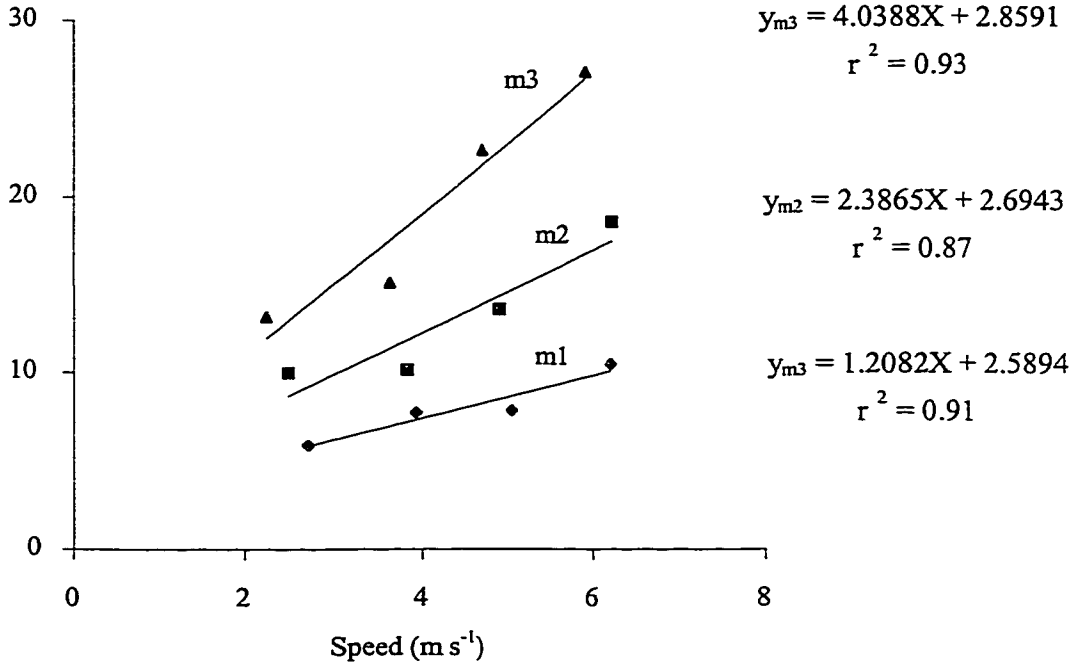

Figure 5.7 Energy used by the flat tool (T2) at different speeds at 60 kPa Cone Index and 11.2%, 14.6%, and 17.6% soil moisture (m1, m2, and m3).

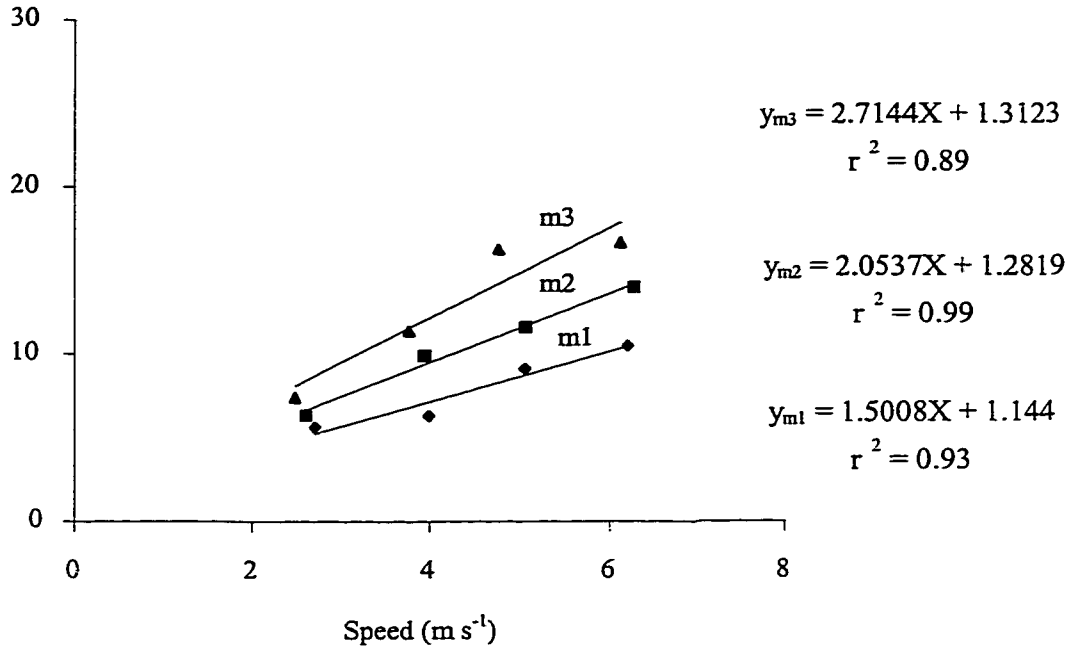

Figure 5.8 Energy used by the elliptical tool (T3) at different speeds at 60 kPa Cone Index and 11.2%, 14.6%, and 17.6% soil moisture (m1, m2, and m3).

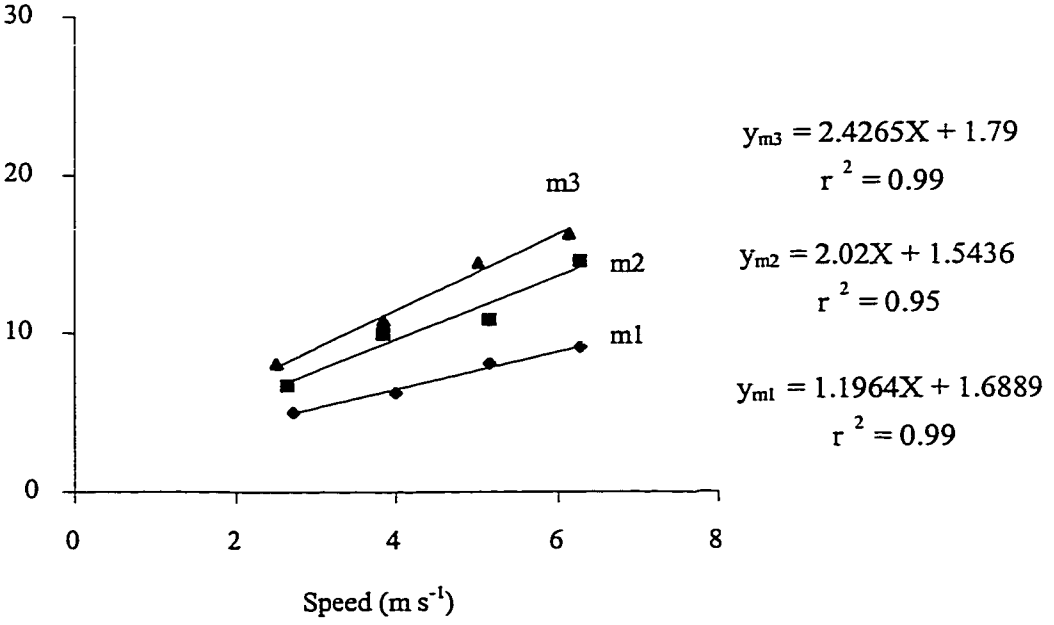

Figure 5.9 Energy used by the 45° triangular tool (T4) at different speeds at 60 kPa Cone Index and 11.2%, 14.6%, and 17.6% soil moisture (m1, m2, and m3).

Table 5.1: Compacted soil body index for different tool shapes at different tool speed, soil compaction, and moisture content.

Compaction	Moisture	Bulk density ($Mg\ m^{-3}$)	Speed $km\ h^{-1}$	Compacted soil body Index*			
				T1	T2	T3	T4
Low	Low	1.15	10	1.00	1.00	0.00	0.00
			15	2.00	1.50	0.00	0.25
			20	2.00	1.50	0.25	0.25
			25	2.50	1.50	0.50	0.50
	Medium	1.18	10	1.50	1.50	0.00	0.00
			15	2.00	1.50	0.25	0.00
			20	2.00	1.50	0.75	0.50
			25	3.00	1.50	0.50	1.00
	High	1.22	10	1.00	1.50	0.00	0.00
			15	1.50	1.50	0.50	0.00
			20	2.00	2.00	2.00	0.00
			25	3.00	2.00	1.75	0.75
Medium	Low	1.24	10	1.00	2.00	0.00	0.00
			15	2.00	3.00	0.25	0.50
			20	2.00	2.00	0.50	0.75
			25	3.00	2.00	1.50	0.75
	Medium	1.31	10	1.00	0.75	0.00	0.00
			15	2.00	1.50	0.00	0.00
			20	2.00	1.50	0.25	0.00
			25	3.00	2.00	0.50	0.75
	High	1.37	10	1.50	1.50	0.50	0.00
			15	2.00	2.00	1.50	0.00
			20	2.00	3.50	2.00	0.50
			25	2.50	1.50	2.00	1.00
High	Low	1.27	10	1.50	1.50	0.25	0.00
			15	3.00	2.00	0.50	0.00
			20	3.50	2.00	0.75	0.50
			25	4.00	3.00	2.00	0.50
	Medium	1.34	10	2.00	2.50	0.50	0.00
			15	2.00	2.50	0.75	0.25
			20	2.50	2.50	1.50	0.25
			25	4.00	3.50	2.00	0.75
	High	1.43	10	2.00	2.00	0.00	0.00
			15	2.00	3.00	0.50	0.25
			20	3.00	3.00	1.50	0.25
			25	4	4	1.5	1
Average compacted soil body Index				2.25	2.03	0.76	0.31

* Compacted soil body Index =average soil lump length/toolwidth

Figure 5.10 Elliptical tool (T3) and soil lump attached to it representing "compacted soil body Index" of 1.

Figure 5.11 Elliptical tool (T3) and soil lump attached to it representing " compacted soil body Index" of 2.

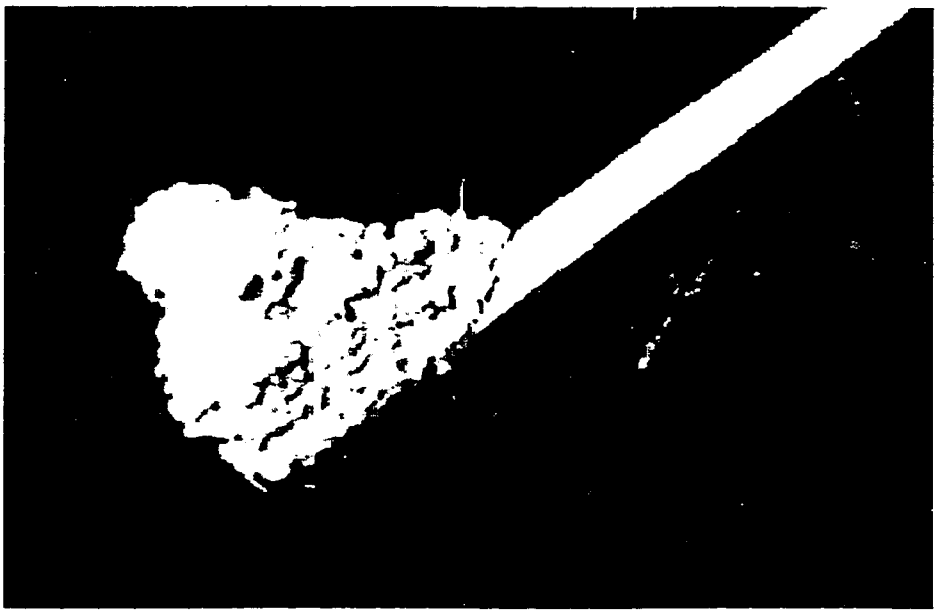

Figure 5.12 90° triangular tool (T1) and soil lump attached to it representing "compacted soil body Index" of 3.

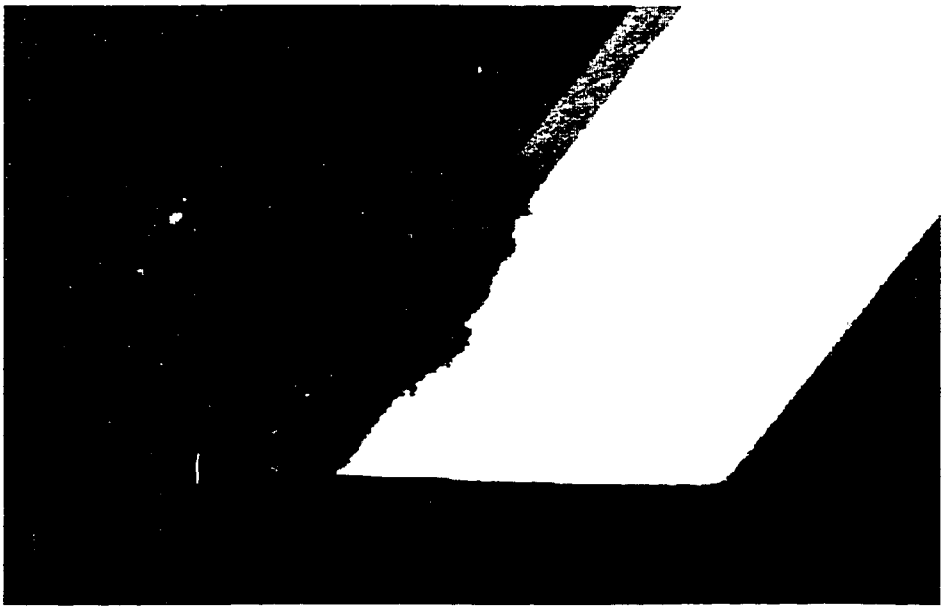

Figure 5.13 Flat tool (T2) and soil lump attached to it representing "compacted soil body Index" of 4.

5.4 Summary and Conclusions

An apparatus using the simple pendulum principle was fabricated. The system was capable of providing up to 25 km h^{-1} speed for tillage tool operation. Four narrow tools with different shapes, 90° triangular, flat, elliptical, and 45° triangular (Figure 5.3) were used at four level of speed of 10, 15, 20, and 25 km h^{-1} and three compaction and three soil moisture levels. Small plastic blocks were used as tracers for soil movement measurements. Soil movement and the energy used in the process of tillage tool movement in the soil were determined. Following conclusions can be drawn from this study:

- Increasing tool operational speed resulted in increase in soil movement for all tools. In some tests at higher speeds, the rate of increase in soil movement with tool speed was decreased, but the trend was not constant for a specific tool or soil condition.
- The 45° triangular tool (T4) and the elliptical tool (T3) exhibited lowest energy requirement and soil movement.
- Measurement of the energy used by tillage tools can not be considered as a measure of soil movement since each tool shape needs a certain amount of energy to start moving in soil.

CHAPTER 6

SOIL PROFILE MEASUREMENTS

6.1 Overview

One of the objectives in some tillage operations is to change the surface topography of soil to form a rough or ridged surface for both conservation and agronomic reasons (Hanna et al., 1993b). Knowing the effects of tillage tool geometry and operational speed under different soil conditions helps in selection or design of more effective tools for different purposes of tillage. A study by Eidet (1974) showed that increasing the approach angle of the plowshare increased the amount of lateral soil displacement. Dowell et al. (1988) found that the ridge height and lateral distance that soil was thrown by a sweep increased with travel speed. Hanna et al. (1993b) in a study of changes in soil microtopography by tillage with a sweep concluded that higher speed and larger rake angle in sweep resulted in more movement of soil to build higher ridges. In this study the soil profile was measured by instrumentation developed specifically for this study. Soil profile measurements were used to study lateral soil movements.

6.2 Materials and Methods

6.2.1 Soil profile meter

A special device was designed and installed on the soil bin carriage to accurately measure the soil profile in the soil bin (Figure 6.1). A visible red laser diode based distance sensor (AccuRange 4000-LV) was used to measure the soil profile. A program in Quick Basic language was developed to control the movement of the sensor by a stepping motor and make communication with the laser sensor to collect the data. Cutting depth was considered 75 mm for the sweep and the knife opener. After each tillage test, the soil profile-meter travelled over the soil profile and measured the distance from the laser sensor to the soil surface. The sampling rate, distance between the samples and the length of sensor travel were software controlled. After each test, the sensor was moved over the soil profile in 5 mm steps by the stepping motor. There were 100 measurements for each point and the the recorded distance for each point was the average of the 100 measurements. This procedure was repeated for the length of the soil profile.

6.3 Results and Discussion

6.3.1 Furrow profile measurements for the sweep and the knife opener

After running the tillage tool through the soil bin, a furrow with two ridges of soil on either side were produced. In general, the furrow width and ridge height, measured as the difference in elevation between ridge top and furrow bottom, for sweep were larger than that of the knife opener. Figures 6.2 and 6.3 show the soil profiles produced by the

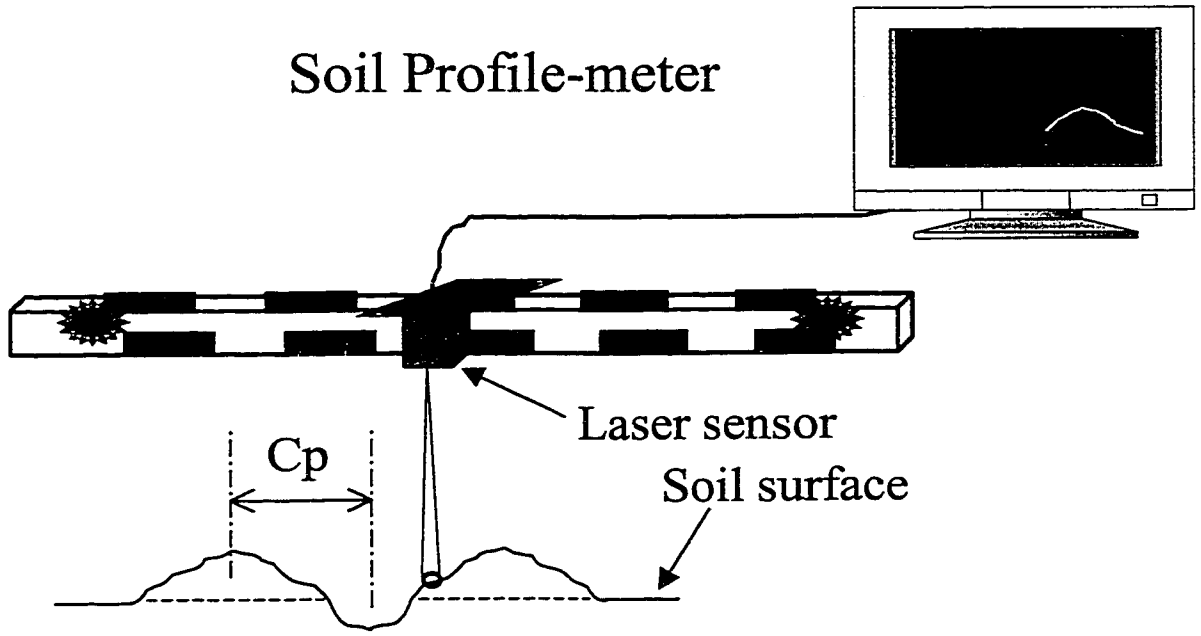

Figure 6.1 Soil profile-meter.

sweep and the knife opener at 5 and 8 km h^{-1} travel speed and at similar soil moisture content and compaction levels.

Flow of the soil particles over the tool surface results in a reduction in speed of soil particles in the direction of travel, as the projection of line AJ on the x-axis (direction of travel) is shorter than AO in Figure 4.9. Considering the continuity of soil flow across the tillage tool, the in-flow and out-flow must be equal (assuming constant mass flow rate). This results in an increase in cross sectional area of the soil leaving the tillage tool to make the output and input mass flow rates equal. Any factor influencing the flow rate of soil particles on tool surface affects the shape of the soil cross-section leaving the tillage tool.

Increasing the travel speed of the tool increased the lateral distance that soil was thrown by the sweep and the knife opener. It also increased the furrow depth, which is mainly due to the fact that, at high speeds, most particles, which are thrown sideways, do not fall back into the opened furrow. Therefore the higher speed resulted in deeper surface furrow and wider ridge, the cross sectional area of the disturbed soil did not change appreciably. This agrees with the findings of McKyes (1985).

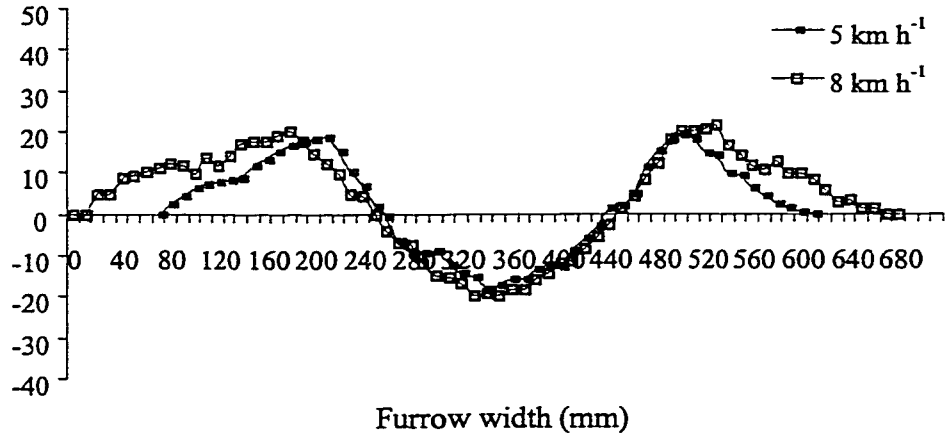

Figure 6.2 Soil profile with sweep at 5 and 8 km h^{-1} speed and 10.3% soil moisture and 205 kPa Cone Index.

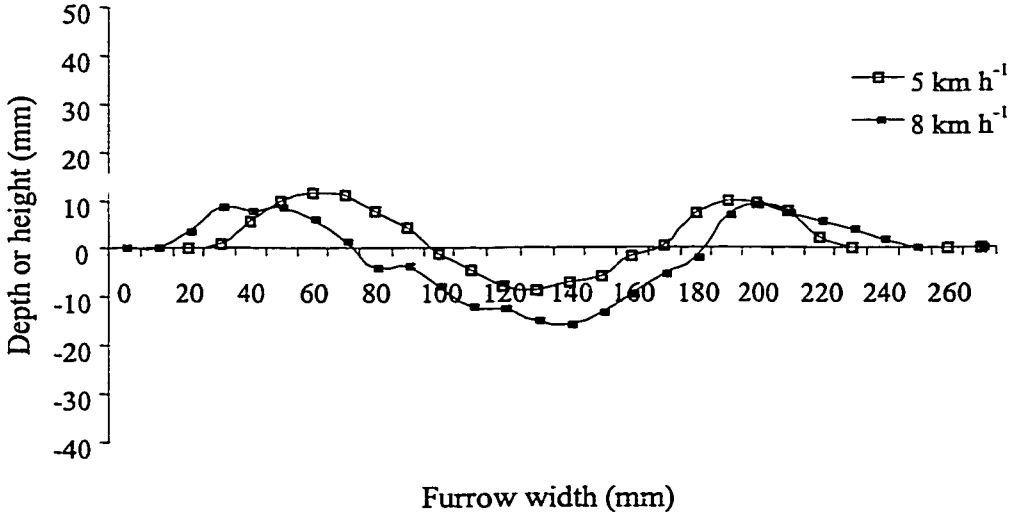

Figure 6.3 Soil profile with knife opener at 5 and 8 km h^{-1} speed and 10.1% soil moisture and 220 kPa Cone Index.

Figures 6.4 and 6.5 show the soil profile produced by the sweep and the knife opener at two different moisture contents. Increasing the moisture content resulted in a wider and higher ridge. In low moisture tests the depth of furrow is larger than that of the high ones. This is due to friability and reduction in plasticity of the soil with lower moisture contents. Increase in moisture content first increases the adhesion of soil particles to tool surface, resulting in a longer time for the soil particle to flow over the tool surface. This in turn results in a larger cross sectional area for the soil leaving the tool surface; in order to make the mass flow rate over the tool surface constant. Further increase in moisture content, will have the lubrication effect.

Figures 6.6 and 6.7 show the soil profile produced by the sweep and the knife opener at two different compaction levels. Increasing the compaction level increased the soil ridge heights for the sweep. The more upward movement of the soil particles moving across the tool indicates the possibility of existence of more lateral stress than the stress above the soil.

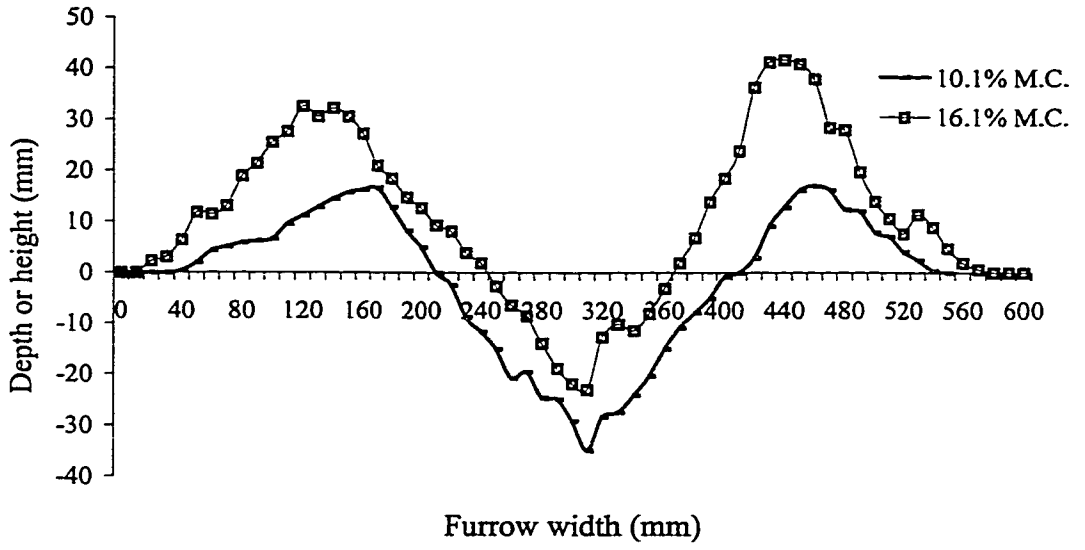

Figure 6.4 Soil profile with sweep at 10.1% and 16.1% soil moisture at 5 km h^{-1} tool travel speed and 205 kPa Cone Index.

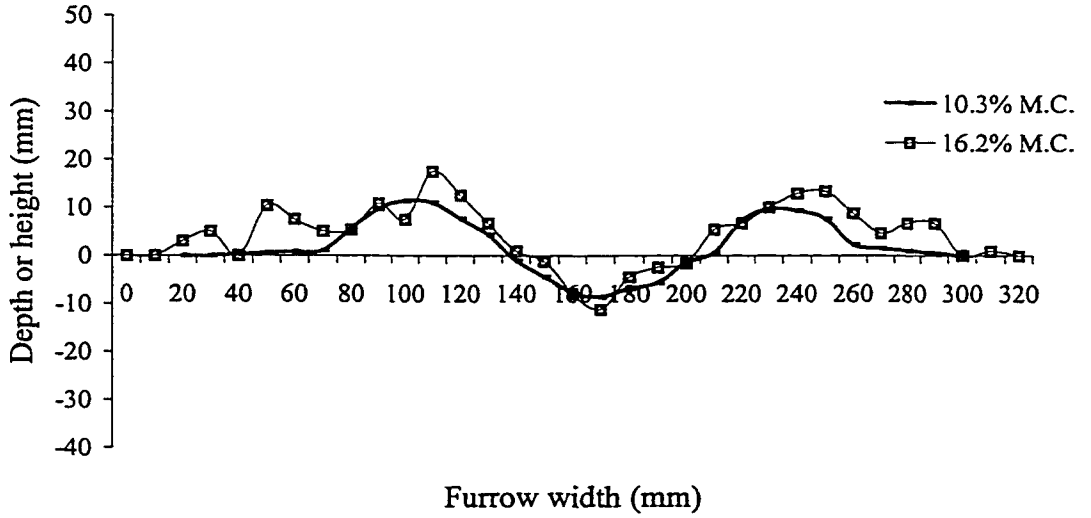

Figure 6.5 Soil profile with knife opener at 10.3% and 16.2% soil moisture at 5 km h^{-1} tool travel speed and 220 kPa Cone Index.

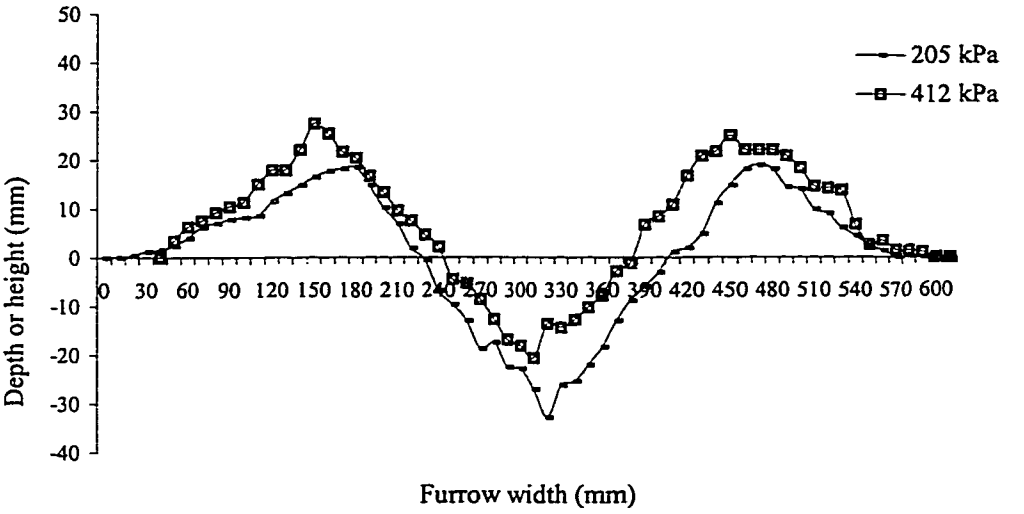

Figure 6.6 Soil profile with sweep at two compaction levels at 10.1% soil moisture and 5 km h^{-1} tool travel speed.

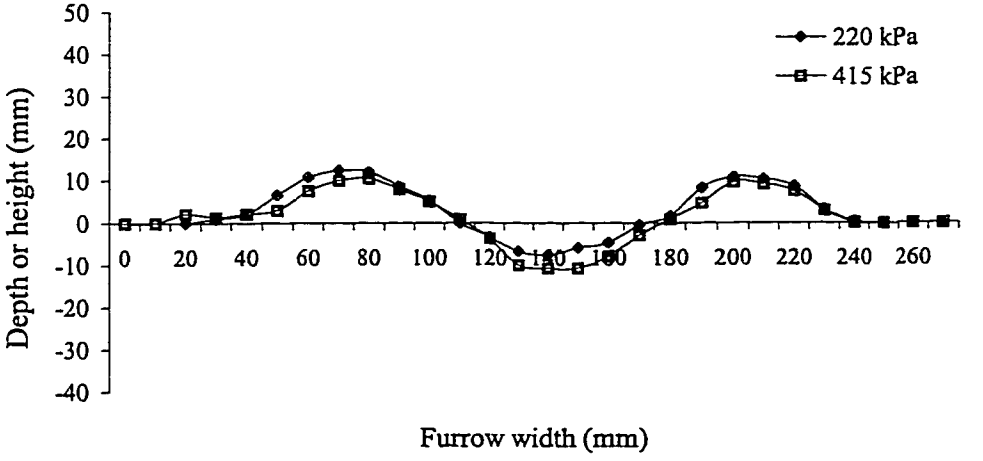

Figure 6.7 Soil profile with knife opener at two compaction levels at 10.3% soil moisture and 5 km h^{-1} tool travel speed.

6.3.2 Analysis of furrow profile for various knife openers

The furrow profiles were analysed for lateral soil movement. The cutting depth for the experiments of Chapter 5 with various knife openers was 50 mm. A furrow profile index, "C_p" was developed to indicate this lateral movement. Considering the symmetry of the cross section of the furrow profile with respect to the center line of the furrow, C_p was defined as the distance of the centroid of the one side of furrow profile cross section to the center line of the furrow. This index became an indicator of the lateral movement of the soil. Greater values of C_p meant greater lateral soil movement. C_p values were calculated from the soil profile measured by the laser profile-meter after the tests with different tool shapes under different soil conditions and tool operational speed. These values are given in Table 6.1. These C_p values show the relative lateral soil movement for various tools and the test conditions. Analysis of variance of C_p values is given in Appendix-A, Table IX. This analysis showed that the effect of soil moisture content, soil compaction, and tool shape on lateral soil movement are highly significant. The effect of speed was just significant. Therefore, similar to forward movement of soil described in previous chapters, the lateral movement of soil is also affected by tool shape, tool operational speed, soil moisture content, and soil compaction.

Table 6.1: Cp Index (Distance of the centroid of one side of soil profile cross section from the furrow center line) values for different knife openers.

Compaction	Moisture	Tool speed	C_p Index*			
		($km\ h^{-1}$)	T1	T2	T3	T4
Low	Low	10	36	38	30	40
		15	39	45	46	41
		20	42	52	47	37
		25	37	47	54	31
	Medium	10	37	48	34	38
		15	40	50	38	31
		20	46	42	37	37
		25	47	41	40	32
	High	10	24	38	32	33
		15	40	43	43	26
		20	34	39	44	33
		25	39	37	36	30
Medium	Low	10	33	32	38	30
		15	33	46	44	35
		20	37	35	37	29
		25	35	49	44	34
	Medium	10	38	44	33	31
		15	43	42	31	28
		20	36	40	35	21
		25	45	46	37	21
	High	10	33	32	26	23
		15	33	30	36	23
		20	37	39	31	26
		25	34	45	22	17
High	Low	10	33	42	47	38
		15	39	52	35	32
		20	36	69	31	40
		25	40	54	38	31
	Medium	10	41	44	37	22
		15	44	44	33	20
		20	37	42	24	17
		25	38	48	29	17
	High	10	34	32	28	20
		15	40	45	33	23
		20	35	42	39	20
		25	28	31	37	22

* C_p Index = Distance of the centroid of one side of soil profile from center line of furrow

Soil flowing around the tools has a lesser speed due to the soil-tool adhesion and soil-soil friction. Adhesion of the soil to tillage tools causes a normal force on the contact surface. Since the frictional force is a function of the normal load, adhesion increases the frictional force. Any parameter contributing to increase in soil-tool adhesion and soil-soil friction reduces the speed of soil flowing around the tool.

Reduction in the speed of the soil flowing around the tool increases the cross sectional area of the soil flowing around the tool to make the input soil flow rate equal to the output soil flow rate.

The values of C_p Means in Appendix-A, Table IX show that the flat tool (T2) has the highest soil lateral movement followed by the 90° triangular face tool (T1). The elliptical tool (T3) and the 45° triangular face tool (T4) have almost the same soil lateral movement with the T4 tool having a lesser value. The size of the soil lump attached to the tool surface was very high for tool shapes T1 and T2. Tool shapes T3 and T4 had the lowest soil lump attached to them (Table 5.1).

Comparing the geometry of the T2 (flat) and T1 (90° triangular), one may conclude that T1 should push more soil in the transverse direction and develop a wider profile and T2 should push the soil mainly in forward direction. This may not happen in practice. Depending on the surface roughness of the tool and soil condition, a compacted soil body may be formed in front of the tillage tool. This compacted soil body attaches to the tool and becomes a part of the tool and changes the shape of the tool interacting with soil (Figures 5.10 to 5.13).

The soil lump attached to the tool surface changed the shape of the tool surface in contact with the soil flowing around the tool. This phenomenon not only increased the

contact surface, but also changed the nature of friction from soil-tool to soil-soil which is higher. Soil flowing around the tool shapes T1 and T2 had more difficulty to move around the tool and their speed was reduced. This reduction in speed resulted in a larger soil profile cross section. It can be concluded that the 45° triangular tip tool has the least soil lateral movement.

Increasing the soil moisture content first increased the soil lateral movement, but a further increase in soil moisture content resulted in decrease of soil lateral movement. Soil moisture content increase, resulted in an increase in the adhesion of the soil to tool surface and that caused the profile cross section to increase. Further increase of moisture, reduced the adhesion of soil to the tool because of its lubrication effect that resulted in lower soil lateral movement.

Increasing the compaction resulted in the reduction in the volume of the input soil flow rate and, therefore, a smaller soil furrow cross section.

Increasing tool operational speed from 10 km h^{-1} to 15 km h^{-1} increased the soil lateral movement, but further increase in speed, reduced it. Although there is disagreement between researchers about the effect of sliding speed and adhesion that was mentioned in literature review section, the author agrees with the finding of Stafford and Tanner (1983) that adhesion decreases with increasing speed. It seems that the adhesion was reduced at the speeds of more that 10 km h^{-1}. This reduction in adhesion made the flow of soil around the tool easier and resulted in a smaller soil profile cross section and decrease of soil lateral movement.

6.4 Summary

In the experiments with the sweep and the knife opener in general, the furrow width and ridge height for the sweep was larger than that of the knife opener. Flow of the soil particles over the tool surface resulted in a reduction in speed of soil particles in the direction of travel. This results in an increase in the volume of the soil leaving the tillage tool to make the output and input mass flow rates equal. Increasing the travel speed of the tool increased the furrow depth and the lateral distance that soil was thrown by the sweep and the knife opener. Increasing the moisture content resulted in a wider and higher ridge. For low moisture content values, the depth of furrow was larger than that of high moisture content values. Increasing the compaction level increased the soil ridge heights.

To study the soil profile in high speed experiments an index C_p, an indicator of the lateral movement of the soil was defined as the distance of the centroid of the furrow profile cross section to the center line of the furrow. Analysis of variance of the data for C_p showed that:

- The effect of soil moisture content, soil compaction, tool shape on lateral soil movement are highly significant.
- The values of C_p Means show that the flat tool (T2) has the highest lateral soil movement followed by the 90° triangular (T1). The elliptical tool (T3) and the 45° triangular tool have almost the same lateral soil movement with the 45° triangular tool (T4) having a lesser value. The amount of the soil lump that was attached to the tool surface was very high for tool shapes T1 and T2. Tool shapes T3 and T4 had the lowest. It can be concluded that the 45° triangular tip tool has the least soil lateral movement.

- Increasing the soil moisture content first increased the lateral soil movement, but further increase in soil moisture resulted in decrease of lateral soil movement. Further increase of moisture, reduced the adhesion of soil to the tool because of its lubrication effect that resulted in lower values for lateral soil movement.
- Increasing the compaction resulted in the reduction in the volume of the input soil flow rate and, therefore, a smaller soil furrow cross section.
- Increasing tool travel speed from 10 km h^{-1} to 15 km h^{-1} increased the lateral soil movement, but further increases in speed, reduced it. It seems that the adhesion was reduced at the speeds of more that 10 km h^{-1}. This reduction in adhesion made the flow of soil around the tool easier and resulted in a smaller soil profile cross section and decrease of lateral soil movement.

CHAPTER 7

SOIL MOVEMENT MODEL DEVELOPMENT

7.1 Overview

Movement of the soil particles during tillage operation is the result of the application of force by the tillage tool. The soil fails due to the action of the applied force, and soil particles move in various directions. The tool geometry, operating speed, and soil physical properties are the important factors in soil movement. Results from previous experiments (Sharifat and Kushwaha, 1997) have shown that soil translocation per unit width or per unit frontal area was higher with a narrow tillage tool (knife opener) than with a wide tool (sweep). A mathematical model for soil movement with speed of operation of the tillage tool was developed. In order to include the effects of soil physical properties and tool shape, a regression analysis of soil bin test data was conducted. The results were compared with the experimental values obtained in the soil bin tests.

7.1.1 Stress distribution in soil

Stress distribution under vertical loads considering elastic soil behavior has been studied for decades. Several methods for estimation of stress distributions have been reported. Some methods have been introduced by civil. Researchers in agricultural soil mechanics have used the stress distribution estimation methods to study the tire-soil

system problems. Boussinesq (Koolen and Kuipers, 1983) used vertical point-load method on a semi-infinite elastic medium for approximating soil-tire system. A small cube was considered at a position represented by radial vector ***r***. The vector ***r*** is perpendicular to one side of the cube (Figure 7.1).

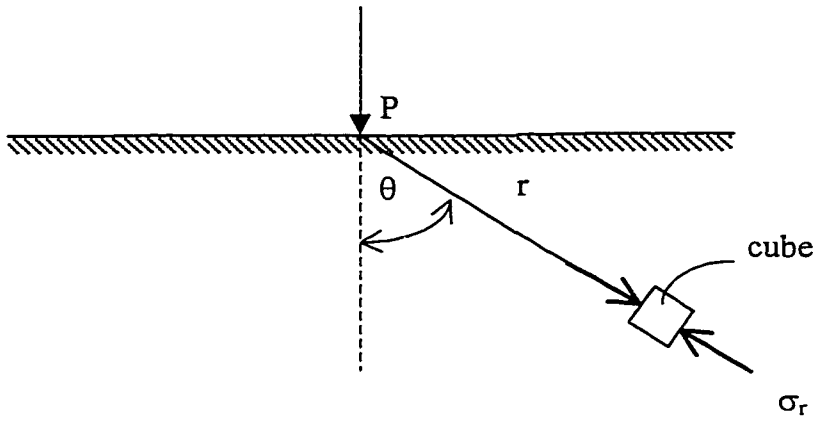

Figure 7.1 Soil stress due to a vertical point load (from Koolen and Kuiper, 1983).

It was concluded that there are no stresses on any side of the cube except on the side perpendicular to the radial vector ***r***. The normal stress on this side which is a principal stress is given by

$$\sigma_r = \sigma_1 = \frac{3P}{2\pi r^2}\cos\theta \qquad (7.1)$$

Using Equation 7.1, the principal stress σ_1 in any point of the soil can be calculated. Direction of the stress is the same as vector ***r***. Equation 7.1 is based on elastic

soil behavior and predicts the same stress distribution for all soils. Since soil behavior is not elastic, soil strength affects stress distribution in soil. Fröhlich modified Equation 7.1 to include a factor ξ which relates to soil condition (Koolen and Kuipers, 1983). The modified equation becomes:

$$\sigma_r = \sigma_1 = \frac{\xi P}{2\pi r^2}\cos^{\xi-2}\theta \qquad (7.2)$$

The factor ξ is called the concentration factor. As soil becomes softer, the value of ξ increases. Suggested values for ξ are 3 for hard soil, 4 for normal soil, and 5 for soft soil. These effects are shown in Figure 7.2. Stress distributions under different loading such as load applied on a circular area, or on an infinite strip were studied and different equations for estimation of the stress distributions were developed. Koolen and Kuipers (1983) reported the following conclusions from their study.

1- Multiplying the applied stress by a factor m, the stress in any point of the soil was multiplied by m.

2- Maximum normal stresses occurred at the contact area.

3- If the normal stresses on the surface elements of the contact area remain unchanged and all linear dimensions of the contact area are multiplied by m, stresses will reach m times deeper into the soil

.

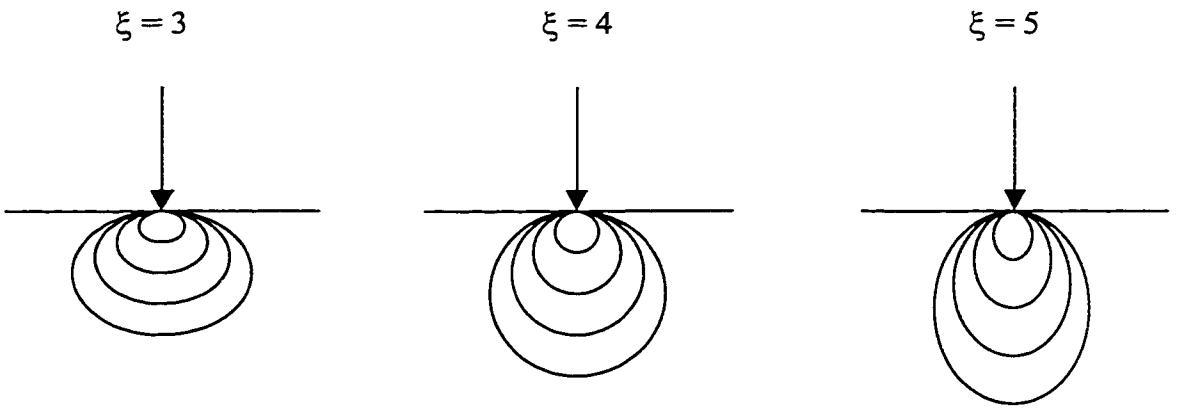

Figure 7.2 Schematic representation of stress distribution under a point load in different soil conditions.

Stress distribution under a horizontally applied load has not been studied adequately. Zelenin (1950) has studied the stress distributions in soil in front of a tillage tool working in a sandy loam soil. Sensors were placed in soil in three directions. One series of sensors was placed in the direction of movement of tillage tool. Two series of sensors were placed in straight lines making ±30° and ±45° angles with tillage tool direction of travel. Figure 7.3 shows the lines of equal stress in front of the tillage tool resulted from this experiment. For normal soil conditions, the stress distribution in soil can be considered to have a circular shape. Although the actual stress distribution may not follow an exact circular pattern, for modeling purposes it can be considered to be circular.

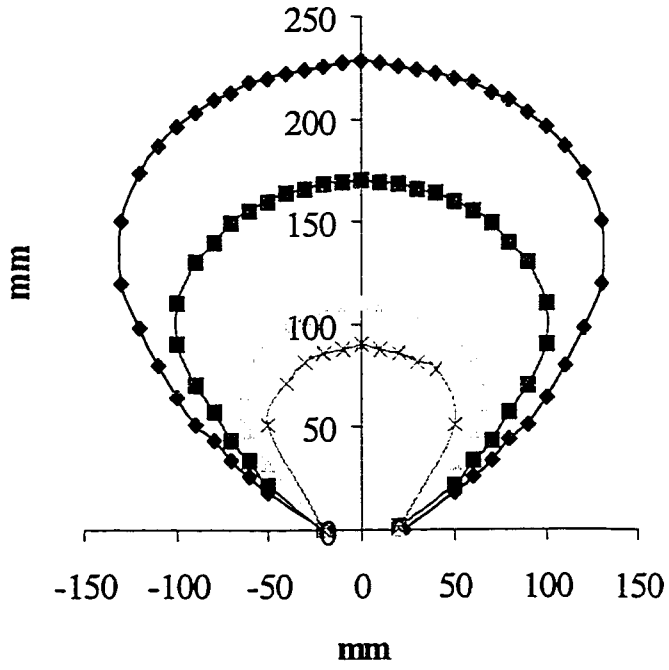

Figure 7.3 Lines of equal stress in front of tillage tool (from Zelenin, 1950).

7.2 Model Development

The tool movement forces the soil located in front of the tillage tool to move. The pattern of soil particle movement depends on tool geometry, speed of operation and soil conditions. Movement of the tillage tool causes the direct movement of the soil particles located right in front of it in the direction of travel of the tool with the same speed as tillage tool. Tillage tool movement also affects the other soil particles located in the sides of the tillage tool. The cohesion and adhesion properties of the soil particles influence the relative movement of soil particles. Some of this movement is in the direction of tillage tool and some toward the sides of the direction of tool travel. Soil particles go forward and at the same time they may move to the sides till they go out of the influence of the tillage tool and finally, the tillage tool passes them and they come to rest.

The pattern of movement of soil particles in front of the tillage tool suggests existence of an influence zone in front of the tillage tool. To simplify the procedure, it was assumed that the influence zone has a circular shape and moves with the tool. The iso-intensity circles that are attached to each other at the contact point create the influence zone. As the radius of the field increases, the soil movement decreases. The smallest circle of the zone has the highest intensity as the soil particles close to the tool have the highest tendency for movement. The largest circle that is representative of the soil particles at some distance from the tool would have the least tendency for movement. The path of movements of the soil particles are lines drawn perpendicular at each circle's perimeter as shown in Figure 7.4. Arrows show the path of movement of soil particles. The magnitude and direction of the movement of each soil particle depends on its location in the influence zone. Soil particles located right in front of the tillage tool will

have the same velocity as the tool. The velocity of the soil particles would decrease toward the perimeter away from the center of influence zone. The points located outside of the influence zone would have no velocity and hence will not move.

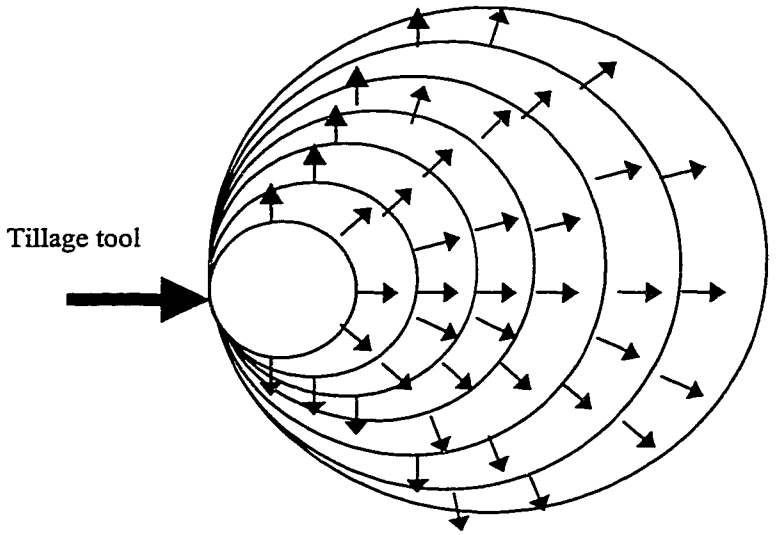

Figure 7.4 Influence zone and iso-intensity circles.

Soil in front of the tool is considered to have a semi-infinite dimension. At the start of tool movement, soil particles located in front of the tool are displaced forward. After rearrangement of the soil particles, when there is no margin for further soil compaction in front of the tool, soil particles start to move to the sides. The influence zone is assumed to move with the tillage tool. The movement of the tillage tool will affect soil particles located in a width equal to the largest diameter of the influence zone. Depending on the position of the soil particle, it will be affected by one of the iso-intensity circles. The movement of the soil particle will be proportional to the intensity of the corresponding circle. The intensity of a circle is a percentage of the tool movement

and depends on its radius. Direction of the movement of the soil particle will be perpendicular to the perimeter of the circle where the particle would be located. After this movement, the soil particle will attain a new position.

During this period, the tillage tool has also advanced and, hence, so does the influence zone that travels with it. This tool advance and the movement of the influence zone will place the soil particle in a new position relative to the influence zone. Depending on the new relative position of the soil particle, it will be affected again by another circle of the influence zone and will reach to a new position. This phenomenon will continue till the soil particle goes out of the area formed by the influence zone. This area is the effective area created by the tillage tool. Figure 7.5 shows the movement of a soil particle by the influence zone. The movement of the soil particle starts even before tillage tool reaches the soil particle and it may not have any contact with the tool in the course of its movement. Soil particles located in front of the tillage tool move perpendicular to the perimeter of the circle of influence which is in direction of motion of tillage tool. There is no lateral movement for the particle and its new position is in the direction of motion of the tillage tool. The next circle of influence will also move the particle in the same manner and this pattern continues. So, soil particles which come in contact with the tool, theoretically should travel with tool as long as the tillage tool is moving. However, the sliding action prevents this from happening in practice. Thus, the model is not applicable for the movement of the soil particles located right in front of the tillage tool since no sliding of particle is taken into account within the model.

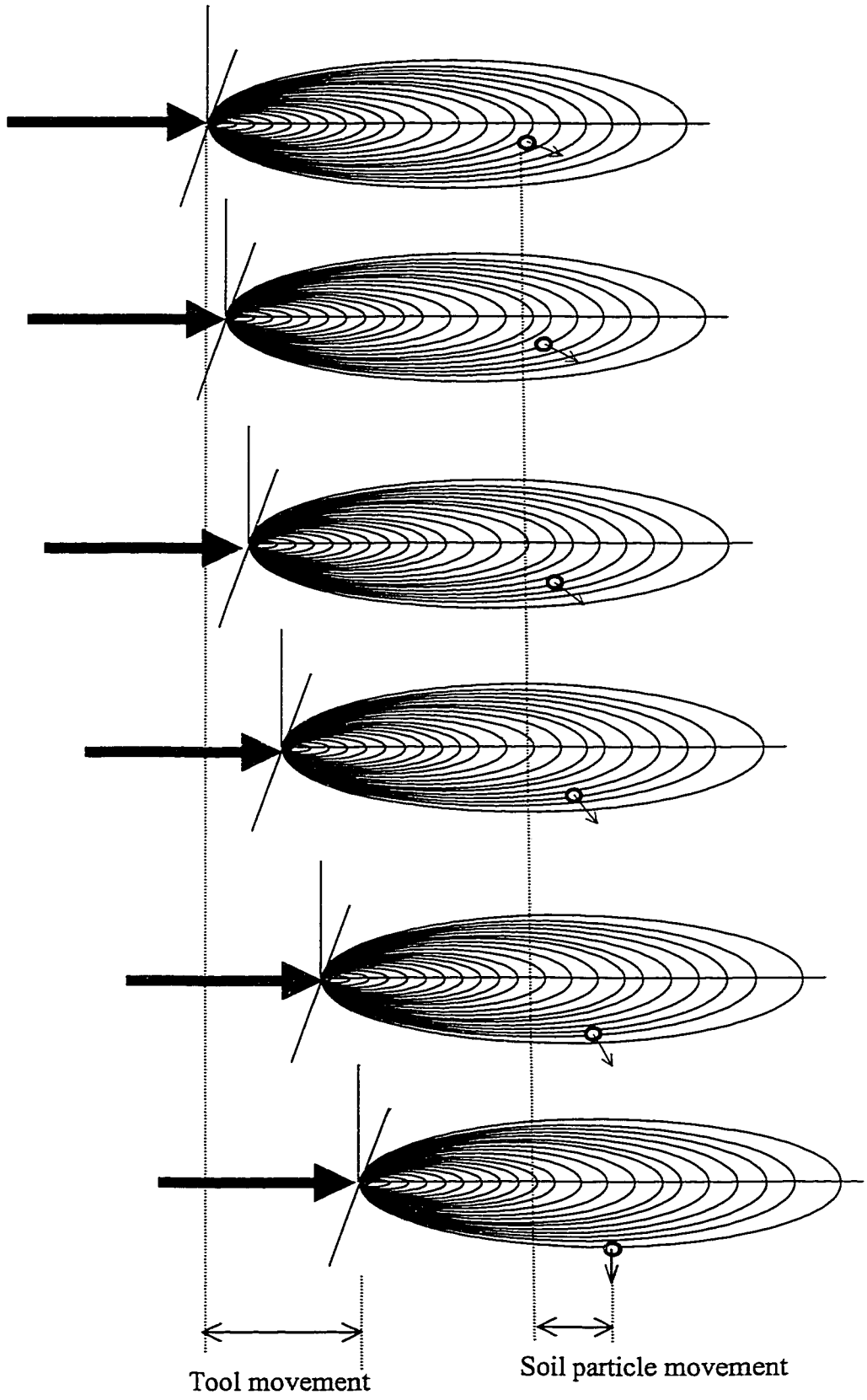

Figure 7.5 Pattern of soil movement in front of tillage tool.

7.3 Theoretical Aspects of Soil Movement Model

Soil influence zone can be described as an oblique conical surface made on the largest circle of the influence zone as shown in Fig. 7.6. The intensity of the zone is defined as a parameter z. The magnitude of the z parameter for each point in the influence zone depends on its reference and it shows the velocity ratio of that point to tool. All the points located on the same iso-intensity circle will have the same Z value. The vertical distance of any point located in the influence zone from the cone surface gives the Z parameter for that point.

$$z = f(x, y)$$

Development of the equation of cone surface is shown in Appendix-B

The equation of the conical surface (influence zone) is:

$$z = f\big((x - v_o t), y\big) = h - \frac{h(x - v_o t)}{2} - \frac{hy^2}{2(x - v_o t)} \tag{7.3}$$

Soil particles movement is in the opposite direction of the gradient vector. The gradient vector is:

$$\vec{\nabla}_t = \begin{pmatrix} -\frac{h}{2} + \frac{hy^2}{2}\left(\frac{1}{(x - v_o t)}\right)^2 \\ \\ \frac{-hy}{(x - v_o t)} \end{pmatrix}_j^i \tag{7.4}$$

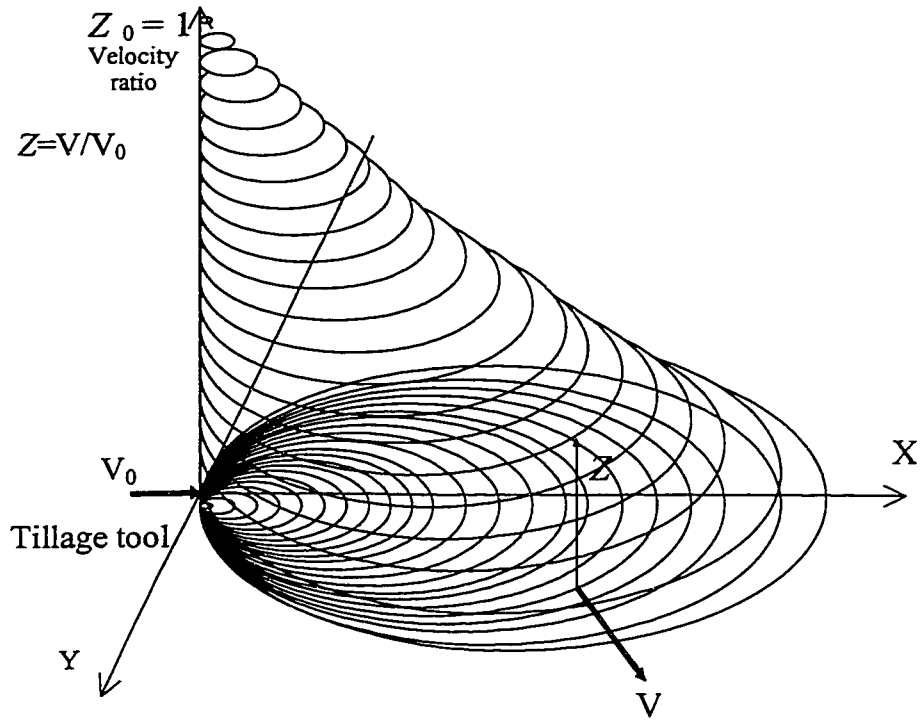

Figure 7.6 Conical surface representing Z parameter.

To calculate the unit vector of gradient, gradient vector is divided by its magnitude.

$$\frac{\nabla_t}{\|\nabla_t\|} = \begin{pmatrix} \dfrac{y^2-(x-v_o t)^2}{y^2+(x-v_o t)^2} \\ \\ \dfrac{-2y(x-v_o t)}{y^2+(x-v_o t)^2} \end{pmatrix} \tag{7.6}$$

The movement vector has the magnitude of Z and is in the direction of the gradient unit vector. To find the movement vector, the gradient unit vector was multiplied by Z.

$$\text{Movement vector} = \frac{\nabla_t}{\|\nabla_t\|} \times Z$$

$$\text{Movement vector} = \begin{pmatrix} \dfrac{y^2-(x-v_o t)^2}{y^2+(x-v_o t)^2} \\ \\ \dfrac{-2y(x-v_o t)}{y^2+(x-v_o t)^2} \end{pmatrix} \times \left(h - \frac{h(x-v_o t)}{2} - \frac{hy^2}{2(x-v_o t)}\right) \tag{7.7}$$

The movement vector shows the velocity vector for any point in front of the tillage tool. Solving this differential equation results in the "equation of motion" for that point. The differential equation was solved by numerical method using the MATLAB software.

Figure 7.7 and Appendix-A, Table X show the results of the numerical solution of the differential equation after 1, 1.5, 2, 2.5, and 3 seconds at tool speed of one unit per second. The lowest curve in Figure 7.7 shows the soil movement after 1 second of tool operation.

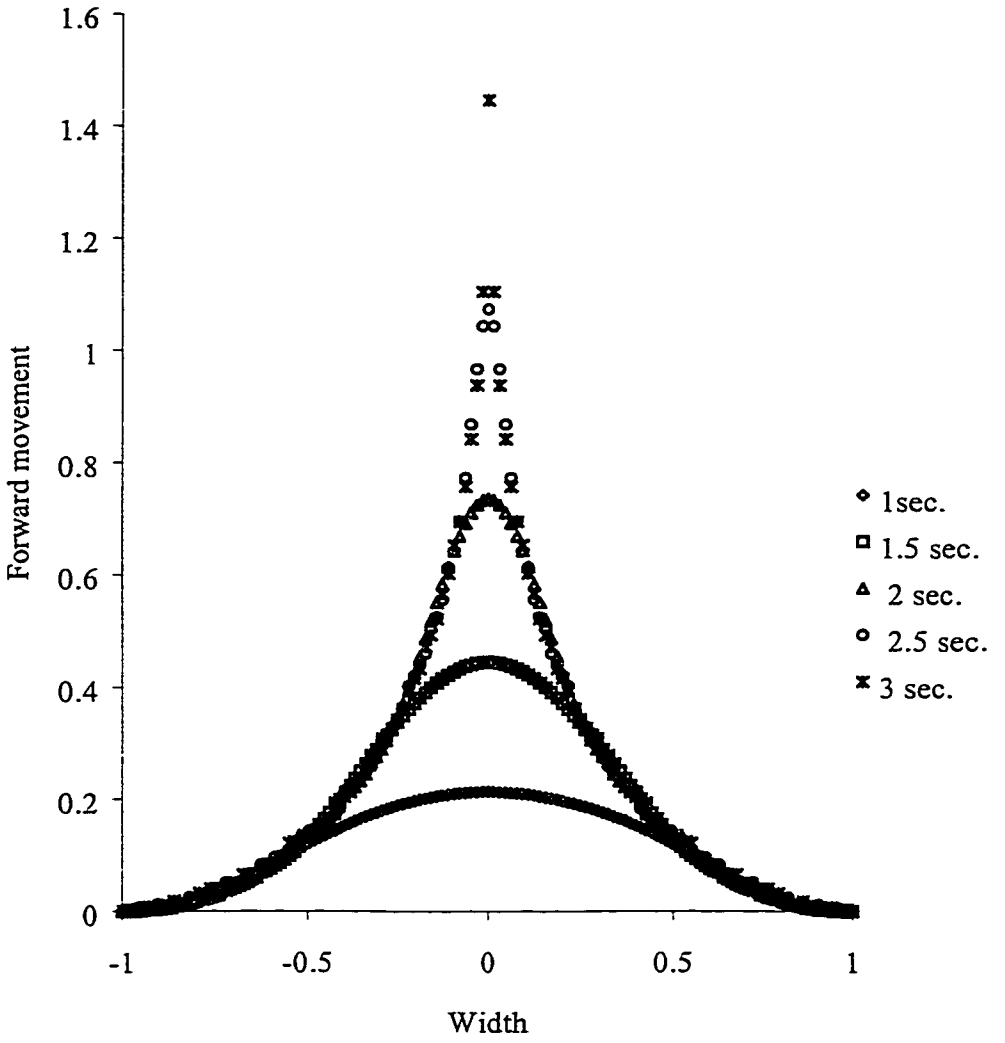

Figure 7.7 Results of the numerical solution of the differential equation of soil movement after 1, 1.5, 2, 2.5 and 3 seconds at unit speed.

For example, if a tillage tool operates at 1 m s^{-1} speed, it will advance one meter in one second and the maximum amount of movement for soil particles will be around 0.2 meter. After 1.5 seconds the maximum particle movement will be around 0.45 meters. After 2 seconds the amount of the soil movement is around 0.7 meter. As the tool advances further, there is no movement for most of the side particles, which means that the tool has passed them and they are now out of the range of the influence zone. The only particles that continue to move are those located right in front of the tillage tool.

7.4 Application of the Model to Experimental Data

The developed soil movement model predicts the soil movement with the speed of operation of tillage tool only. Four tool shape factors and soil physical properties were used in regression analysis to predict soil movement with different tool shapes, speed of operation, and soil conditions of moisture and compaction level. Appendix A, Table X shows the results of the numerical solution of the differential equation of soil forward movement. The results are based on the tillage tool operational speed of 1 unit. The model was calibrated by using the results of the high speed tillage experiments by Sharifat and Kushwaha (1998). In high speed experiments 19 plastic blocks of 10 x 10 x 11 mm with total width of 190 mm were used to the depth of 10 mm. Four tool shapes of 90° triangular (T1), Flat (T2), elliptical (T3), and 45° triangular (T4) were used. To apply the model to experimental data, the results from the model were converted to the soil movement corresponding to the tool speed of 10, 15, 20, and 25 km h^{-1} used in the experiments. The calculated soil movement for the speeds used in the experiments are shown in Figure 7.8.and Table XI Appendix-A.

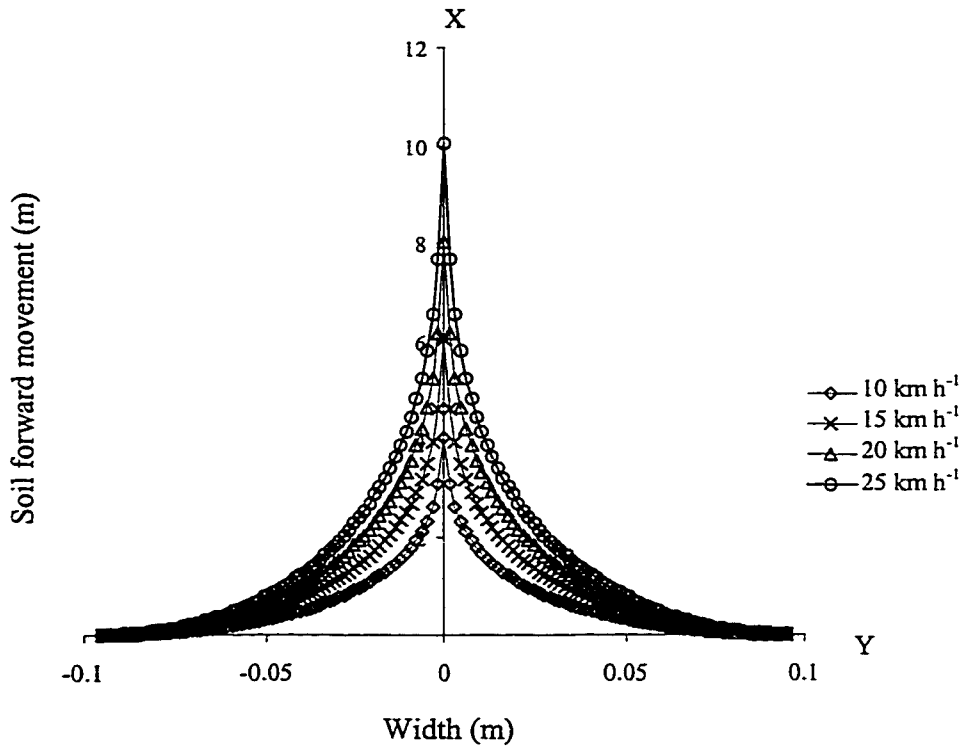

Figure 7.8 Graphical representation of the soil movement at different speeds predicted by the model.

Since the model is not applicable for calculation of movement of the soil particles located right in front of the tillage tool, in comparing the results obtained from the model to experimental data, soil movement of the block located directly in front of the tillage tool was removed from the calculation. Its movement was replaced with the average movements of its two adjacent blocks in both sides. The same procedure was used for the data from the model. To determine the relationship of the soil movement measured in the experiments and the values obtained from the model, and tool and soil parameters, regression analysis and analysis of variance were performed on the data. The actual soil movement was considered as a dependent variable. The soil movement was calculated from the model, and the influence of soil moisture content, and soil compaction were considered as independent variables. The results are shown in Tables XII to XV in Appendix-A. The equations of soil movement determined from the regression analysis are given below.

$$S.M\ (90^\circ\ \text{triangular}) = -0.00786 - 0.000003\ C - 0.000023\ M + 0.288\ S.F \quad (7.8)$$

$$S.M\ (\text{Flat}) = -0.00878 + 0.000011\ C - 0.000081\ M + 0.288\ S.F \quad (7.9)$$

$$S.M\ (\text{Elliptical}) = -0.00734 - 0.000008\ C + 0.000435\ M + 0.109\ S.F \quad (7.10)$$

$$S.M\ (45^\circ\ \text{triangular}) = -0.00235 - 0.000009\ C + 0.000055\ M + 0.139\ S.F \quad (7.11)$$

where:

S.M = soil movement (m)

C = soil compaction (C.I)

M = soil moisture content (%)

S.F = soil movement predicted by the "speed soil movement model"

Examining the Equations 7.8 to 7.11, it can be concluded that the major contribution to the value of actual soil movement is from the model term or speed factor (S.F) that is representative of tool speed. The coefficients of the model term (SF) in the regression equations may be considered as "Shape Factors" representing different tool shapes. Since the soil movement by the 90° triangular and the flat tools are very close, their shape factors are similar and equal to 0.29. Elliptical and 45° triangular have shape factors of 0.11 and 0.14 respectively.

The values of soil movement for different tool shapes and speeds under different soil conditions were calculated from the model and from the regression equations that includes the model. Results are shown in Tables 7.1 to 7.4. Comparison of the results of soil movement measurement with predicted soil movement show that the regression equations give satisfactory results and the error for the 90° triangular, flat, elliptical, and 45° triangular were 7%, 13%, 20%, and 13% respectively.

The model was also applied to the data obtained with knife opener by Sharifat and Kushwaha (1995). The regression analysis for the knife opener is shown in Appendix-A, Table XVI. The regression equation for the knife opener is:

$$S.M\ (Knife\ opener) = -0.00851 + 0.000009C + 0.000155\,M + 0.215\,S.F \qquad (7.12)$$

Soil movement for the knife opener using the above equation was calculated and compared with the actual values measured in the experiments and are shown in Table 7.5.

Table 7.1: Soil movement by the 90° triangular tool (T1) by experiment, movement model, and regression analysis.

Compaction (kPa)	Moisture (%)	Speed (kmh^{-1})	Actual movement from experiments (m)	Movement calculated from model (m)	Movement calculated from regression (m)	Error (%)
59	11	10	0.008	0.071	0.012	32
59	11	15	0.021	0.106	0.022	5
59	11	20	0.031	0.142	0.032	3
59	11	25	0.045	0.177	0.043	5
60	14.58	10	0.011	0.071	0.012	6
60	14.58	15	0.022	0.106	0.022	1
60	14.58	20	0.032	0.142	0.032	2
60	14.58	25	0.042	0.177	0.043	0
66	16.85	10	0.012	0.071	0.012	3
66	16.85	15	0.024	0.106	0.022	9
66	16.85	20	0.036	0.142	0.032	10
66	16.85	25	0.043	0.177	0.042	1
148	11.17	10	0.011	0.071	0.012	7
148	11.17	15	0.023	0.106	0.022	3
148	11.17	20	0.034	0.142	0.032	4
148	11.17	25	0.043	0.177	0.042	0
160	14.94	10	0.013	0.071	0.012	10
160	14.94	15	0.023	0.106	0.022	3
160	14.94	20	0.032	0.142	0.032	1
160	14.94	25	0.042	0.177	0.042	0
194	17.07	10	0.013	0.071	0.012	11
194	17.07	15	0.017	0.106	0.022	20
194	17.07	20	0.031	0.142	0.032	2
194	17.07	25	0.041	0.177	0.042	3
264	11.17	10	0.010	0.071	0.011	14
264	11.17	15	0.021	0.106	0.022	3
264	11.17	20	0.034	0.142	0.032	8
264	11.17	25	0.043	0.177	0.042	2
320	15.06	10	0.016	0.071	0.011	42
320	15.06	15	0.022	0.106	0.021	2
320	15.06	20	0.028	0.142	0.032	12
320	15.06	25	0.043	0.177	0.042	3
300	17.63	10	0.013	0.071	0.011	12
300	17.63	15	0.022	0.106	0.021	4
300	17.63	20	0.031	0.142	0.032	3
300	17.63	25	0.038	0.177	0.042	9
					Average error for tool T1	7

Table 7.2: Soil movement by the flat tool (T2) by experiment, movement model, and regression analysis.

Compaction (kPa)	Moisture (%)	Speed (km h^{-1})	Actual movement from experiments (m)	Movement calculated from model (m)	Movement calculated from regression (m)	Error (%)
59	11	10	0.009	0.071	0.011	20
59	11	15	0.018	0.106	0.022	18
59	11	20	0.035	0.142	0.032	11
59	11	25	0.034	0.177	0.042	19
60	14.58	10	0.016	0.071	0.011	44
60	14.58	15	0.021	0.106	0.021	3
60	14.58	20	0.039	0.142	0.031	23
60	14.58	25	0.044	0.177	0.042	6
66	16.85	10	0.009	0.071	0.011	21
66	16.85	15	0.022	0.106	0.021	6
66	16.85	20	0.034	0.142	0.031	8
66	16.85	25	0.043	0.177	0.041	3
148	11.17	10	0.010	0.071	0.012	17
148	11.17	15	0.028	0.106	0.023	23
148	11.17	20	0.036	0.142	0.033	9
148	11.17	25	0.043	0.177	0.043	1
160	14.94	10	0.010	0.071	0.012	20
160	14.94	15	0.021	0.106	0.022	6
160	14.94	20	0.027	0.142	0.033	17
160	14.94	25	0.043	0.177	0.043	2
194	17.07	10	0.017	0.071	0.012	39
194	17.07	15	0.024	0.106	0.023	8
194	17.07	20	0.027	0.142	0.033	19
194	17.07	25	0.036	0.177	0.043	17
264	11.17	10	0.010	0.071	0.014	26
264	11.17	15	0.026	0.106	0.024	8
264	11.17	20	0.035	0.142	0.034	2
264	11.17	25	0.046	0.177	0.044	5
320	15.06	10	0.011	0.071	0.014	21
320	15.06	15	0.025	0.106	0.024	5
320	15.06	20	0.040	0.142	0.034	17
320	15.06	25	0.047	0.177	0.044	5
300	17.63	10	0.013	0.071	0.013	7
300	17.63	15	0.026	0.106	0.024	9
300	17.63	20	0.033	0.142	0.034	3
300	17.63	25	0.043	0.177	0.044	2
				Average error for tool T2		**13**

Table 7.3: Soil movement by the elliptical tool (T3) by experiment, movement model, and regression analysis.

Compaction (kPa)	Moisture (%)	Speed (km h^{-1})	Actual movement from experiments (m)	Movement calculated from model (m)	Movement calculated from regression (m)	Error %
59	11	10	0.003	0.071	0.005	26
59	11	15	0.006	0.106	0.009	26
59	11	20	0.014	0.142	0.012	13
59	11	25	0.017	0.177	0.016	4
60	14.58	10	0.004	0.071	0.006	33
60	14.58	15	0.012	0.106	0.010	19
60	14.58	20	0.017	0.142	0.014	22
60	14.58	25	0.016	0.177	0.018	12
66	16.85	10	0.004	0.071	0.007	46
66	16.85	15	0.010	0.106	0.011	5
66	16.85	20	0.018	0.142	0.015	20
66	16.85	25	0.016	0.177	0.019	14
148	11.17	10	0.003	0.071	0.004	19
148	11.17	15	0.009	0.106	0.008	8
148	11.17	20	0.011	0.142	0.012	2
148	11.17	25	0.018	0.177	0.016	17
160	14.94	10	0.004	0.071	0.006	29
160	14.94	15	0.006	0.106	0.009	41
160	14.94	20	0.013	0.142	0.013	4
160	14.94	25	0.020	0.177	0.017	17
194	17.07	10	0.009	0.071	0.006	46
194	17.07	15	0.015	0.106	0.010	44
194	17.07	20	0.017	0.142	0.014	20
194	17.07	25	0.017	0.177	0.018	5
264	11.17	10	0.003	0.071	0.003	11
264	11.17	15	0.007	0.106	0.007	6
264	11.17	20	0.008	0.142	0.011	22
264	11.17	25	0.016	0.177	0.015	6
320	15.06	10	0.006	0.071	0.004	49
320	15.06	15	0.009	0.106	0.008	11
320	15.06	20	0.010	0.142	0.012	16
320	15.06	25	0.015	0.177	0.016	3
300	17.63	10	0.008	0.071	0.006	45
300	17.63	15	0.008	0.106	0.009	18
300	17.63	20	0.012	0.142	0.013	13
300	17.63	25	0.014	0.177	0.017	21
					Average error for tool T3	**20**

Table 7.4: Soil movement by the 45° triangular tool (T4) by experiment, movement model, and regression analysis

Compaction (kPa)	Moisture (%)	Speed (km h^{-1})	Actual movement from experiments (m)	Movement calculated from model (m)	Movement calculated from regression (m)	Error (%)
59	11	10	0.006	0.071	0.008	25
59	11	15	0.009	0.106	0.012	30
59	11	20	0.018	0.142	0.017	3
59	11	25	0.022	0.177	0.022	0
60	14.58	10	0.007	0.071	0.008	11
60	14.58	15	0.017	0.106	0.013	32
60	14.58	20	0.018	0.142	0.018	1
60	14.58	25	0.025	0.177	0.022	12
66	16.85	10	0.006	0.071	0.008	22
66	16.85	15	0.014	0.106	0.013	7
66	16.85	20	0.018	0.142	0.018	4
66	16.85	25	0.020	0.177	0.023	10
148	11.17	10	0.009	0.071	0.007	32
148	11.17	15	0.010	0.106	0.012	16
148	11.17	20	0.017	0.142	0.017	3
148	11.17	25	0.020	0.177	0.021	9
160	14.94	10	0.006	0.071	0.007	12
160	14.94	15	0.014	0.106	0.012	18
160	14.94	20	0.017	0.142	0.017	1
160	14.94	25	0.023	0.177	0.022	6
194	17.07	10	0.009	0.071	0.007	36
194	17.07	15	0.011	0.106	0.012	2
194	17.07	20	0.016	0.142	0.017	3
194	17.07	25	0.019	0.177	0.021	11
264	11.17	10	0.005	0.071	0.006	6
264	11.17	15	0.011	0.106	0.011	5
264	11.17	20	0.016	0.142	0.016	1
264	11.17	25	0.021	0.177	0.020	3
320	15.06	10	0.009	0.071	0.005	61
320	15.06	15	0.008	0.106	0.010	26
320	15.06	20	0.016	0.142	0.015	2
320	15.06	25	0.021	0.177	0.020	4
300	17.63	10	0.004	0.071	0.006	28
300	17.63	15	0.009	0.106	0.011	16
300	17.63	20	0.015	0.142	0.016	6
300	17.63	25	0.021	0.177	0.020	2
					Average error for tool T4	**13**

Table 7.5: Soil movement by the knife opener by experiment, movement model, and regression analysis.

Compaction (kPa)	Moisture (%)	Speed (km h^{-1})	Actual movement from experiments (m)	Movement calculated from model (m)	Movement calculated from regression (m)	Error (%)
220	10.3	5	0.0069	0.0513	0.0061	11
220	10.3	6.5	0.0087	0.0668	0.0094	8
220	10.3	8	0.0128	0.0819	0.0127	1
220	13.8	5	0.0077	0.0513	0.0066	14
220	13.8	6.5	0.0093	0.0668	0.0100	7
220	13.8	8	0.0126	0.0819	0.0132	5
210	16.13	5	0.0075	0.0513	0.0069	9
220	16.4	6.5	0.0096	0.0668	0.0104	7
210	16.13	8	0.0126	0.0819	0.0135	7
296	10.1	5	0.0066	0.0513	0.0067	2
285	10.3	6.5	0.0106	0.0668	0.0100	5
296	10.1	8	0.0143	0.0819	0.0133	7
300	13.8	5	0.0080	0.0513	0.0074	9
300	13.8	6.5	0.0107	0.0668	0.0107	0
300	13.8	8	0.0158	0.0819	0.0139	12
323	15.24	5	0.0093	0.0513	0.0078	16
320	15.7	6.5	0.0111	0.0668	0.0112	1
323	15.24	8	0.0141	0.0819	0.0144	2
412	10.2	5	0.0062	0.0513	0.0078	26
420	10.7	6.5	0.0116	0.0668	0.0113	3
412	10.2	8	0.0147	0.0819	0.0144	2
425	14.1	5	0.0087	0.0513	0.0085	2
425	14.1	6.5	0.0117	0.0668	0.0119	2
425	14.1	8	0.0162	0.0819	0.0151	7
432	16.5	5	0.0084	0.0513	0.0090	6
432	16.5	6.5	0.0130	0.0668	0.0123	5
432	16.5	8	0.0158	0.0819	0.0155	1
				Average error for the knife opener		**7**

In this case, the model provided satisfactory results and the average error was about 7%. Attempts have been made to incorporate effects of depth with the final model. The knife opener exponential model of soil movement with depth of Chapter 4 was used to predict the soil movement by four different tool shapes used in the high speed experiments under the same speed of operation and soil moisture content and compaction levels. The knife opener exponential model predicted lower values for the soil movement with all four tools. Results are shown in Appendix-A, Tables XVII and XVIII. This disagreement with results could be attributed to the difference in the nature of the tests at low and high speed. With high speed tests, the length of the soil sample to be cut by the tool was only 200 mm and the plastic blocks were placed in the middle of the 200-mm length. After coming under the influence of the tool, plastic blocks were in contact with soil only for less than 100 mm of their total movement. Since no further retarding media was available, the plastic blocks moved freely. However, at low speed tests, the tools were cutting a continuous mass of soil and the plastic blocks were in contact with soil for almost all of their path of movement. Thus, knife opener exponential model of soil movement with depth was the result of low speed tests, and that is why it predicted lower values for soil movement compared to the measured values of soil movement at high speed tests. The 200-mm length was sufficient to study energy, soil disturbance, and to evaluate tool shape factors in relation to soil movement.

Considering soil non-uniformity and difficulties in accurate measurements of soil parameters, the "speed soil movement" model combined with the equations resulted from the regression analysis produced satisfactory results.

7.5 Summary

Stress distribution in front of the tillage tool in a normal soil condition can be considered to follow a circular pattern. To model the movement of soil particles in front of the tillage tool, it was assumed that there is an influence zone in front of the tillage tool that moves with the tool. The influence zone was considered to be made of circular shapes attached to the tillage tool in the direction of travel of the tool. Moving from the center toward the perimeter of the influence zone, the intensity of the field decreases. During the movement of the tillage tool in the soil, the influence zone affects the soil particles in front of the tillage tool and causes the soil particles to move. The amount of movement is proportional to the position of the particles with respect to the influence zone. An oblique conical surface was established with the largest circle of the influence zone as the base of the cone. The influence zone intensity was defined as a parameter Z. The parameter Z, the ratio of the soil particle velocity to the tool velocity, was defined as the vertical distance of a point in the influence zone from the surface of the cone. The equation of the conical surface was determined and the differential equation of the movement of soil particles under the influence of the influence zone of a tillage tool was developed. The differential equation was solved numerically by the MATLAB software.

The developed soil movement model predicts the soil movement with the speed of operation of tillage tool only. Four tool shape factors and soil physical properties were used in regression analysis to predict soil movement with different tool shapes, speed of operation and soil conditions of moisture and compaction level. Some of the soil particles located right in front of the tillage tool will come in contact with the tool. These particles in practice will get some direct impact from the tool that might give them a higher

movement that is not explainable by this model. Attempts have been made to incorporate the effects of depth with the final model. The knife opener exponential model of soil movement with depth of Chapter 4 was used to predict the soil movement by four different tool shapes used in the high speed experiments under the same speed of operation and soil moisture content and compaction levels. The knife opener exponential model predicted lower values for the soil movement with all four tools

7.6 Conclusions

- Soil movement with speed of operation of tillage tools can be modeled by considering a circular influence zone in front of tillage tool and by describing the motion of particles by differential equations.
- In order to include the effects of soil physical properties, and tool shape, a regression analysis of soil bin test data was conducted. The results were compared with the experimental values obtained in the soil bin tests. The comparison showed an error of 7-20% for different tool shapes and soil conditions. The model was also applied to the knife opener and the results showed about 7% error.
- Considering the complexity of soil conditions and the difficulties in modeling soil parameters, the model appears to relate very well the soil movement to the experimental data. The developed soil movement model predicts the soil movement with the speed of operation of tillage tool only. Four tool shape factors and soil physical properties were used in regression analysis to predict

soil movement with different tool shapes, speed of operation and soil conditions of moisture and compaction level.

CHAPTER 8

CONCLUSIONS AND SUGGESTIONS FOR FURTHER RESEARCH

8.1 Conclusions

Soil translocation measurements with a sweep and a knife opener in soil bin showed an exponential relation between forward soil movement and the depth of soil layer. Tool shape and operational speed showed a very strong correlation with forward and lateral soil movement. The specific conclusions from this study are:

8.1.1 Soil movement by a narrow and a wide tool

- The soil movement by the sweep was greater than knife opener, but a larger soil movement per frontal area by the knife opener was observed.
- Soil movement was inversely proportional to depth of the block layers and had an exponential relationship.
- Increasing tool travel speed from 5 to 8 km h^{-1} increased soil movement by the sweep and the knife opener by factors of 1.5 ± 0.2 and 1.7 ± 0.3, respectively.
- Increasing moisture content of the soil from 10-11% to 15-16% resulted in an 18% increase of soil movement by the sweep.

8.1.2 Soil movement in high speed tillage experiments

- In high speed experiments, increasing tool operational speed generally resulted in increase in soil movement for all tools. In some tests at higher speeds, the rate of increase in soil movement with tool speed decreased, but the trend was not constant for a specific tool or soil condition.
- T4 (45° triangular) and T3 (elliptical) tool had the lowest energy usage and soil movement.
- Measurement of the energy used by tillage tools can not be used as a measure of soil movement since each tool shape needs a certain amount energy to move in soil at zero speed.

8.1.3 Soil profile analysis

- In soil profile measurement experiments, the furrow width and ridge height for sweep was larger than that for the knife opener.
- Increasing the travel speed of the tool increased the furrow depth and the lateral distance that soil was thrown by the sweep and the knife opener.
- Increasing the moisture content resulted in a wider and higher ridge.
- Increasing the compaction level increased the soil ridge heights.
- In soil profile measurements for high speed experiments, flat tool (T2) had the highest lateral soil movement followed by the 90° triangular (T1). The elliptical tool (T3) and the 45° triangular tool had almost the same lateral soil movement with the T4 tool having a lesser value.

- The compacted soil body that was attached to the tool surface was very high for the 90° triangular (T1) and Flat tool T2. The elliptical tool (T3) and the 45° triangular tool (T4) had the lowest. It was concluded that the 45° triangular tip tool had the least soil lateral movement.
- Increasing the soil moisture content first increased the lateral soil movement, but further increases in soil moisture resulted in decrease of lateral soil movement. Further increases of moisture, reduced the adhesion of soil to the tool because of its lubrication effect that resulted in lower lateral soil movement.
- Increasing the compaction resulted in the reduction in the amount of the input soil flow rate and, therefore, a smaller soil furrow cross section.
- Increasing tool travel speed from 10 km h^{-1} to 15 km h^{-1} increased the lateral soil movement, but further increases in speed, reduced it. It seems that the adhesion was reduced at the speeds of more that 10 km h^{-1}. This reduction in adhesion made the flow of soil around the tool easier and resulted in a smaller soil profile cross section and decrease of lateral soil movement.

8.1.4 Soil movement model

- A model for soil movement with speed of operation of tillage tools was developed by considering a circular influence zone and by describing the motion of particles by differential equations.
- In order to include the effects of soil physical properties, and tool shape, a regression analysis of soil bin test data was conducted. The results were compared with the experimental values obtained in the soil bin tests.

- The comparison showed an average error of 7-20% for different tool shapes and soil conditions. The model was also applied to the knife opener and the results showed about 7% error.
- Considering the complexity of soil conditions and the difficulties in modelling soil parameters, the model appears to relate very well the soil movement to the experimental data.

8.2 Suggestions for Further Research

In developing soil movement model in this research, it was assumed that the movement field for a narrow tillage tool has a perfect circular shape for a normal soil condition. It was also assumed that the tillage tool influencing the movement field in one point. It is suggested that further research should be done to find out the soil movement pattern for different soil conditions and wide tillage tool. It is also desirable to design an instrumentation system to record the pattern of movement of the tracers placed in soil with time to simulate soil movement.

References

ASAE Standards, 31st Edition. 1984. ASAE S 313.1. Soil cone penetrometer. St. Joseph, MI.: ASAE. (124).

Boyd, C. W., and S. J. Windisch. 1966. A technique for measuring deformations within a sand under controlled wheel loads. 2nd international conference of the International Society for Terrain-Vehicle Systems :72 Lyme Road, Hanover, NH:ISTVS.

Chancellor, W. J. 1994. Soil physical properties. In *Advances in Soil Dynamics*. Ed. P. D. Hansen ASAE Monograph Number 12, pp 21-254. St. Joseph, MI: ASAE.

Chase, L. W. 1942. A study of subsurface tiller blades. *Agricultural Engineering* 23:43-45, 50.

deJong, E., C. B. M. Begg and R. G. Kachanoski. 1983. Estimates of soil erosion and deposition for some Saskatchewan soils. *Canadian Journal of Soil Science* 63:607-617.

Dowell, F.E., J.C. Siemens and L. E. Bode. 1988. Cultivator speed and sweep spacing effects on herbicide incorporation. *Transactions of the ASAE* 31(5):1315-1321.

Eidet, J. H. 1974. Effect of varied approach angle on high speed moldboard plow performance. Unpublished M.Sc. thesis. Iowa State University, Ames, IA.

Ellison, W. D. 1947. Soil erosion studies-Part II. *Agricultural Engineering* 28:197-201.

Fredlund, D. G. and H. Rahardjo. 1993. *Soil Mechanics for Unsaturated Soils*. New York, NY: John Wiley & Sons, Inc.

Govers, G., K. Vandaele, P. J. J. Desmet, and J. Poesen. 1994. Characterizing soil tillage as a geomorphological process. *In proc. 13th International conference. "Soil*

Tillage for Crop Production and Protection of the Environment". Vol. I. H. E. Jensen. P. Schjonning, S. A. Mikkelsen, K. B. Madsen (eds.) ISTRO. pp. 269-274.

Gill, W. R. and G.E. VandenBerg. 1968. *Soil Dynamics in Tillage and Traction.* Agriculture Handbook, No. 316. Agricultural Research Service, U. S. Department of Agriculture. Auburn, AL

Godwin, R. J. and G. Spoor. 1977. Soil failure with narrow tines. *Journal of Agricultural Engineering Research* 22(4):213-228.

Goryachkin, V. P. 1968. *Collected Works in Three Volumes.* Ed. N. D. Luchinskii. Translated 1972. Jerusalem, Israel: Ketter Press.

Hanna, H.M., D.C. Erbach, S.J. Marley, and S.W. Melnin.1993a. Comparison of the Goryachkin theory to soil flow on a sweep. *Transactions of ASAE* 36(2):293-299.

Hanna, H.M., D.C. Erbach, S.J. Marley, and S.W. Melnin.1993b. Changes in soil microtopography by tillage with a sweep. *Transactions of ASAE* 36(2): 301-307

Hittiaratchi, D. R. P. and A. R. Reece. 1967. Symmetrical three-dimensional soil failure. *Journal of Terramechanics* 4(3):45-67.

Kachanoski, R. G. 1992. Evaluation of soil loss rates under different soil and cropping practices in Prince Edward Island. University of Guelph. Guelph. 75 p.

Kachanoski, R. G. 1993. Estimating soil loss from changes in soil ^{137}Cs. *Canadian Journal of Soil Science* 73: 627-632.

Koolen, A. J. and H. Kuipers. 1983. *Agricultural Soil Mechanics.* Berlin: Springer-Verlag.

Kuiper, H. and B. Kroesbergen. 1966 The significance of moisture content, pore space, method of sample preparation and type of shear annulus on laboratory torsional shear testing of soils. *Journal of Terramechanics*. 3(4): 17-28.

Kushwaha. R. L. and F. W. Bigsby. 1989. Tillage practices In *Handbook on Conservation Agriculture,* eds. J. A. Gillies and R. L. Kushwaha. University of Saskatchewan, Saskatoon, SK, Canada

Kushwaha, R. L., L. Chi and J. Shin. 1993. Analytical and Numerical models for predicting soil forces on narrow tillage tools-A review. *Canadian Agricultural Engineering* 35(3):183-192.

Lambe, T. W. and R. V. Whitman. 1969. *Soil Mechanics*. New York, NY:John Wiley & Sons, Inc.

Lindstrom M. J., W. W. Nelson, T. E. Schumacher and G. D. Lemme.1990. Soil movement by tillage as affected by slope. *Soil and Tillage Research*, 17: 225-264.

Lobb, D. A., R. G. Kachanoski, and M. H. Miller. 1995. Tillage translocation and tillage erosion on shoulder slope landscape positions measured using ^{137}Cs as a tracer. *Canadian Journal of Soil Science* 75: 211-218.

Lobb, D. A., R. G. Kachanoski, and M. H. Miller. 1995. The effect of slope gradient, tillage speed and depth on tillage translocation and tillage erosion measured using Cl as a tracer. Quebec City, QB, Canada:CSSS.

Lobb, D. A., R. G. Kachanoski. 1996. The impact of tillage translocation and tillage erosion on the estimation of soil loss using Cs-137. *Canadian Journal of Soil Science* 76: 241.

Lobb, D. A.and R. G. Kachanoski. 1997. Quantification of tillage translocation and tillage erosion. Presented at the *Tillage Translocation and Tillage Erosion: An International Symposium,* Part of the 52nd Annual Conference of the Soil and Water Conservation Society, Toronto, ON, Canada.

McKyes, E. and O. S. Ali. 1977. The cutting of soil by narrow blades. *Journal of Terramechanics*. 14(2): 43-58.

McKyes, E. 1985. *Soil cutting and tillage* . Amsterdam, The Netherland: Elsevier.

McKyes, E. 1989. *Agricultural Engineering Soil Mechanics*. Amsterdam, The Netherland: Elsevier.

Mech, S. J. and Free, G. A., 1942. Movement of soil during tillage operations. *Agricultural Engineering* 23: 379-382.

Neal, M. S. 1966. Friction and adhesion of between soil and rubber. *Journal of Agricultural Engineering Research.* 11(2):108-112.

Nichols, M. L. 1931. The dynamic properties of soil II. Soil and metal friction. *Agricultural Engineering*, 12:321-324.

Nichols, M. L., and I. F. Reed, 1934. Soil dynamics: VI. Physical reactions of soils to moldboard surfaces. *Agricultural Engineering*, 15:187-190.

Nikiforov, P. E. and M. I. Bredun. 1965. *The sliding friction of soil on metal and plastic surfaces.* Moscow, Russia: Nukai.

O'Callaghan J. R. and K. M. Farrelly. 1964. Cleavage of soil tined implements. *Journal of Agricultural Engineering Research* 9:259-270.

Payne, P. C. 1956. The relationship between the mechanical properties of soil and the performance of simple cultivation implements. *Journal of Agricultural Engineering Research.* 1(1):23-50.

Perumpral, J. V., R. D. Drisso, and C. S. Desai. 1983. A soil-tool model based on limit equilibrium analysis. *Transactions of ASAE* 26(4):991-995.

Pimental, D. 1993. *World soil erosion and conservation.* Cambridge, England:Cambridge University Press

Plante, A. F., W. B. McGill, M. J. M. Duke, and J. C. Stensrud. 1998. Development of a tracer method for studying soil aggregate dynamics. Department of Renewable Resources, University of Alberta, Edmonton, AB, Canada

Rajaram G. and A. Oida, 1992. Deformation of sand caused by tine implements. *Journal of Terramechanics* 29(1):149-159.

Schafer, R. L., and C. E. Johnson. 1982. Changing soil condition-The soil dynamics of tillage. p. 14-15. In *tillage effects on soil physical properties and processes.* American Society of Agronomy special publication number 44, Madison.

Sharifat, K. and R. L. Kushwaha 1997. Soil translocation by two tillage tools. *Canadian Agricultural Engineering* 39(2):77-84. (Chapter 4).

Sharifat, K. and R. L. Kushwaha. 1998. Soil translocation by narrow tillage tools at high speeds. CSAE paper 98-409, Saskatoon, SK, :CSAE. (Chapter 5).

Sibbesen, E., C. E. Anderson, S. Anderson, and M. Flensted-Jensen. 1985. Soil movement in long-term experiments as a result of cultivations: I. A model for approximating soil movement in one horizontal dimension by repeated tillage. *Journal of Experimental Agriculture* 21:101-107.

Sibbesen, E., and C. E. Anderson. 1985. Soil movement in long-term experiments as a result of cultivations: II. How to estimate the two-dimentional movement of substances accumulating in the soil. *Journal of Experimental Agriculture.* (21): 109-117.

Söhne, W. 1960. Suiting the plow body shape to higher speeds. *National Institute of Agricultural Engineering* Translation No. 101(12):51-62.

Stafford, J. V. and D. W. Tanner. 1983. Effect of rate on soil shear strength and soil-metal friction.. *Soil and Tillage Research* 3(1983):321-330.

Staricka, J. A., R. R. Allmaras, W. W. Nelson, and W. E. Larson. 1992.Soil aggregate longevity as determined by the incorporation of ceramic spheres. *Soil Science Society of America Journal.* 56:1591-1597.

Sweek, W. C. and J. V. Perumpral. 1988. A model for predicting soil-tool interaction. *Journal of Terramechanics* 25(1):43-56.

Turkelboom, F., J. Poesen, I. Ohler, K. Van Keer, S. Ongprasert and K. Vlassak. 1996. Assessment of tillage erosion rates on steep slopes in northern Thailand. *Catena* 29: 29-44.

Walling, D. E. and T. A. Quine. 1990. Calibration of ^{137}Cs measurements to provide quantitative erosion rate data. *Land Degradation & Rehabilitation Journal.* 2: 161-175.

Zelenin, A. N. 1950. *Basic physics of the theory of soil cutting.* Moscow, Russia: Kolos

Zeng, D. and Y. Yao. 1992. A dynamic model for soil cutting by blade and tine. *Journal of Terramechanics* 29(3):317-328.

Zhang, J.X., Z. Z. Sang and L. R. Gao. 1986. Adhesion and friction between soils and solids. *Transaction of Chinese Society of Agricultural Machinery*. 17(1):32-40

APPENDICES

Appendix-A: Statistical analysis tables

Appendix-B: Model development

Appendix-C: Instrumentation system for measuring x-y-z references

Appendix A

Table I: Analysis of variance results for the sweep and the knife opener.

Analysis of variance for soil movement by the knife opener

Source	df	MS	F	P
Compaction	2	0.568	79.69	0.000
Moisture	2	0.234	33.99	0.000
Speed	2	3.045	416.87	0.000
Compaction*moisture	4	0.016	2.19	0.152
Compaction*speed	4	0.039	5.33	0.022
Moisture*speed	4	0.013	1.76	0.207

Means

Compaction	Movement	Moisture	Movement	Speed	Movement
1	1.790	1	1.900	1	1.491
2	2.182	2	2.114	2	2.084
3	2.258	3	2.216	3	2.654

Analysis of variance for soil movement by the sweep

Source	df	MS	F	P
Compaction	2	23.570	24.54	0.000
Moisture	2	37.829	39.24	0.000
Speed	2	121.059	125.58	0.000
Compaction*moisture	4	3.955	4.10	0.043
Compaction*speed	4	1.423	1.48	0.296
Moisture*speed	4	0.640	0.66	0.634

Means

Compaction	Movement	Moisture	Movement	Speed	Movement
1	16.372	1	13.023	1	11.727
2	15.984	2	15.670	2	14.979
3	13.396	3	17.059	3	19.047

Table II: Analysis of variance results for all of data.

Source	df	MS	F	P
Tool	1	2343.009	4479.14	0.000
Compaction	2	15.724	30.06	0.000
Moisture	2	22.004	42.06	0.000
Speed	2	81.193	155.23	0.000
Tool*compaction	2	8.413	16.08	0.002
Tool*moisture	2	16.059	30.70	0.000
Tool*speed	2	42.907	82.02	0.000
Compaction*moisture	4	1.774	3.39	0.067
Compaction*speed	4	0.602	1.15	0.400
Moisture*speed	4	0.251	0.48	0.751
Tool*compaction*moisture	4	2.197	4.20	0.040
Tool*compaction*speed	4	0.860	1.64	0.254
Tool*moisture*speed	4	0.402	0.77	0.574
Compaction*moisture*speed	8	0.448	0.86	0.584

MEANS

Tool	Movement	Compaction	Movement	Moisture	Movement	Speed	Movement
1	2.077	1	9.315	1	7.462	1	6.609
2	15.251	2	9.083	2	8.892	2	8.532
		3	7.593	3	9.637	3	10.851

Table III: Analysis of data for determination of coefficient A of the exponential function model for soil movement by the knife opener.

The regression equation is
$A = -440 + 219\ S + 0.43\ M^2 - 2.12x10^9/C^3$

Predictor	Coef	Stdev	t-ratio	P
Constant	-440	107.70	-4.47	0.000
$S^{\dagger}$	219	14.14	15.47	0.000
$(M^{\dagger\dagger})^2$	0.43	0.2753	1.73	0.097
$1/(c^{\dagger\dagger\dagger})^3$	$-2.12x10^9$	19724	-4.26	0.000

† Speed (km h^{-1}) †† Moisture content (%) ††† Compaction (kPa)

$s = 90.01$ $r^2 = 92\%$

Analysis of variance

Source	df	SS	MS	F	P
Regression	3	2108246	702749	86.75	0.000
Error	23	186326	8101		
Total	26	2294571			

Source	df	SEQ SS
S	1	1939334
M^2	1	21669
$1/c^5$	1	147243

Table IV: Analysis of data for determination of the coefficient B of the exponential function model for soil movement by the knife opener.

The regression equation is
$B = 37.3 + 4.25\ S - .0287\ A + .0374\ M^2 - 0.110/C^3$

Predictor	Coef	Stdev	t-ratio	P
Constant	37.255	2.855	13.05	0.000
S†	4.2467	0.9653	4.40	0.000
A	-0.028709	0.004221	-6.80	0.000
(M††)^2	0.037444	0.005751	6.51	0.000
1/(c†††)^3	-0.10955	0.01314	-8.33	0.000

† Speed (km h^{-1}) †† Moisture content (%) ††† Compaction (kPa)

$s = 1.786$ $r^2 = 87\%$

Analysis of variance

Source	df	SS	MS	F	P
Regression	4	467.66	116.91	36.66	0.000
Error	22	70.16	3.19		
Total	26	537.82			

Source	SEQ SS
Speed	167.81
A	147.53
M^2	70.75
$1/C^3$	81.57

Table V: Analysis of data for determination of the coefficient A of the exponential function model for soil movement by the sweep.

The regression equation is

$A = -3802 + 1.68\ C + 204\ M + 781\ S$

Predictor	Coef	Stdev	t-ratio	P
Constant	-3801.9	321.7	-11.82	0.000
C†	1.6834	0.4444	3.79	0.001
M††	204.06	16.57	12.31	0.000
S†††	780.70	31.22	25.01	0.000

† Compaction (kPa) †† Moisture content (%) ††† Speed (km h^{-1})

$s = 198.7$ $r^2 = 97.2\%$

Analysis of variance

Source	df	SS	MS	F	P
Regression	3	31639792	10546597	267.18	0.000
Error	23	907904	39474		
Total	26	32547696			

Source	df	SEQ SS
Compaction	1	970390
Moisture	1	5984722
Speed	1	24684680

Table VI: Analysis of data for determination of the coefficient B of the exponential function model for soil movement by the sweep.

The regression equation is

$B = 260 + 5108\ 1/C^{6} - 67.6\ M^{0.5} + 531/S$

Predictor	Coef	Stdev	t-ratio	P
Constant	259.55	56.99	4.55	0.000
$1/(C^{\dagger})^{6}$	5108.4	896.6	5.70	0.000
$(M^{\dagger\dagger})^{0.5}$	-67.63	14.21	-4.76	0.000
$1/S^{\dagger\dagger\dagger}$	531.2	149.2	3.56	0.000

† Compaction (kPa) †† Moisture content (%) ††† Speed (km h^{-1})

$s = 23.93$ $r^{2} = 76\%$

Analysis of variance

Source	df	SS	MS	F	P
Regression	3	40937	13646	23.82	0.000
Error	23	13176	573		
Total	26	54113			

Source	df	SEQ SS
$1/C^{6}$	1	20696
$M^{0.5}$	1	12977
1/S	1	7264

Table VII: Analysis of variance for soil movement.

Source	df	SS	MS	F	P
Block	2	2900929	1450465	1.69	0.187
Moisture	2	49083304	24541652	28.58	0.000
Compaction	2	12324278	6162139	7.18	0.001
Tool	3	241331440	80443816	93.67	0.000
Speed	3	1056446016	352148672	410.10	0.000
Block*moisture	4	7757401	1939350	2.26	0.063
Moisture*compaction	4	23067538	5766885	6.72	0.000
Moisture*tool	6	4408258	734710	0.86	0.528
Moisture*speed	6	108839832	18139972	21.12	0.000
Compaction*tool	6	16460011	2743335	3.19	0.005
Compaction*speed	6	19562634	3260439	3.80	0.001
Tool*speed	9	43199284	4799921	5.59	0.000
Moisture*compaction*tool	12	35810304	2984192	3.47	0.000
Moisture*compaction*speed	12	72556304	6046358	7.04	0.000
Moisture*tool*speed	18	42323324	2351296	2.74	0.000
Compaction*tool*speed	18	48322188	2684566	3.13	0.000
Moisture*compaction*tool*speed	36	111911568	3108655	3.62	0.000
Error	282	242176256	858781		
Total	431	2138480896			

Means

Moisture	No. of tests	Movement
1	144	3527.0
2	144	4049.6
3	144	3234.8

Compaction	No. of tests	Movement
1	144	3774.9
2	144	3662.6
3	144	3373.9

Tool	No. of tests	Movement
1	108	4231.8
2	108	4451.5
3	108	2993.9
4	108	2738.0

Speed	No. of tests	Movement
1	108	1452.6
2	108	2984.7
3	108	4305.5
4	108	5672.3

Table VIII: Analysis of Variance for used energy.

Source	df	SS	MS	F	P
Block	2	0.0041	0.0020	0.63	0.533
Moisture	2	117.12	58.5618	1.8E+04	0.000
Compaction	2	95.50	47.7505	1.5E+04	0.000
Tool	3	50.10	16.7023	5196.42	0.000
Speed	3	96.99	32.3304	1.0E+04	0.000
Block*moisture	4	0.0139	0.0035	1.08	0.365
Moisture*compaction	4	15.59	3.8973	1212.53	0.000
Moisture*tool	6	5.88	0.9804	305.01	0.000
Moisture*speed	6	3.42	0.5705	177.49	0.000
Compaction*tool	6	9.51	1.5841	492.84	0.000
Compaction*speed	6	3.39	0.5643	175.58	0.000
Tool*speed	9	97.41	0.8234	256.19	0.000
Moisture*compaction*tool	12	9.541	0.7948	247.27	0.000
Moisture*compaction*speed	12	2.73	0.2277	70.86	0.000
Moisture*tool*speed	18	7.10	0.3946	122.76	0.000
Compaction*tool*speed	18	2.91	0.1614	50.22	0.000
Moisture*compaction*tool*speed	36	8.59	0.2385	74.20	0.000
Error	282	0.91	0.0032		
Total	431	436.71			

Means

Moisture	No. of tests	Energy
1	144	13.356
2	144	17.441
3	144	25.862

Compaction	No. of tests	Energy
1	144	13.266
2	144	18.619
3	144	24.774

Tool	No. of tests	Energy
1	108	23.155
2	108	20.950
3	108	17.110
4	108	14.330

Speed	No. of tests	Energy
1	108	12.624
2	108	16.677
3	108	20.905
4	108	25.339

Table IX: Analysis of variance for the position of the " C_p".

Source	df	SS	MS	F	P
Moisture	2	2865.13	1432.56	76.79	0.000
Compaction	2	1226.29	613.15	32.87	0.000
Tool	3	502.35	167.45	8.98	0.000
Speed	3	180.52	60.17	3.23	0.003
Moisture*compaction	4	595.58	148.90	7.98	0.000
Moisture*tool	6	1408.87	234.81	12.59	0.000
Moisture*speed	6	476.71	79.45	4.26	0.002
Compaction*tool	6	250.38	41.73	2.24	0.062
Compaction*speed	6	296.88	49.48	2.65	0.031
Tool*speed	9	231.56	25.73	1.38	0.234
Moisture*compaction*tool	12	390.58	32.55	1.74	0.098
Moisture*compaction*speed	12	271.58	22.63	1.21	0.312
Moisture*tool*speed	18	276.62	15.37	0.82	0.662
Compaction*tool*speed	18	401.79	22.32	1.20	0.314
Error	36	671.58	18.66		
Total	143	10046.44			

MEANS

Moisture	No. of tests	C_p
1	48	38.81
2	48	40.00
3	48	30.00

Compaction	No. of tests	C_p
1	48	39.79
2	48	36.38
3	48	32.65

Tool	No. of tests	C_p
1	36	37.56
2	36	38.64
3	36	34.56
4	36	34.33

Speed	No. of tests	C_p
1	36	34.42
2	36	37.39
3	36	36.81
4	36	36.47

Table X: Results of the numerical solution of the differential equation of soil movement (m).

Distance from center	forward movement	Distance from center	forward movement	Distance from center	forward movement	Distance from center	forward movement
0.0000	1.4462	0.3972	0.1955	0.7290	0.0325	0.9409	0.0022
0.0157	1.1068	0.4115	0.1847	0.7396	0.0300	0.9461	0.0025
0.0314	0.9422	0.4258	0.1752	0.7501	0.0279	0.9511	0.0008
0.0471	0.8356	0.4399	0.1665	0.7604	0.0260	0.9558	0.0006
0.0628	0.7570	0.4540	0.1535	0.7705	0.0244	0.9603	0.0006
0.0785	0.6957	0.4679	0.1447	0.7804	0.0232	0.9646	0.0006
0.0941	0.6420	0.4818	0.1366	0.7902	0.0187	0.9686	0.0007
0.1097	0.5978	0.4955	0.1291	0.7997	0.0169	0.9724	0.0008
0.1253	0.5590	0.5090	0.1222	0.8090	0.0153	0.9759	0.0011
0.1409	0.5260	0.5225	0.1160	0.8182	0.0141	0.9792	0.0001
0.1564	0.4896	0.5358	0.1093	0.8271	0.0130	0.9823	0.0001
0.1719	0.4616	0.5490	0.0991	0.8358	0.0121	0.9851	0.0002
0.1874	0.4356	0.5621	0.0930	0.8443	0.0114	0.9877	0.0003
0.2028	0.4126	0.5750	0.0873	0.8526	0.0110	0.9900	0.0003
0.2181	0.3849	0.5878	0.0822	0.8607	0.0077	0.9921	0.0004
0.2335	0.3641	0.6004	0.0774	0.8686	0.0069	0.9940	0.0006
0.2487	0.3453	0.6129	0.0731	0.8763	0.0063	0.9956	0.0000
0.2639	0.3280	0.6252	0.0692	0.8838	0.0059	0.9969	0.0000
0.2790	0.3061	0.6374	0.0612	0.8910	0.0052	0.9980	0.0001
0.2940	0.2894	0.6495	0.0571	0.8980	0.0051	0.9989	0.0001
0.3090	0.2741	0.6613	0.0534	0.9048	0.0050	0.9995	0.0001
0.3239	0.2600	0.6730	0.0495	0.9114	0.0028	0.9999	0.0002
0.3387	0.2470	0.6846	0.0464	0.9178	0.0024	1.0000	0.0000
0.3535	0.2351	0.6959	0.0436	0.9239	0.0022		
0.3681	0.2179	0.7071	0.0411	0.9298	0.0020		
0.3827	0.2062	0.7181	0.0353	0.9354	0.0020		

Table XI: Soil movement calculated from the model for different speeds.

D†,m	10 km h^{-1}	15 km h^{-1}	20 km h^{-1}	25km h^{-1}	D,m	10 km h^{-1}	15 km h^{-1}	20 km h^{-1}	25km h^{-1}
0.0000	4.0205	6.0308	8.0411	10.0369	0.0682	0.0982	0.1474	0.1965	0.2453
0.0015	3.0769	4.6153	6.1538	7.6811	0.0693	0.0905	0.1357	0.1809	0.2258
0.0030	2.6193	3.9290	5.2386	6.5389	0.0703	0.0835	0.1253	0.1670	0.2085
0.0045	2.3230	3.4845	4.6459	5.7991	0.0713	0.0774	0.1161	0.1548	0.1933
0.0060	2.1046	3.1569	4.2091	5.2539	0.0722	0.0722	0.1083	0.1444	0.1803
0.0075	1.9341	2.9011	3.8681	4.8282	0.0732	0.0679	0.1018	0.1358	0.1695
0.0089	1.7848	2.6772	3.5696	4.4555	0.0741	0.0645	0.0967	0.1289	0.1609
0.0104	1.6619	2.4928	3.3238	4.1487	0.0751	0.0519	0.0779	0.1039	0.1296
0.0119	1.5541	2.3312	3.1083	3.8797	0.0760	0.0469	0.0704	0.0939	0.1171
0.0134	1.4623	2.1934	2.9245	3.6504	0.0769	0.0426	0.0640	0.0853	0.1065
0.0149	1.3611	2.0417	2.7222	3.3979	0.0777	0.0391	0.0586	0.0781	0.0975
0.0163	1.2832	1.9248	2.5664	3.2034	0.0786	0.0360	0.0540	0.0720	0.0899
0.0178	1.2109	1.8164	2.4219	3.0230	0.0794	0.0336	0.0503	0.0671	0.0838
0.0193	1.1470	1.7205	2.2940	2.8634	0.0802	0.0317	0.0476	0.0634	0.0792
0.0207	1.0699	1.6049	2.1399	2.6710	0.0810	0.0305	0.0458	0.0610	0.0762
0.0222	1.0122	1.5183	2.0244	2.5269	0.0818	0.0213	0.0319	0.0426	0.0532
0.0236	0.9598	1.4397	1.9196	2.3961	0.0825	0.0191	0.0286	0.0381	0.0476
0.0251	0.9118	1.3677	1.8236	2.2762	0.0832	0.0174	0.0261	0.0349	0.0435
0.0265	0.8511	1.2766	1.7021	2.1246	0.0840	0.0164	0.0246	0.0327	0.0409
0.0279	0.8045	1.2067	1.6090	2.0083	0.0846	0.0146	0.0219	0.0291	0.0364
0.0294	0.7619	1.1428	1.5237	1.9019	0.0853	0.0141	0.0211	0.0281	0.0351
0.0308	0.7227	1.0840	1.4453	1.8041	0.0860	0.0140	0.0210	0.0280	0.0350
0.0322	0.6867	1.0301	1.3734	1.7143	0.0866	0.0078	0.0118	0.0157	0.0196
0.0336	0.6535	0.9803	1.3070	1.6315	0.0872	0.0068	0.0101	0.0135	0.0169
0.0350	0.6058	0.9088	1.2117	1.5124	0.0878	0.0060	0.0090	0.0121	0.0151
0.0364	0.5733	0.8600	1.1467	1.4313	0.0883	0.0056	0.0085	0.0113	0.0141
0.0377	0.5435	0.8152	1.0870	1.3568	0.0889	0.0057	0.0085	0.0113	0.0142
0.0391	0.5134	0.7701	1.0268	1.2817	0.0894	0.0061	0.0091	0.0122	0.0152
0.0404	0.4870	0.7305	0.9741	1.2158	0.0899	0.0069	0.0104	0.0138	0.0173
0.0418	0.4628	0.6941	0.9255	1.1552	0.0904	0.0021	0.0032	0.0042	0.0053
0.0431	0.4266	0.6399	0.8532	1.0650	0.0908	0.0017	0.0025	0.0034	0.0042
0.0445	0.4023	0.6034	0.8046	1.0043	0.0912	0.0016	0.0023	0.0031	0.0039
0.0458	0.3797	0.5695	0.7593	0.9478	0.0916	0.0016	0.0024	0.0032	0.0040
0.0471	0.3588	0.5383	0.7177	0.8958	0.0920	0.0019	0.0028	0.0037	0.0046
0.0484	0.3398	0.5097	0.6797	0.8483	0.0924	0.0023	0.0035	0.0046	0.0058
0.0496	0.3226	0.4839	0.6452	0.8053	0.0927	0.0030	0.0045	0.0059	0.0074
0.0509	0.3039	0.4558	0.6078	0.7586	0.0930	0.0003	0.0005	0.0006	0.0008
0.0522	0.2756	0.4134	0.5512	0.6880	0.0933	0.0003	0.0005	0.0007	0.0008
0.0534	0.2585	0.3878	0.5170	0.6454	0.0936	0.0005	0.0007	0.0009	0.0012
0.0546	0.2428	0.3642	0.4856	0.6061	0.0938	0.0008	0.0011	0.0015	0.0019
0.0558	0.2285	0.3427	0.4569	0.5703	0.0941	0.0008	0.0012	0.0016	0.0019
0.0570	0.2152	0.3228	0.4304	0.5372	0.0943	0.0011	0.0017	0.0022	0.0028
0.0582	0.2032	0.3047	0.4063	0.5072	0.0944	0.0015	0.0023	0.0031	0.0038
0.0594	0.1925	0.2887	0.3849	0.4805	0.0946	0.0000	0.0000	0.0001	0.0001
0.0606	0.1701	0.2552	0.3403	0.4247	0.0947	0.0001	0.0001	0.0001	0.0001
0.0617	0.1586	0.2379	0.3173	0.3960	0.0948	0.0001	0.0002	0.0003	0.0003
0.0628	0.1483	0.2225	0.2966	0.3702	0.0949	0.0003	0.0004	0.0005	0.0006
0.0639	0.1377	0.2065	0.2753	0.3437	0.0950	0.0004	0.0006	0.0008	0.0010
0.0650	0.1289	0.1933	0.2578	0.3217	0.0950	0.0006	0.0009	0.0012	0.0015
0.0661	0.1211	0.1816	0.2422	0.3023	0.0950	0.0000	0.0000	0.0000	0.0000
0.0672	0.1143	0.1715	0.2286	0.2854					

† D= distance from the center

Table XII: Regression analysis and analysis of variance for 90° triangular tool (T1).

MTB > Regress 'Actual' 3 'Compaction' 'Moisture' 'Model';
SUBC> Constant.

The regression equation is
Actual = - 0.00786 -0.000003 Compaction -0.000023 Moisture + 0.288 Model

Analysis of variance

Source	df	SS	MS	F	P
Regression	3	0.0046437	0.0015479	379.14	0.000
Error	32	0.0001306	0.0000041		
Total	35	0.0047744			

Source	df	SEQ SS
Compaction	1	0.0000031
Moisture	1	0.0000001
Model	1	0.0046406

Unusual Observations

Observation	Compaction	Actual	Fit	Stdev.Fit	Residual	St.Resid
1	59	0.008180	0.012076	0.000790	-0.003896	-2.09R
22	194	0.017370	0.021725	0.000515	-0.004355	-2.23R
29	320	0.015870	0.011230	0.000757	0.004640	2.48R

R denotes an observation. with a largest. resid.

Table XIII: Regression analysis and analysis of variance for the flat tool (T2).

MTB > Regress 'Actual' 3 'Compaction' 'Moisture' 'Model';
SUBC> Constant.

The regression equation is
Actual = - 0.00878 +0.000011 Compaction -0.000081 Moisture + 0.288 Model

Analysis of variance

Source	df	SS	MS	F	P
Regression	3	0.0047042	0.0015681	106.97	0.000
Error	32	0.0004691	0.0000147		
Total	35	0.0051732			

Source	df	SEQ SS
Compaction	1	0.0000413
Moisture	1	0.0000014
Model	1	0.0046614

Unusual Observations

Observation	Compaction	Actual	Fit	Stdev.Fit	Residual	St.Resid
4	59	0.033880	0.041929	0.001495	-0.008049	-2.28R
24	194	0.035540	0.042988	0.001266	-0.007448	-2.06R

R denotes an obs. with a large st. resid.

Table XIV: Regression analysis and analysis of variance for the Elliptical tool (T3).

MTB > Regress 'Actual' 3 'Compaction' 'Moisture' 'Model';
SUBC> Constant.

The regression equation is
Actual = - 0.00734 -0.000008 Compaction +0.000435 Moisture + 0.109 Model

Analysis of variance

Source	df	SS	MS	F	P
Regression	3	0.00071877	0.00023959	44.97	0.000
Error	32	0.00017047	0.00000533		
Total	35	0.00088924			

Source	df	SEQ SS
Compaction	1	0.00001082
Moisture	1	0.00004119
Model	1	0.00066675

Table XV: Regression analysis and analysis of variance for the 45° triangular tool (T4).

MTB > Regress 'Actual' 3 'Compaction' 'Moisture' 'Model';
SUBC> Constant.

The regression equation is
Actual = - 0.00235 -0.000009 Compaction +0.000055 Moisture + 0.139 Model

Analysis of variance

Source	df	SS	MS	F	P
Regression	3	0.00110590	0.00036863	108.15	0.000
Error	32	0.00010907	0.00000341		
Total	35	0.00121497			

Source	df	SEQ SS
Compaction	1	0.00002638
Moisture	1	0.00000066
Model	1	0.00107886

Unusual Observations

Observation	Compaction	Actual	Fit	Stdev.Fit	Residual	St.Resid
2	59	0.008770	0.012438	0.000607	-0.003668	-2.10R
6	60	0.016770	0.012626	0.000506	0.004144	2.33R

R denotes an obs. with a large st. resid.

Table XVI: Regression analysis for the knife opener.

Regression Analysis for the knife opener
Actual=-0.00851+0.000009Compaction+0.000155Moisture+0.215 Model

Predictor	Coef	Stdev	t-ratio	P
Constant	-0.008514	0.001358	-6.27	0.000
Compaction	0.00000948	0.00000191	4.96	0.000
Moisture	0.00015497	0.00006777	2.29	0.003
Model	0.21540	0.01293	16.66	0.000

$s = 0.0008398$ $r^2 = 93.1\%$

Table XVII: Soil movement measured from the experiments by the 90° triangular tool (T1) and the Flat tool (T2), and predicted by knife opener exponential model.

Tool	compaction level (kPa)	moisture content (%)	speed (km h^{-1})	measured soil movement (m)	soil movement predicted by knife model (m)	measured/predicted ratio
1	194	17.07	10	0.0128	0.0013	9.75
1	194	17.07	15	0.0174	0.0022	8.01
1	194	17.07	20	0.0312	0.0030	10.49
1	194	17.07	25	0.0407	0.0037	10.96
1	264	11.17	10	0.0099	0.0015	6.79
1	264	11.17	15	0.0209	0.0023	9.05
1	264	11.17	20	0.0343	0.0031	11.02
1	264	11.17	25	0.0430	0.0039	11.15
1	320	15.06	10	0.0159	0.0015	10.24
1	320	15.06	15	0.0218	0.0024	9.03
1	320	15.06	20	0.0279	0.0032	8.65
1	320	15.06	25	0.0431	0.0040	10.86
1	300	17.63	10	0.0126	0.0016	7.91
1	300	17.63	15	0.0222	0.0025	9.03
1	300	17.63	20	0.0308	0.0033	9.42
1	300	17.63	25	0.0380	0.0040	9.45
					Average ratio	9.49
2	194	17.07	10	0.0172	0.0013	13.14
2	194	17.07	15	0.0243	0.0022	11.18
2	194	17.07	20	0.0266	0.0030	8.96
2	194	17.07	25	0.0355	0.0037	9.57
2	264	11.17	10	0.0100	0.0015	6.90
2	264	11.17	15	0.0257	0.0023	11.13
2	264	11.17	20	0.0348	0.0031	11.19
2	264	11.17	25	0.0464	0.0039	12.03
2	320	15.06	10	0.0110	0.0015	7.10
2	320	15.06	15	0.0254	0.0024	10.50
2	320	15.06	20	0.0401	0.0032	12.45
2	320	15.06	25	0.0466	0.0040	11.74
2	300	17.63	10	0.0125	0.0016	7.89
2	300	17.63	15	0.0259	0.0025	10.54
2	300	17.63	20	0.0329	0.0033	10.07
2	300	17.63	25	0.0433	0.0040	10.75
					Average ratio	10.32

Table XVIII: Soil movement measured from the experiments by the elliptical tool (T3) and 45° triangular tool (T4) and predicted by knife opener exponential model.

Tool	compaction level (kPa)	moisture content (%)	speed (km h^{-1})	measured soil movement (m)	soil movement predicted by knife model	measured/prerdicted ratio
3	194	17.07	10	0.0091	0.0013	6.95
3	194	17.07	15	0.0146	0.0022	6.72
3	194	17.07	20	0.0168	0.0030	5.65
3	194	17.07	25	0.0170	0.0037	4.57
3	264	11.17	10	0.0035	0.0015	2.39
3	264	11.17	15	0.0074	0.0023	3.20
3	264	11.17	20	0.0085	0.0031	2.72
3	264	11.17	25	0.0156	0.0039	4.05
3	320	15.06	10	0.0065	0.0015	4.19
3	320	15.06	15	0.0091	0.0024	3.76
3	320	15.06	20	0.0102	0.0032	3.16
3	320	15.06	25	0.0154	0.0040	3.87
3	300	17.63	10	0.0082	0.0016	5.15
3	300	17.63	15	0.0078	0.0025	3.18
3	300	17.63	20	0.0116	0.0033	3.56
3	300	17.63	25	0.0136	0.0040	3.38
					Average ratio	4.16
4	194	17.07	10	0.0091	0.0013	6.93
4	194	17.07	15	0.0113	0.0022	5.22
4	194	17.07	20	0.0160	0.0030	5.38
4	194	17.07	25	0.0190	0.0037	5.11
4	264	11.17	10	0.0054	0.0015	3.72
4	264	11.17	15	0.0111	0.0023	4.82
4	264	11.17	20	0.0157	0.0031	5.06
4	264	11.17	25	0.0210	0.0039	5.46
4	320	15.06	10	0.0087	0.0015	5.64
4	320	15.06	15	0.0077	0.0024	3.17
4	320	15.06	20	0.0155	0.0032	4.82
4	320	15.06	25	0.0209	0.0040	5.27
4	300	17.63	10	0.0042	0.0016	2.62
4	300	17.63	15	0.0090	0.0025	3.64
4	300	17.63	20	0.0147	0.0033	4.49
4	300	17.63	25	0.0208	0.0040	5.17
					Average ratio	4.78

APPENDIX B

MODEL DEVELOPMENT

To find the equation of cone surface, point P considered as the tip of the cone and point Q is any arbitrary point on the cone surface (Fig. 1). The radius of the cone base was considered as one. The references of P and Q are:

$$P=\begin{pmatrix}0\\0\\h\end{pmatrix} \qquad Q=\begin{pmatrix}x\\y\\z\end{pmatrix}$$

A line drawn from P through Q crosses the base of the cone at point R.

$$\vec{V}=\vec{Q}-\vec{P}=\begin{pmatrix}x\\y\\z-h\end{pmatrix}$$

$$\vec{M}=\vec{P}+t_{\circ}\vec{V}=\vec{P}+t_{\circ}(\vec{Q}-\vec{P})=\begin{pmatrix}\cos\theta_{\circ}+1\\\sin\theta_{\circ}\\0\end{pmatrix}$$

$$\begin{pmatrix}0\\0\\h\end{pmatrix}+t_{\circ}\begin{pmatrix}x\\y\\z-h\end{pmatrix}=\begin{pmatrix}\cos\theta_{\circ}+1\\\sin\theta_{\circ}\\0\end{pmatrix};$$

$$\begin{aligned} t_{\circ}x&=\cos\theta_{\circ}+1 & x&=(\cos\theta_{\circ}+1)/t_{\circ}\\ t_{\circ}y&=\sin\theta_{\circ} & y&=\sin\theta_{\circ}/t_{\circ}\\ h+t_{\circ}(z-h)&=0 & t_{\circ}&=h/(h-z)\end{aligned}$$

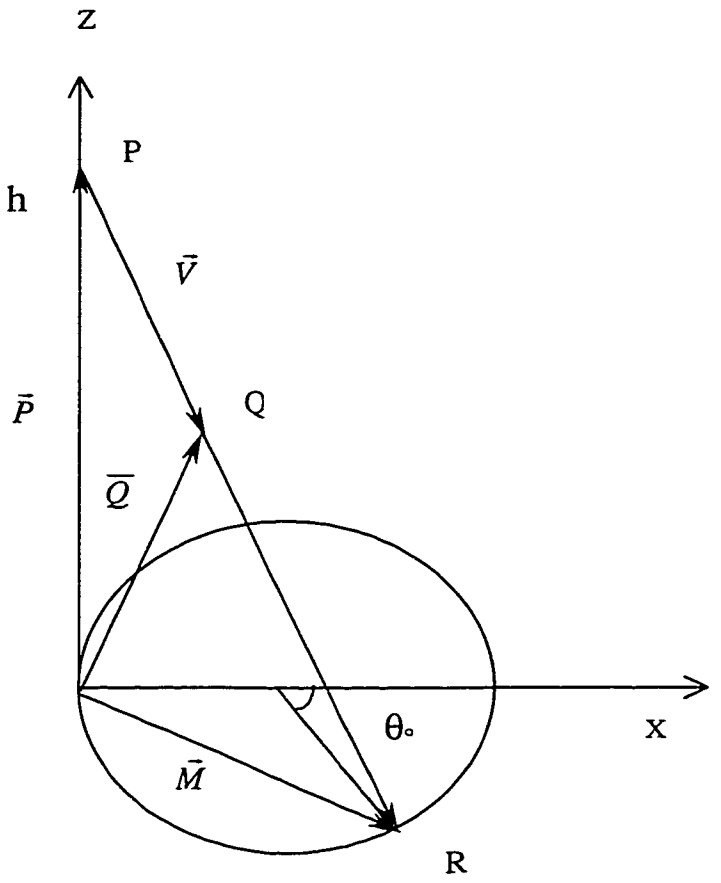

Figure 1 Development of the conical surface representing the Z parameter.

Let $a = \frac{y}{x}$

$$a = \frac{\sin\theta_\circ / t_\circ}{(\cos\theta_\circ + 1)/t_\circ}$$

$$a = \frac{\sqrt{1-\cos^2\theta_\circ}}{\cos\theta_\circ + 1}$$

$$\sqrt{1-\cos^2\theta_\circ} = a(\cos\theta_\circ + 1)$$

$$1-\cos^2\theta_\circ = a^2(\cos\theta_\circ + 1)^2$$

$$1-\cos^2\theta_\circ = a^2\cos\theta_\circ^{\,2} + 2a^2\cos\theta_\circ + a^2$$

$$(a^2+1)\cos^2\theta_\circ + 2a^2\cos\theta_\circ + a^2 - 1 = 0$$

$$\cos\theta_\circ = \frac{-2a^2 \pm \sqrt{4a^4 - 4(a^2+1)(a^2-1)}}{2(a^2+1)}$$

$$\cos\theta_\circ = \frac{-a^2 \pm 1}{a^2+1}$$

by taking $\cos\theta_\circ = \dfrac{1-a^2}{1+a^2}$

$$t_\circ = \frac{\cos\theta_\circ + 1}{x}$$

$$t_\circ = \frac{\dfrac{1-a^2}{1+a^2} + \dfrac{1+a^2}{1+a^2}}{x}$$

$$t_\circ = \frac{2}{(1+a^2)x}$$

$$t_o = \frac{2}{(1+\frac{y^2}{x^2})x}$$

$$t_o = \frac{2}{x+\frac{y^2}{x}}$$

$$t_o = \frac{2x}{x^2+y^2} \qquad \text{but} \qquad t_o = h/(h-z)$$

$$h+\frac{2x}{x^2+y^2}(z-h)=0 \qquad ; \qquad (x^2+y^2)h+2x(z-h)=0$$

$$(z-h)=\frac{-h(x^2+y^2)}{2x};$$

$$z=\frac{-h(x^2+y^2)}{2x}+h=\frac{-h(x^2+y^2)+2hx}{2x}=\frac{2hx-hx^2-hy^2}{2x}$$

$$\text{so} \qquad z=f(x,y)=\frac{2hx-hx^2-hy^2}{2x}=\frac{h(2x-x^2-y^2)}{2x}$$

$$z=f\big((x-v_o t),y\big)=\frac{h(2(x-v_o t)-(x-v_o t)^2-y^2)}{2(x-v_o t)}=h-\frac{h(x-v_o t)}{2}-\frac{hy^2}{2(x-v_o t)}$$

So, the equation of the conical surface (influence zone) is:

$$z=f\big((x-v_o t),y\big)=h-\frac{h(x-v_o t)}{2}-\frac{hy^2}{2(x-v_o t)}$$

Soil particles movement is in the opposite direction of the gradient vector. The gradient vector is:

$$\vec{\nabla}_t = \begin{pmatrix} -\frac{h}{2} - \frac{hy^2}{2}\left(\frac{-1}{(x-v_o t)^2}\right) \\ \\ \frac{-2hy}{2(x-v_o t)} \end{pmatrix}_j^i = \begin{pmatrix} -\frac{h}{2} + \frac{hy^2}{2}\left(\frac{1}{(x-v_o t)}\right)^2 \\ \\ \frac{-hy}{(x-v_o t)} \end{pmatrix}_j^i$$

To calculate the unit vector of gradient, gradient vector is divided by the its magnitude.

$$\|\nabla_t\| = \sqrt{\frac{h^2 y^2}{(x-v_o t)^2} + \left(\frac{-(x-v_o t)^2 h + hy^2}{2(x-v_o t)^2}\right)^2}$$

$$\|\nabla_t\| = \sqrt{\frac{h^2 y^4 - 2hy^2(x-v_o t)^2 h + (x-v_o t)^4 h^2 + 4h^2 y^2 (x-v_o t)^2}{4(x-v_o t)^4}}$$

$$\|\nabla_t\| = \sqrt{\frac{(hy^2 + (x-v_o t)^2 h)^2}{(2(x-v_o t)^2)^2}}$$

The magnitude of the gradient vector is:

$$\|\nabla_t\| = \frac{hy^2 + (x-v_o t)^2 h}{2(x-v_o t)^2}$$

To normalize the gradient, the vector is divided by its magnitude.

$$\frac{\nabla_t}{\|\nabla_t\|} = \begin{pmatrix} \frac{hy^2 - (x-v_o t)^2}{2(x-v_o t)^2} \\ \\ \frac{-hy}{(x-v_o t)} \end{pmatrix} \frac{2(x-v_o t)^2}{hy^2 + (x-v_o t)^2 h}$$

$$\frac{\nabla_t}{\|\nabla_t\|} = \begin{pmatrix} \dfrac{hy^2 - h(x - v_o t)^2}{hy^2 + h(x - v_o t)^2} \\ \dfrac{-2(x - v_o t)hy}{hy^2 + (x - v_o t)^2 h} \end{pmatrix}$$

$$\frac{\nabla_t}{\|\nabla_t\|} = \begin{pmatrix} \dfrac{y^2 - (x - v_o t)^2}{y^2 + (x - v_o t)^2} \\ \dfrac{-2y(x - v_o t)}{y^2 + (x - v_o t)^2} \end{pmatrix}$$

The movement vector has the magnitude of Z and is in the direction of the gradient unit vector. To find the movement vector, the gradient unit vector was multiplied by Z.

$$\text{Movement vector} = \frac{\nabla_t}{\|\nabla_t\|} \times Z$$

$$\text{Movement vector} = \begin{pmatrix} \dfrac{y^2 - (x - v_o t)^2}{y^2 + (x - v_o t)^2} \\ \dfrac{-2y(x - v_o t)}{y^2 + (x - v_o t)^2} \end{pmatrix} \times \left(h - \frac{h(x - v_o t)}{2} - \frac{hy^2}{2(x - v_o t)}\right) \qquad (7.7)$$

Appendix C

Schematic representation of the Instrumentation system for measuring x-y-z references